

10-4-2021

Oxidative DNA damage modulates genome and epigenome integrity via base excision repair

Pawlos S. Tsegay
ptseg001@fiu.edu

Follow this and additional works at: <https://digitalcommons.fiu.edu/etd>



Part of the [Biochemistry Commons](#), and the [Molecular Biology Commons](#)

Recommended Citation

Tsegay, Pawlos S., "Oxidative DNA damage modulates genome and epigenome integrity via base excision repair" (2021). *FIU Electronic Theses and Dissertations*. 4902.
<https://digitalcommons.fiu.edu/etd/4902>

This work is brought to you for free and open access by the University Graduate School at FIU Digital Commons. It has been accepted for inclusion in FIU Electronic Theses and Dissertations by an authorized administrator of FIU Digital Commons. For more information, please contact dcc@fiu.edu.

FLORIDA INTERNATIONAL UNIVERSITY

Miami, Florida

OXIDATIVE DNA DAMAGE MODULATES GENOME AND EPIGENOME
INTEGRITY VIA BASE EXCISION REPAIR

A dissertation submitted in partial fulfillment of
the requirements for the degree of

DOCTOR OF PHILOSOPHY

in

BIOCHEMISTRY

by

Pawlos S. Tsegay

2021

To: Dean Michael R. Heithaus
College of Arts, Sciences and Education

This dissertation, written by Pawlos S. Tsegay, and entitled Oxidative DNA Damage Modulates Genome and Epigenome Integrity via Base Excision Repair, having been approved in respect to style and intellectual content, is referred to you for judgment.

We have read this dissertation and recommend that it be approved.

Lou Kim

Yuk-Ching Tse-Dinh

Xiaotang Wang

Yuan Liu, Major Professor

Date of Defense: October 4, 2021

The dissertation of Pawlos S. Tsegay is approved.

Dean Michael R. Heithaus
College of Arts, Sciences and Education

Andrés G. Gil
Vice President for Research and Economic
Development and Dean of the University Graduate School

Florida International University, 2021

© Copyright 2021 by Pawlos S. Tsegay

All rights reserved.

DEDICATION

I dedicate this dissertation to my beloved wife, Danait Andemichael Solomon
and all my family for their endless love, encouragement, and support.

ACKNOWLEDGMENTS

I want to express my most sincere gratitude to all the people that directly or indirectly help me to achieve this work. First, I would like to thank my advisor/mentor Dr. Yuan Liu for her guidance, mentorship, and support through graduate studies. She motivated me to pursue this magnificent and fulfilling career path in biochemistry and molecular biology. Under her tutelage, I developed many skills such as critical thinking, writing/oral communication, and experimental procedures that will serve me well in every step of my career.

I also want to convey my deep gratitude to my committee members Dr. Lou W, Kim, Dr. Yuk-Ching Tse-Dihn, and Dr. Xiaotang Wang, for their guidance, comments, support, and collaboration through my Ph.D. training.

My sincere thank also goes to Dr. Chapagain for his collaboration and generating the docking and molecular dynamics results for my projects.

I would like to give my appreciation to my present and past lab members who helped me through this period of my life. I would especially like to thank Dr. Zhongliang Jiang, Dr. Yanhao Lai and Dr. Eduardo Laverde for their training and guidance. I would like to thank Dr. Yaou Ren, Daniela Hernandez, Fei Qu, Christopher Brache, other members of the Liu laboratory and all the neighboring labs for their assistance with my experiments and data analysis, help, cooperation, and friendship.

My special thanks go out to my wife Danait Andemichael Solomon, my parents Semere Tsegay and Mliete Foto, my brother Samuel S. Tsegay with his wife Mhret Girmatsion, as well as all my family for their continuous support and motivation throughout my graduate studies. I would not have had the

forbearance to make the achievement during my Ph.D. training without their support.

Finally, I would like to thank the FIU Dissertation Year Fellowship (DYF) which provided me great support to finish the last part of my graduate research.

ABSTRACT OF THE DISSERTATION

OXIDATIVE DNA DAMAGE MODULATES GENOME AND EPIGENOME INTEGRITY VIA BASE EXCISION REPAIR

by

Pawlos S Tsegay

Florida International University, 2021

Miami, Florida

Professor Yuan Liu, Major Professor

Oxidative DNA damage is one of the leading causes of genome instability, cell death, and diseases. It is repaired by DNA base excision repair (BER), during which repair and translesion DNA polymerases may incorporate damaged nucleotides and mediate RNA-guided DNA repair induced by DNA replication and gene transcription leading to the modulation of genome stability. On the other hand, oxidative DNA damage may result in cellular epigenetic responses to regulate DNA repair, altering genome stability and integrity. In this dissertation, we revealed the molecular mechanisms underlying the misincorporation of oxidized nucleotides, 5',8-cyclo-2-cyclodeoxyadenosine (cdA) and RNA-guided base lesion repair mediated by repair and translesion DNA polymerases. We then explored how oxidative DNA damage induced cellular epigenetic responses by disrupting microRNA expression to regulate BER. We found that DNA polymerase β (pol β) and DNA polymerase η (pol η) incorporated cdA that basepaired with dC, resulting in an A:C mismatch. We further demonstrated that cdA lesions were readily extended and ligated in duplex DNA. We showed that the polymerases incorporated cdAs independent of their hydrogen bonding with a template nucleotide using molecular docking.

Our study reveals a unique mechanism underlying the accumulation of cyclodeoxypurine lesions in the genome. We then explored the mechanisms by which DNA polymerases can utilize RNA as a template to synthesize DNA and repair a DNA base lesion. We found that translesion DNA polymerases, pol η , θ , and ν and repair DNA polymerases, pol β , λ and κ exhibited DNA synthesis activity, i.e., reverse transcriptase activity to mediate RNA-guided DNA base lesion repair. We further demonstrated that the completion of base lesion repair was accomplished by the RNA-guided translocation of a nick into duplex DNA via the strand displacement synthesis of the polymerases. We then explored the cellular mechanisms by which oxidative DNA damage modulates microRNA expression to regulate DNA repair. Our study revealed that oxidative DNA damage upregulated the expression of microRNA-499-5p (miR-499-5p) that subsequently downregulated the expression of the key BER enzyme, pol β , in human cells. Further analysis showed that the inhibition of 8-oxoG DNA glycosylase 1 (OGG1) activity significantly suppressed the upregulation of miR-499-5p, suggesting the epigenetic role of OGG1 in mediating the expression of miR-499-5p as cellular DNA damage response. Our study provides new insights into the crosstalk among oxidative DNA damage and repair, miRNAs, RNA-guided base lesion repair in modulating genome stability and integrity.

TABLE OF CONTENTS

CHAPTER	PAGE
INTRODUCTION	1
1. DNA Damage and Their Biological Consequences	1
1.1. Endogenous DNA damage	1
1.2. Exogenous DNA damage	9
1.3. Repair and Bypass of DNA Damage	12
1.4. DNA damage and epigenetic stability	19
2. The DNA Base Excision Repair Pathway.....	22
3. Cyclo-deoxypurines (cdPus) and Their Impact on RNA and DNA Metabolism.....	28
4. RNA-Templated/Guided DNA Repair.....	40
5. DNA Damage and Modulation of miRNA Expression.....	42
OVERVIEW.....	45
CHAPTER 1. INCORPORATION OF 5',8-CYCLO-2'DEOXYADENOSINES BY DNA REPAIR POLYMERASES VIA BASE EXCISION REPAIR.....	48
1.1. ABSTRACT	48
1.2. INTRODUCTION	49
1.3. MATERIALS AND METHODS.....	53
1.4. RESULTS.....	57
1.5. DISCUSSION	72
CHAPTER 2. RNA-GUIDED DNA BASE EXCISION REPAIR VIA DNA POLYMERASE SWITCHING	80
2.1. ABSTRACT	80
2.2. INTRODUCTION.....	81
2.3. MATERIALS AND METHODS.....	85
2.4. RESULTS.....	88
2.5. DISCUSSION	103

CHAPTER 3. OXIDATIVE DNA DAMAGE ALTERS MIR-49-5P ASSOCIATED WITH DNA POLYMERASE β	110
3.1. ABSTRACT	110
3.2. INTRODUCTION	111
3.3. MATERIALS AND METHODS.....	113
3.4. RESULTS.....	119
3.5. DISCUSSION	128
REFERENCE.....	131
VITA.....	156

LIST OF TABLES

TABLE	PAGE
INTRODUCTION	
Table 1.1. Proteins Involved in DNA Replication, Repair, and Replication Stress Response and Associated Diseases	6
Table 1.2. Translesion DNA Polymerases and Their Bypass Properties DNA Base Lesions	18
CHAPTER 1	
Table 1.1. Oligonucleotides sequence.....	54
Table 1.2. The steady state kinetics of the incorporation of cdA by Pol β	70
Table 1.3. The Steady State Kinetics of the Incorporation of cdA by pol η	71
CHAPTER 2	
Table 2.1. Oligonucleotides sequence.....	86
Table 2.2, Table 2.3, Table 2.4, Table 2.5. Steady-state Kinetics of RNA guided DNA synthesis by pol β , η	100

LIST OF FIGURES

FIGURE	PAGE
INTRODUCTION	
Figure 1.1. Sources of Oxidative Stress-Induced Oxidative DNA Damage	2
Figure 1.2. DNA Replication Stress Leads to Genomic and Epigenomic Instability Associated with Diseases	4
Figure 1.3. Oxidative Stress Induced by KBrO ₃	10
Figure 1.4. Types of DNA Damage and DNA Repair Pathways	12
Figure 1.5. Heterochromatin Formation During Replication Stress to Prevent Loss of Genetic Information	21
Figure 2.1. The dRP lyase mechanism of pol β	24
Figure 2.2. Base excision repair pathway	23
Figure 3.1. The Diastereomeric Cyclo-Deoxy Purine Lesions (cdPu).....	29
Figure 3.2. Mechanisms of cdPu accumulation and their impact on DNA and RNA metabolism.....	31
Figure 3.3. A cdA Located at DNA Repeat Sequences Induces Repeat Instability Through Pol β Bypass of a Loop Structure.....	39
Figure 5.1. miRNA Biogenesis. RNA polymerase II transcribes miRNA from their respective genes.	42
Figure 5.2. miRNAs associated with DNA damage and response.....	44
CHAPTER 1	
Figure 1.1. The structure of 5', 8-cyclo-2'-deoxyadenosine in 5'R and 5'S diastereoisomeric forms.	50
Figure 1.2. The incorporation of cdA by pol β during BER.....	59
Figure 1.3. The incorporation of cdA by pol η during BER.....	61
Figure 1.4. The misincorporation of cdA with a dC by pol β and pol η during BER.	63
Figure 1.5. Extension of cdA base paired with dT or dC by pol β and pol η .	64
Figure 1.6. Ligation of cdA by DNA LIG I. Ligation of cdA basepaired with dT or dC by LIG I.	66
Figure 1.7. The molecular docking analysis on the interaction between pol β and pol η and cdAd.....	69

CHAPTER 2

Figure 2.1. RNA and DNA template-dependent DNA synthesis by DNA polymerases	89
Figure 2.2. RNA dependent DNA synthesis by DNA polymerases.....	90
Figure 2.3. DNA synthesis on viral RNA by DNA polymerases.	92
Figure 2.4. RNA template-dependent DNA repair.	94
Figure 2.5. A. RNA dependent DNA repair.....	96
Figure 2.6. DNA synthesis on RNA-templated nick substrate.	98
Figure 2.7. Molecular dynamics simulation of the ternary complexes of pol β with a 1 nt gap.	102
Figure 2.8. Ligation of RNA templated nick using titrated concentration of DNA ligases.....	104
Figure 2.9. Hypothetical model for RNA guided DNA repair.....	107

CHAPTER 3

Figure 3.1. Oxidative DNA damage induces alteration of miR-499-5p to deregulate Pol β mRNA level.	120
Figure 3.2. Oxidative DNA damage decreases pol β protein level.....	121
Figure 3.3. Oxidative DNA damage does not alter the DNA methylation pattern in the promoter region of miR-499-5p.....	122
Figure 3.4. inhibition of OGG1 downregulated miR-499a-5p level.....	123
Figure 3.5. miR-499a-5p level is upregulated in OGG1 knockdown HEK 293H cells.....	124
Figure 3.6. DNA damage landscape profiles at the promoter region of miR-499a-5p.....	126
Figure 3.7. DNA base damage is correlated with the expression of miR-499a-5p.....	127

ABBREVIATIONS AND ACRONYMS

°C	Degree Celsius
3-meA	3-methyladenine
5',8-cdA	5',8-cyclo-2'-deoxyadenosine
5'-dRP	5'-deoxyribose phosphate
5-hU	5-hydroxyuracil
5-meC	5-methylcytosine
6-FAM	6-carboxyfluorescein
A	Adenine
AAO	Age at onset
AID	Activation-induced cytosine deaminase
AOA2	Ataxia with oculomotor apraxia 2
ALS4	Amyotrophic lateral sclerosis type 4
APE1	AP Endonuclease 1
AP site	Apurinic/aprimidinic site
APOBEC	Apolipoprotein B mRNA editing enzyme
AQR	Aquarius helicase
AR	Androgen receptor
ASF1	Alternative splicing factor 1
ATP	Adenosine triphosphate
ATR	Ataxia telangiectasia and Rad3-related protein
BER	Base excision repair
Bis-Tris	2,2-Bis(hydroxymethyl)-2,2',2'-nitrilotriethanol
bp	Base pair
BRCA1	Breast cancer type 1

BRCA2	Breast cancer type 2
BSA	Bovine serum albumin
C	Cytosine
Cdc45	Cell division cycle 45
Cdc6	Cell division cycle 6
CDK	Cyclin dependent kinase
cdPu	5',8-cyclo-2'-deoxypurines
Cdt1	Cdc10-dependent transcript 1
Chk1	Checkpoint kinase 1
CSR	Class switch recombination
CMG	CDC45-MCM-GINS
Cordycepin	3'-deoxyadenosine
CPDs	Pyrimidine dimers
Ctf4	Chromosome transmission fidelity 4
dAMP	Deoxyadenosine monophosphate
Dbf4	Dumbbell former 4
DDC	DNA damage checkpoint
DDK	Dbf4 dependent kinase
DDR	DNA damage response
DDSBs	DNA double-strand breaks
DGCR8	DiGeorge syndrome critical region 8
DNA	Deoxyribonucleic acid
dNDPs	Deoxyribonucleotide diphosphate
DNMT1	DNA methyltransferase 1
dNTP	Deoxyribonucleotide triphosphate

DRC	DNA replication checkpoint
dRP	Deoxyribose phosphate
dsDNA	Double-stranded DNA
DTT	Dithiothreitol
dUTP	Deoxyuracil monophosphate
dUTP	Deoxyuracil triphosphate
dUTPase	dUTP pyrophosphate
8-oxoG	8-oxoguanine
E. coli	Escherichia coli
EDTA	Ethylenediaminetetraacetic acid
EME1	Essential meiotic structure-specific endonuclease 1
EXO1	Exonuclease 1
FaPy	Formamidopyrimidine
FA	Fanconi Anemia
FAN1	Fanconi-anemia associated nuclease 1
FANCM	Fanconi anemia complementation complex M
FEN1	Flap endonuclease 1
FMR1	Fragile X mental retardation 1
FPLC	Fast protein liquid chromatography
FRDA	Friedreich's ataxia
FXN	Frataxin
FXS	Fragile X syndrome
G	Guanine
GINS	Go-inchi-ni-san
GST	Glutathione S-transferase

HCC	Hepatocellular carcinoma
HD	Huntington's disease
HDAC1	Histone deacetylase 1
HEK	Human embryonic kidney
HEPES	4-(2-hydroxyethyl)-1-piperazineethanesulfonic acid
His	Histadine
HMGB1	High-mobility group protein B1
HR	Homologous recombination
H ₂ O ₂	Hydrogen peroxide
HU	Hydroxyurea
ICL	Interstrand crosslink
IPTG	Isopropyl β-D-1-thiogalactopyranoside
IR	Ionizing radiation
KCl	Potassium chloride
KBRO ₃	Potassium bromate
LB	Lysogeny/Luria broth
LIG I	DNA ligase I
LIG III	DNA ligase III
LP-BER	Long patch-base excision repair
MAM	Methylazoxymethanol
MBD4	Methyl-binding domain glycosylase 4
MCM	Minichromosome maintenance protein
MD	Myotonic dystrophy

MEC1	Mitosis entry checkpoint 1
MEF	Mouse embryonic fibroblast
MgCl ₂	Magnesium chloride
miRNA	MicroRNA
MLH	MutL homologue
MMR	Mismatch repair
MMS	Methyl methanesulfonate
MRE11	Microhomology-mediated end-joining 11
mRNA	Messenger RNA
MSH	MutS homologue
Mus81	MUS81 structure-specific endonuclease subunit
MutSβ	MSH2/MSH3
MW	Molecular weight
MYH	MutY homologue
MNNG	N-methyl-N'-nitro-N-nitrosoguanidine
N	Nitrogen
NaCl	Sodium chloride
NaH ₂ PO ₄	Sodium dihydrogen phosphate
NaOH	Sodium hydroxide
N ⁷ -mG	N ⁷ -methylguanine
N ³ -mA	N ³ -methyl adenine
NEIL	Endonuclease VIII-like
NER	Nucleotide excision repair
NHEJ	Nonhomologous end-joining
NP-40	Nonidet P-40

nM	Nanomolar
nt	Nucleotide
O ₂	Oxygen
O ₂ ⁻	Superoxide
O•	Oxygen radical
¹ O ₂	Singlet oxygen
OH ⁻	Hydroxyl radical
O ⁶ -mG	O ⁶ -methylguanine
OGG1	8-oxoguanine DNA glycosylase
ORC	Origin recognition complex
PAGE	Polyacrylamide gel electrophoresis
PARP1	Poly(ADP-ribose) polymerase 1
PCNA	Proliferating cell nuclear antigen
pH	Potential of hydrogen
pI	Isoelectric point
PIP	PCNA-interacting protein
PMSF	Phenylmethylsulfonyl fluoride
pol β	DNA polymerase β
pol δ	DNA polymerase δ
pol ε	DNA polymerase ε
polyA	Polyalanine
polyQ	Polyglutamine
PTMs	Post-transcriptional modifications
RAD2	Radiation sensitivity 2
RFC	Replication factor C

RISC	RNA-induced silencing complex
RNA	Ribonucleic acid
RNR	Ribonucleotide reductase
ROS	Reactive oxygen species
ROOH	Lipid peroxides
ROO•	Peroxyl radicals
RPA	Replication protein A
SAM	S-adenosylmethionine
SETX	Human senataxin
SAMHD1	SAM domain and HD domain-containing protein 1
Sen1	Yeast senataxin
SF2	Splicing factor 2
siRNA	Small interference RNA
SMUG 1	Single-strand selective monofunctional uracil DNA glycosylase
SN-BER	Single-nucleotide base excision repair
SRSF1	Serine/arginine-rich splicing factor 1
ssDNA	Single-stranded DNA
T	Thymine
TDG	Thymine DNA glycosylase
Tg	Thymine glycol
THF	Tetrahydrofuran
TL	Translesion synthesis
TLS	Translesion polymerases
TNR	Trinucleotide repeat
TOP1	DNA topoisomerase 1

TopBP1	Topoisomerase II Binding Protein 1
TPC	Topotecan
TRCs	Transcription-replication conflicts
Tris	Tris(Hydroxymethyl)aminomethane
TSGs	Tumor suppressor genes
U	Uracil
U2OS	Human bone osteosarcoma
UBZ	Ubiquitin-binding domain
ub-PCNA	Ubiquitylated PCNA
UDG	Uracil DNA glycosylase
μM	Micromolar
UDG	Uracil DNA glycosylase
UNG	Uracil DNA N-glycosylase
UTR	Untranslated region
UV	Ultraviolet
WT	Wild-type
XPF	Xeroderma pigmentosum complementation group F
XPG	Xeroderma pigmentosum complementation group G
XRCC1	X-ray repair cross-complementing protein 1

INTRODUCTION

1. DNA Damage and Their Biological Consequences

1.1. Endogenous DNA damage

All living organisms store their genetic information on deoxyribonucleic acid (DNA) in the genome and strive to maintain genome integrity and stability to ensure the accurate pass of genetic information to the next generation. However, DNA is frequently subject to damage and mutations resulting from spontaneous base loss and deamination of DNA bases, endogenous and exogenous DNA damaging agents (Hoeijmakers, 2001; Lindahl, 1993). Spontaneous base loss, also known as self-decomposition of bases, can result from spontaneous hydrolysis of N-glycosidic bond and deamination under normal physiological conditions (Lindahl, 1993). Loss of a base results in an abasic or apurinic/apyrimidinic (AP) site at a rate of 10,000 abasic sites per day per cell (Lindahl and Nyberg, 1972). Subsequently, the AP site is converted to a single-strand break through β -elimination and 5'-incision of the AP site (Doetsch and Cunningham, 1990; Gates, 2009; Lindahl and Andersson, 1972). If not repaired efficiently, single-strand DNA breaks can cause mutagenesis and cytotoxicity (Auerbach et al., 2005; Bailly et al., 1989; Bailly and Verly, 1988; Boiteux and Guillet, 2004; Gates, 2009). In a scenario where the sugar is converted to open ring aldehyde, an interstrand crosslink (ICL) can also be generated by forming a covalent bond between the aldehyde and a guanine in the opposite strand leading to the blockage of replication and transcription (Dutta et al., 2007). Spontaneous DNA hydrolytic deamination is another major cause of DNA base damage. A typical example is the deamination of cytosine

(C) and 5-methylcytosine (5mC) that occur in cells with a high frequency. The deamination of C and 5mC are resulting in the conversion of C to uracil (U) and 5mC to thymine (T), respectively (Ehrlich et al., 1990; Lindahl, 1979; Lindahl and Nyberg, 1974).

The nitrogenous bases and backbone of DNA can also be damaged by endogenous and exogenous DNA damaging agents (*Figure 1.1*) (Ana L. Zamora Perez, 2016; Friedberg, 2003; Hoeijmakers, 2001; Lindahl, 1993; Pfeifer et al., 2002). Endogenous DNA damaging agents can be generated from cellular biochemical reactions, respiration, and metabolic processes. These internal DNA damaging sources mainly generate reactive oxygen species

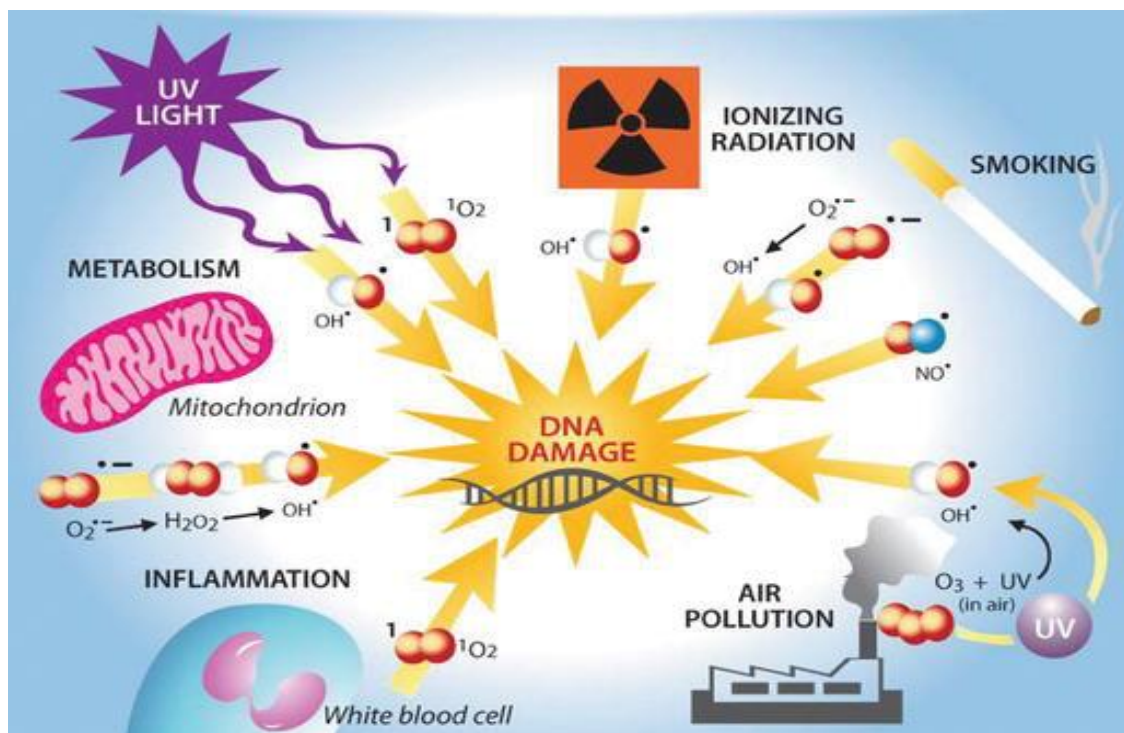


Figure 1.1. Sources of Oxidative Stress-Induced Oxidative DNA Damage (Ana L. Zamora Perez, 2016). DNA damaging agents are generated from endogenous and exogenous sources that lead to the formation of ROS causing DNA damage. Endogenously, ROS can be generated from cellular respiration and inflammation and UV light, Ionizing radiation, environmental toxicants and among others as the sources of exogenous ROS.

(ROS). ROS include superoxide anion radicals ($O_2^{\cdot-}$), hydroxyl radicals ($\cdot OH$) that can, hydrogen peroxides (H_2O_2), lipid peroxides (ROOH), singlet oxygen (1O_2) peroxy radicals ($ROO\cdot$) and so forth (De Bont and van Larebeke, 2004; Gaschler and Stockwell, 2017).that damage DNA by causing oxidized DNA bases and can directly oxidize DNA bases and cause single and double-strand DNA breaks (De Bont and van Larebeke, 2004). ROS can also indirectly attack DNA through oxidized polyunsaturated fatty acids and residues of phospholipids or oxidized amino acid residue. DNA damage resulted from peptide-DNA and lipid-DNA crosslinks can be generated by oxidized proteins and lipid respectively (De Bont and van Larebeke, 2004). Bulky DNA base

lesions, including cyclopurines and intra- and

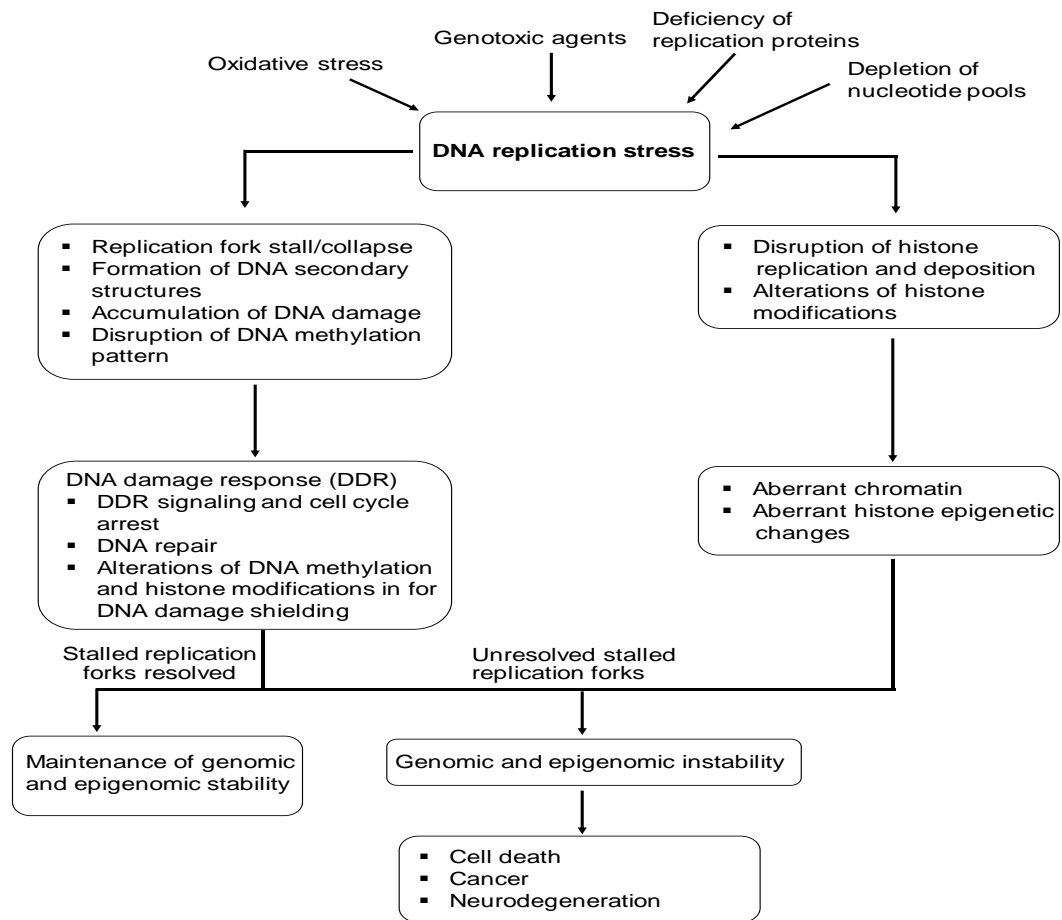


Figure 1.2. DNA Replication Stress Leads to Genomic and Epigenomic Instability Associated with Diseases (Tsegay et al., 2019). DNA replication stress arises from oxidative stress, genotoxic agents, deficiency of replication proteins, depletions of nucleotides, and others are the endogenous causes of genomic and epigenomic instability.

interstrand crosslinks that block DNA replication and transcription can also be generated by hydroxyl radicals (Kuraoka et al., 2000; Sczepanski et al., 2009). These bulky DNA lesions can cause nucleotide misincorporation and mutations during DNA replication and repair. The other significant sources of endogenous DNA damage are DNA replication and gene transcription. During cell division, 6 billion nucleotides are incorporated to duplicate the 3 billion paired bases of the human genome per cell (Voet, 2011). The cellular process provides a

variety of chances to cause genome instability through DNA replication. Among them, replication stress is the most common one and can cause a series of adverse biological consequences (*Figure 1.2*). These effects include physical impediments of replication fork progression (Lopes et al., 2001b), insufficient synthesis of histone proteins (Clemente-Ruiz and Prado, 2009), and depletion of dNTPs (Bester et al., 2011; Chabosseau et al., 2011; Gay et al., 2010). In some cases, DNA replication and repair enzymes can also cause replication stress by producing DNA repair intermediates such as abasic sites and ssDNA breaks and incorporating damaged nucleotides through repair and translesion DNA polymerases (Grollman and Moriya, 1993b; Patel and Weiss, 2018; Shibutani et al., 1991; Wallace, 2002). In addition, replication stress can be facilitated by the insufficiency of proteins involved in DNA replication, repair, and response to replication stress leading to diseases (*Table 1.1*). DNA damage can also result from repeated DNA sequences in the genome that include microsatellites, minisatellites, isolated repeated motifs comprising homopolymers, elevation transposable elements, pseudogenes, and terminal repeats.

Table 1.1. Proteins Involved in DNA Replication, Repair, and Replication Stress Response and Associated Diseases (Tsegay et al., 2019)

DNA Repair Protein	Function	Human Diseases
CDT1	Facilitates MCM loading on origins	Meier-Gorlin syndrome (Zeman and Cimprich, 2014b)
Pre-RC (CDT1, ORC1-ORC6, Cdc6, MCM2-7)	Recruitment of DNA polymerase and phosphorylation by both the Cdc7/Dbf4 and CDK2-cyclin A protein kinases	Meier-Gorlin syndrome (Zeman and Cimprich, 2014b)
Nbs1	ATR/ATM activation	Nijmegen breakage syndrome (Zeman and Cimprich, 2014b)
Rad50	ATR/ATM activation	Nijmegen breakage syndrome-like disorder (Zeman and Cimprich, 2014b)
RecQL4	DNA remodeling, replication fork structure resolution	Rothmund-Thomson syndrome (Bernstein et al., 2010; Zeman and Cimprich, 2014b)
RNase H2	Removal of embedded ribonucleotides Resolution of RNA-DNA hybrid	Aicardi-Goutières syndrome (Crow et al., 2006)
Senataxin	Resolution of RNA-DNA hybrid	Amyotrophic lateral sclerosis (Zeman and Cimprich, 2014b)
Mre 11	ATM/ATR activation	Ataxia-telangiectasia-like diseases (Zeman and Cimprich, 2014b)
BLM	DNA remodeling, replication fork stall resolution	Bloom syndrome (Chabosseau et al., 2011)
FANC family	DNA inter-strand cross-link repair	Fanconi anemia (Kim and D'Andrea, 2012; Zeman and Cimprich, 2014b)
FANCD2	Replication fork protection	Fanconi anemia (Kim and D'Andrea, 2012; Zeman and Cimprich, 2014b)
WRN	DNA remodeling, replication fork structure resolution	Werner syndrome (Zeman and Cimprich, 2014b)
BRCA1, BRCA2	Checkpoint mediators, DNA repair and recombination	Breast and ovarian carcinoma (Bartek et al., 2004)
MSH2 and MLH1	DNA mismatch repair	Colorectal cancer (Bartek et al., 2004)

The repeat sequences constitute 50% of the human genome and can result in DNA replication fork stalling in the absence of exogenous genome stress (Liu

et al., 2012; Techer et al., 2017). This is because the repeats can form non-B form DNA structures during DNA replication and repair. Among them, minisatellites and microsatellites are the major sources of causing replication stalling and DNA damage resulting in “dynamic mutations,” i.e., repeat deletions and expansions (Sutherland et al., 1998; Techer et al., 2017). The non-B form DNA structures resulting from repeated DNA sequences include triplex DNA, hairpins, DNA loops, Z-DNA, and G-quadruplexes (Gordenin and Resnick, 1998; Mirkin and Mirkin, 2007; Usdin et al., 2015; Wang and Vasquez, 2014). They form the roadblocks of replicative and repair DNA polymerases to cause polymerase pausing, impeding replication for progression and DNA repair, leading to replication stress. In addition, the non-B form structures are susceptible to DNA damage and DNA strand breaks. Thus, repeat DNA sequences also form as part of DNA fragile sites.

DNA replication fork stalling can also be induced as a result of gene transcription. During S phase, genes involved in DNA replication are highly expressed. This may result in a conflict between replication and transcription, i.e., transcription-replication conflicts (TRCs) when both replication and transcription occur simultaneously in the same DNA templates creating a head-on collision (Garcia-Muse and Aguilera, 2016; Mirkin and Mirkin, 2007). The collision slows down replication fork progression subsequently leading to fork stalling and genome stress and instability (Garcia-Muse and Aguilera, 2016; Mirkin and Mirkin, 2007). Furthermore, gene transcription can impede the replication fork progression by forming an R-loop that contains RNA-DNA hybrid and a single-stranded non-template strand that forms hotspots of DNA damage (Aguilera and Garcia-Muse, 2012; Mirkin and Mirkin, 2007; Santos-

Pereira and Aguilera, 2015). The RNA-DNA hybrid in an R-loop can be generated when nascent RNA transcripts reanneal to their template DNA by displacing the non-template strand into single-stranded DNA, making an R-loop a potent barrier of co-transcription and replication (Aguilera and Garcia-Muse, 2012; Huertas and Aguilera, 2003). R-loops can be stabilized by regulating DNA replication and transcription proteins and factors (Hamperl et al., 2017; Huertas and Aguilera, 2003; Li and Manley, 2005). Also, the formation of R loops can be facilitated by trinucleotide repeats, including CAG, GAA, CGG repeats that can stabilize DNA-RNA hybrid in the repeats (Grabczyk et al., 2007; Groh and Gromak, 2014; Groh et al., 2014; Reddy et al., 2011). The persistence of R-loops in the GC rich repeated sequences may facilitate somatic repeat expansion or deletion (Lin et al., 2010) by causing replication fork stalling and resulting in the progression of trinucleotide repeat expansion diseases such as Huntington's disease (HD) and Friedreich's ataxia (FRDA), respectively (Groh and Gromak, 2014; Groh et al., 2014; Lin et al., 2010; McIvor et al., 2010).

Endogenous DNA damage can also result from dNTP pool. The progression of the replication fork and fidelity of DNA replication during S phase (Bester et al., 2011; Chabosseau et al., 2011; Gay et al., 2010; Techer et al., 2016; Wilhelm et al., 2016) can be regulated by the balance of dNTPs and the size of the nucleotide pool (Anglana et al., 2003; Bester et al., 2011). dNTPs are periodically synthesized and degraded at the different phases of the cell cycle (Mathews, 2015; Nordlund and Reichard, 2006; Pontarin et al., 2008). A key step for the synthesis of dNTPs is the conversion of ribonucleotides triphosphate (NTPs) to deoxyribonucleotides (dNTPs) by ribonucleotide

reductase (RNR), the rate-limiting enzyme for the synthesis of deoxynucleotide (Mathews, 2015). Inhibition of RNR by hydroxyurea (HU) depletes dNTPs leading to replication fork stalling and genomic instability (Anglana et al., 2003; Bester et al., 2011). On the other hand, degradation/hydrolysis of dNTPs also modulates the fidelity of replication and fork progression impacting genomic stability. For example, knockdown of the dNTP triphosphohydrolase, sterile alpha motif, and HD-domain containing protein 1 (SAMHD1) in G1 phase disrupts the dNTP balance stopping the progression of the cell cycle increasing cellular susceptibility to DNA damage (Clifford et al., 2014; Franzolin et al., 2013). The level of dUTP can also impact the fidelity of DNA replication. This is because replicative DNA polymerases cannot differentiate dUTP from dTTP (Bessman et al., 1958; Chen et al., 2016). The degradation of dUTP to dUMP by dUTP pyrophosphatase (dUTPase) plays a critical role in controlling dUTP to a low level in cells to ensure the high fidelity of DNA replication. Thus, the rate of DNA replication fork progression and genomic stability is regulated by the balance of dNTPs and nucleotide pool size. Disruption of the balance between purine and pyrimidine can promote nucleotide misincorporations leading to replication fork stalling, DNA damage and genomic instability (Reijns et al., 2012).

1.2. Exogenous DNA damage

Exogenous DNA damage sources include ionizing radiation (IR), ultraviolet (UV) radiation, chemotherapeutic drugs, and environmental pollutants are the major sources of DNA damage. Ionizing radiation (IR) causes severe strand breaks and oxidized DNA bases. A low dose of IR can induce ROS that in turn

causes oxidative DNA base damage (Hashem and Sinden, 2002). IR can also directly attack DNA to create a covalent linkage between nitrogenous bases and thymine dimer (Su et al., 2010). The DNA damage generated by IR can

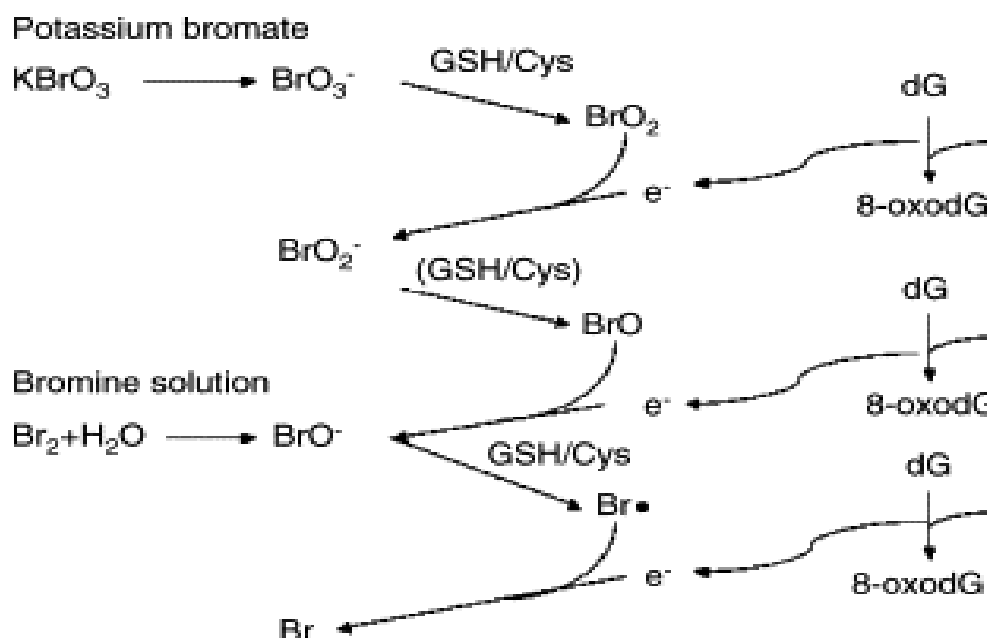


Figure 1.3. Oxidative Stress Induced by KBrO_3 (Kawanishi and Murata, 2006): Bromate, an environmental oxidative DNA damage and carcinogen generates 8-oxoG in the presence thiols such as glutathione and cysteine.

hinder DNA replication and transcription. High dose of IR generates free radicals by reacting with water and cause single-strand and double-strand DNA breaks (Acharya, 1976). UV radiation is another source of DNA damage that can induce bulky lesions, such as cyclobutane–pyrimidine dimers (CPDs) and 6–4 photoproducts (6–4PPs) thymine dimers (Fuss and Cooper, 2006). The bulky DNA lesions can distort DNA helix and block DNA replication and transcription. Chemotherapeutic drugs such as cisplatin, temozolomide, and environmental pollutants such as potassium bromate (KBrO_3), chromate, and tobacco smoke can cause interstrand cross-link (ICL), alkylating DNA damage, bulky DNA adducts, and oxidative DNA damage (Breitling et al., 2011; Hashem et al., 2004; Hashem and Sinden, 2002). KBrO_3 , an environmental DNA

damaging agent and carcinogen, was widely used in cheese making, beer malting, and food additive in the bread-making process (Ahmad et al., 2014). In 1999, bromate was prohibited as a food additive by the international agency for research on cancer (IARC) since oral administration of bromate in F344 rats can induce renal cell tumors (Kurokawa et al., 1986). However, bromate exposure still can result from drinking water disinfection, cold-wave hair lotions, and textile dyeing with sulfur dyes (Ahmad and Mahmood, 2012; Ahmad et al., 2012; Ajarem et al., 2016; Campbell, 2006; Dongmei et al., 2015; Khan et al., 2004; Kurokawa et al., 1986). Bromate exposure significantly increases the level of 8-oxo-7,8-dihydro-2'- deoxyguanine (8-oxodG) in human HL-60 cells and HP100 cells (Murata et al., 2001). It predominantly induces 8-oxodG but not DNA backbone breakage (*Figure 1.3*). Considering bromate exposure is inevitable and that it can cause mutagenic oxidative DNA damage in G-rich regions in the genome such as trinucleotide repeats and CpG islands of gene promoter regions, it is crucial to understand the impact of bromate exposure on genome and epigenome stability to tackle environmentally induced diseases such as cancer and neurodegenerative diseases.

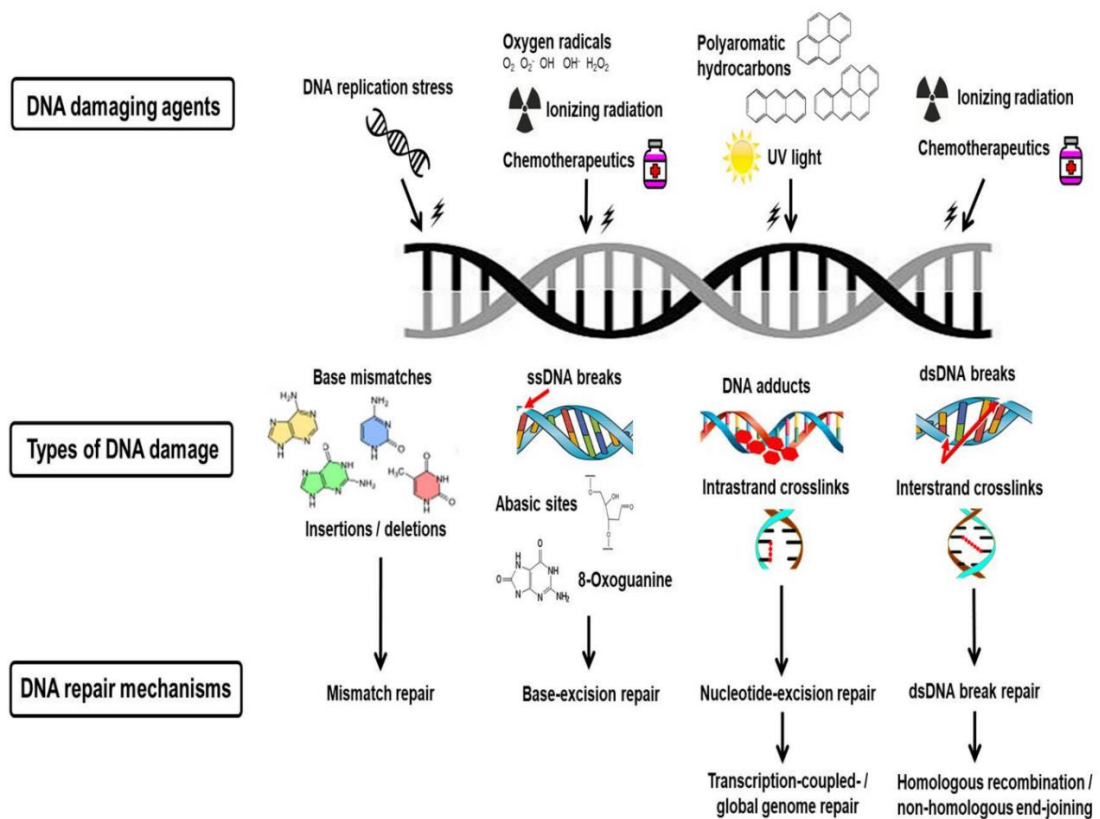


Figure 1.4. Types of DNA Damage and DNA Repair Pathways (Helena et al., 2018).

Cells are equipped with several DNA repair mechanisms to combat DNA damages generated by different DNA damaging agents in order to maintain the genome stability and faithful passage of genetic information to the next generation.

1.3. Repair and Bypass of DNA Damage

To combat the unintended adverse effects from different types of DNA damage and maintain genome stability and integrity, cells have evolved several DNA repair pathways, such as DNA base excision repair (BER), nucleotide excision repair (NER), mismatch repair (MMR), non-homologous end joining (NHEJ), and homologous recombination (HR) (Figure 1.4) (Helena et al., 2018).

Depending on the types of DNA damage, different DNA repair pathway is activated. BER primarily removes oxidized and alkylated base lesions, deaminated bases, and misincorporated nucleotides. These types of lesions are small and do not distort the helical structure of DNA, and are recognized

and removed by damage-specific DNA glycosylases followed by the incision of an abasic site generating a single-strand break that initiates BER. NER is responsible for bulky DNA adducts such as thymine dimers that distort DNA helix and impede DNA replication and transcription. The NER pathway is initiated by the distorted DNA helix and excises a fragment of DNA (25-30 nucleotides) that containing the bulky lesions creating a large gap. DNA polymerases then fill in the gap generating a nick that is ligated by DNA ligases (Hoogstraten et al., 2008). On the other hand, misincorporated/mismatched bases and small loops generated during DNA replication and repair including adenine misbasepaired with 8-oxodG are removed by the MMR pathway (Constantin et al., 2005). The Fanconi Anemia (FA) repair pathway can resolve ICLs and stalled replication forks (Rodriguez and D'Andrea, 2017). Homologous recombination (HR) and non-homologous end-joining (NHEJ) are activated due to double-strand break generated by severe single-strand breaks in both DNA strands and stalled replication fork. HR is an error-free repair pathway for dsDNA breaks that occurs in proliferating cells and relies on the presence of sister chromatids as the template for damage repair. However, NHEJ that occurs in both proliferating and non-proliferating cells is an error-prone repair for dsDNA breaks.

As part of DNA repair, cells also use DNA damage response to regulate DNA repair capacity and coordinate DNA damage repair and cell cycle progression. Cells respond to DNA damage by initiating the DNA damage response signaling pathway to arrest cell cycle (Lanz et al., 2019). The signaling pathway allows the coordination between DNA damage repair and replication fork processing. This prevents stalled replication forks, DNA damage, and strand breaks from

being passed to the next phase in the cell cycle (Patel and Weiss, 2018). The DNA damage response signaling pathway is activated by activating cell cycle checkpoints known as the DNA damage checkpoint (DDC) and DNA replication checkpoint (DRC). DDC is activated by DNA damage recognition, whereas DRC is activated by stalled replication forks (Macheret and Halazonetis, 2015; Magdalou et al., 2014; Techer et al., 2017; Zeman and Cimprich, 2014a). For the cell cycle checkpoints, G1/S and G2/M (Kastan and Bartek, 2004), the G1/S phase checkpoint plays a major role in preventing the progression of cells that carry replication stress products such as stalled fork and DNA damage (Macheret and Halazonetis, 2015; Magdalou et al., 2014; Techer et al., 2017). Thus, the checkpoint allows DNA damage to be repaired in the S phase so that DNA replication can proceed to M phase. Both checkpoints demand DNA damage generated during the G1 and G2 phases to be repaired before the cell cycle progresses (Bartek et al., 2004; Rhind and Russell, 2000, 2012). Activation of DRC is initiated by the slow progression of the replication fork along with the activation of the DNA replication checkpoints (Koundrioukoff et al., 2013). It has been shown that a decrease of replication fork progression by 5- to 10-fold can activate the ATR-mediated DNA damage response pathway. Further, it has also been found that a moderate level of replication stress induces ATR activation (Dungrawala et al., 2015). More severe replication stress induces the activation of both ATR and its downstream target pathways, such as FANC and CHK1 pathways (Dungrawala et al., 2015; Lossaint et al., 2013; Sirbu et al., 2013). Thus, cellular response to replication stress through DRC is dependent on the ATR pathway (Dominguez-Kelly et al., 2011; Koundrioukoff et al., 2013; Wilhelm et al., 2014). Through the activation of the

checkpoints, cell cycles are arrested, and DNA repair machineries are recruited to the damaged sites. Finally, DNA damage is repaired, and the stalled replication forks are resolved allowing replication and cell division to proceed (Marians, 2018). Thus, cell cycle checkpoints play a vital role in coordinating DNA damage repair and resolution of stalled replication forks with cell cycle progression (Iyer and Rhind, 2017), leading to maintenance of genome stability.

Unresolved stalled replication forks will collapse replication forks, causing severe consequences such as DNA breakage and cell death. To solve the challenging problem, DNA replication needs to be restarted. One strategy for resolving stalled replication forks in eukaryotic cells such as budding yeast on the lagging strand is to create new RNA primers downstream of DNA lesions that occur in the forks to restart DNA synthesis, a process named repriming. It has been found that the repriming mechanism is used in the lagging strand DNA synthesis as the synthesis of the Okazaki fragments is not affected by DNA damage and fork stalling as long as DNA is unwound continuously (Mezzina et al., 1988). In this process, a stalled DNA polymerase dissociates from the template strand and rebinds to the newly synthesized primer to synthesize DNA, thereby leading to the restart of stalled forks (Lopes et al., 2006). It has been found that discontinuous DNA synthesis can occur on both leading and lagging strands after UV damage in budding yeast, suggesting that the repriming mechanism is also used to resolve stalled replication fork induced by DNA damage in the leading strand (Lopes et al., 2006). Also, eukaryotic cells can use a backup replication origin, i.e., the licensed replication origin to rescue stalled replication forks (Friedberg, 2005; Wickramasinghe et al., 2015) because the reduced rate of replication fork progression can result in the

accumulation of the ssDNAs causing the uncoupling between DNA polymerase and helicase activities and large single-stranded DNA gaps (Leon-Ortiz et al., 2014b). In this scenario, the pol α -primase can be recruited to the ssDNA gaps and synthesize RNA primers to initiate DNA replication. Since the recruitment of pol α -primase depends on TopBP1, which is also involved in the activation of ATR/MEC1 pathway (Yan and Michael, 2009), this suggests that the reactivating the replication forks and the signaling pathway are coupled.

Stalled replication forks induced by DNA damage can also be broken down, resulting in genomic instability and carcinogenesis (Aguilera and Gomez-Gonzalez, 2008; Hastings et al., 2009). Eukaryotes have evolved the MEC1/ATR pathway to combat this challenge (Feng, 2017). In addition, a stalled replication fork is protected by checkpoint and homologous recombination (HR) proteins (Costanzo, 2011). Current models propose that the repair protein MRE11 expands the ssDNA gaps at a stalled replication fork behind the replisome creating the substrate for the post-replicative repair. In contrast, RAD51 is loaded onto the stalled replication fork through BRCA2 to limit the expansion of the ssDNA gaps and protect the stalled forks from being broken (Costanzo, 2011).

DNA damage that occurs on stalled replication forks must be removed by DNA repair or bypassed by DNA helicases and polymerases, allowing the restart, continuation, and completion of DNA replication. Failure of repairing DNA lesions can result in DNA strand breaks causing chromosomal rearrangement and cell death (Chun and Jin, 2010; Lehmann, 2005; Lehmann et al., 2007). To ensure cell survival and completion of replication and cell cycle, cells may adopt

lesion bypass if DNA damage at replication forks fails to be repaired (Chun and Jin, 2010). The lesion bypass mechanisms include template switching, downstream repriming, recombination, lesion bypass through translesion synthesis (TLS) DNA polymerases, and FANCDJ (Leon-Ortiz et al., 2014a; Mendoza et al., 2016; Wickramasinghe et al., 2015). However, the lesion bypass processes are usually error-prone and can result in rearrangement of chromosome and genome instability that is associated with cancer. Unrepaired DNA lesions can be bypassed by TLS carried out by Y-family DNA polymerases (Goodman and Woodgate, 2013; Lehmann, 2005; Lehmann et al., 2007; Vaisman and Woodgate, 2017b) and some of the polymerases from X- and A-family (Yang and Gao, 2018). Since replicative DNA polymerases pause at DNA lesions, they are dislodged and substituted by TLS DNA polymerases, i.e., polymerase switching. This allows the incorporation of a nucleotide opposite the lesions by TLS polymerases for lesion bypass (Lehmann et al., 2007; Macheret and Halazonetis, 2015; Zeman and Cimprich, 2014b). However, lesion bypass by TLS often results in nucleotide misincorporation and mismatches, causing mutations (Lehmann et al., 2007). For example, incorporation of dAMP opposite 8-oxoG by TLS polymerases can induce the T→C transversion mutation. Many other examples of base lesions that can be bypassed by translesion DNA polymerases are listed in *Table 1.2*. In addition, TLS polymerases can incorporate damaged dNTPs and create mismatches to bypass a base lesion. It has been shown that oxidized dGTP can be incorporated opposite to dA on the template strand by TLS inducing C→T transversion and genomic instability (Grollman and Moriya, 1993a, b; Patel and Weiss, 2018; Shibutani et al., 1991). It is well-known that in the leading strand,

DNA lesions need to be either repaired or bypassed by TLS for DNA synthesis to be continued during replication (Courcelle et al., 1999; Goodman and Woodgate, 2013; Rudolph et al., 2007). However, in the lagging strand, DNA lesions can be bypassed by TLS and repriming (Lehmann, 2005; Lehmann et al., 2007; Lopes et al., 2006). Thus, TLS polymerases play a crucial role in bypassing DNA lesions to maintain continuous DNA synthesis in the leading strand (Goodman and Woodgate, 2013). Upon the completion of DNA lesion bypass, TLS polymerases will be dislodged by replicative polymerases through polymerase switching restoring leading strand synthesis (Kannouche et al., 2004; Moldovan et al., 2007).

Table 1.2. Translesion DNA Polymerases and Their Bypass Properties DNA Base Lesions (Tsegay et al., 2019)

Proteins	DNA lesions	Properties of proteins to bypass base lesion
Pol η	Thymine dimer	Preferably dA followed dG > dT > dC (Masutani et al., 2000)
	8-oxodG	Preferably dC and dA (Haracska et al., 2000)
	Acetyl amino fluorene-dG	Preferably dC followed dG > dT > dA (Masutani et al., 2000)
	N6-ethenodeoxyadinosine	Preferably dT followed dA > dG > dC (Washington et al., 2001)

	Abasic-site	Preferably (Masutani et al., 2000)	A
Pol κ	Thymine dimers	Could not bypass(Haracska et al., 2002)	
	N6- ethenodeoxyadinosine	Preferably followed >dC>dG (Washington et al., 2001)	dT dA
	Abasic site	Preferably followed >dT>dC (Haracska et al., 2002)	dA dG
Pol ι	Thymine dimer	Preferably T and A followed by dG >dC (Johnson et al., 2000a)	
	Abasic site	Preferably dA(Johnson et al., 2000a)	

1.4. DNA damage and epigenetic stability

DNA damage can also induce epigenetic instability. Typical epigenetic instability includes hypermethylation of CpGs in the promoter of tumor suppressor genes (TSGs), and hypomethylation of oncogenes and non-promoter repetitive elements and satellite DNA. The former causes transcriptional inactivation of TSGs, while the latter induces abnormal activation of oncogenes and mobile genetic elements and chromosomal instability. It has

been found that a high level of ROS can lead to aberrant DNA hypermethylation in the gene promoter of TSGs and their silencing suggesting an association between oxidative DNA damage with cancer-associated DNA methylation pattern changes. For example, hydrogen peroxide causes hypermethylation of the promoter of the E-cadherin gene via snail-induced recruitment of histone deacetylase 1 (HDAC1) and DNA methyltransferase 1 (DNMT1) (Lim et al., 2008) in hepatocellular carcinoma (HCC) cells. Further, oxidative DNA damage can inactivate TSGs through the recruitment of the polycomb repressive complex, which includes DNMT1, histone deacetylase (sirtuin-1), and histone methyltransferase to the CpGs containing 8-oxodGs (O'Hagan et al., 2011). It is possible that in responding to oxidative DNA damage, cells may use DNA hypermethylation to create heterochromatin in the genes such as TSG. This may shield DNA and protect them from further attack by DNA damaging agents. Interestingly, oxidative DNA damage can also result in DNA demethylation by inhibiting the binding of methyl-CpG binding protein 2 (MBP2) to methyl-CpGs, an epigenetic regulator that recruits DNMTs and histone HDAC to DNA (Valinluck et al., 2004). This is because 8-oxodGs next to the 5mC at the CpGs inhibits the substrate binding of MBP (Turk et al., 1995; Weitzman et al., 1994). Furthermore, the oxidized 5-methylcytosine, hydroxyl-5-methyl-cytosine can also decrease the binding affinity of MBPs resulting in DNA hypomethylation (Donkena et al., 2010). Thus, oxidative DNA damage can cause passive DNA demethylation, which in turn result in epigenetic instability leading to cancer and other diseases. Since double-helical DNA is wrapped around histone octamers that consist of H2A, H2B, H3, and H4 histone proteins, respectively (Kornberg and Lorch, 1999), histone modifications that govern the structures of chromatin,

i.e., open (euchromatin) and closed (heterochromatin) conformation (Li and Reinberg, 2011; Luger and Hansen, 2005; Zhou et al., 2011) play an important role in shielding DNA during cellular responses to DNA damage. It has been proposed that the formation of heterochromatin induced by genome stress, such as replication fork stalling stops DNA replication (Figure 1.5) and prevents genomic instability. Since histone tails are subject to different types of posttranslational modifications for the regulation of chromatin structures,

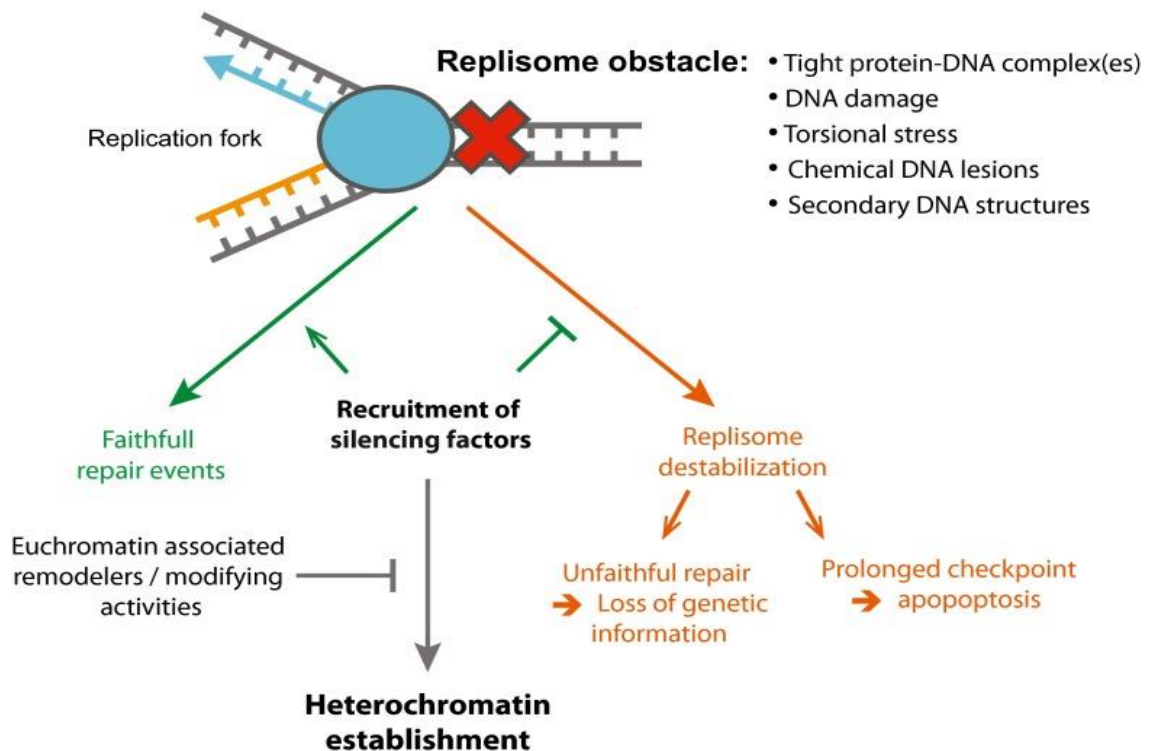


Figure 1.5. Heterochromatin Formation During Replication Stress to Prevent Loss of Genetic Information (Nikolov and Taddei, 2016). DNA replication is stopped by heterochromatin formation to prevent unfaithful DNA repair and loss of genetic information induced by replisome obstacles.

upon transcriptional activation or repression or chromatin opening or closing (Bannister and Kouzarides, 2011), specific histone modifications have also been identified as the response to replication stress (Jasencakova and Groth, 2010). The unscheduled firing of origin, fork stalling, and repair of the collapsed fork can result in dramatic changes in chromatin structures. The methylation of newly synthesized histone proteins can be altered as a result of replication stress. This can alter the arrangement of old and newly synthesized histone proteins, restoration of chromatin and patterning of epigenetic marks. It has been found that when the replication fork is stalled by genome stress, histones along with antisilencing factor 1 (Asf1) fail to be incorporated into chromatin, thereby increasing the level of H3K9me1 (Jasencakova et al., 2010). Subsequently, methylation of H3K9 prevents histone acetylation. H3K9me1 can also be further methylated into H3K9me3, the suppressive mark. These can then lead to the suppression of replication (Bernstein et al., 2005; Jasencakova and Groth, 2010; Jasencakova et al., 2010; Loyola et al., 2006; Loyola et al., 2009; Singh et al., 2009; Wang et al., 2008). Further, histone methylation can recruit endonucleases to degrade the stalled replication fork. It has been found that methylation of H3K4 triggers MRE11-mediated degradation of the replication fork, whereas H3K27me3 recruits MUS81 to cleave stalled forks (Chaudhuri et al., 2016; Rondinelli et al., 2017). The results indicate cells adopt the epigenetic mechanisms to resolve replication forks stalling induced by DNA damage.

2. The DNA Base Excision Repair Pathway

Oxidized DNA bases are the most common lesions. More than 100 types of oxidized bases are known to exist in the DNA (Iyama and Wilson, 2013; Neeley

and Essigmann, 2006). These base lesions are repaired by BER. BER also repairs alkylated, deaminated, depurinated bases, and single-strand breaks. BER enzymes coordinate in a sequential way to accomplish the repair. The pathway is initiated by the removal of a damaged base by lesion-specific DNA glycosylases followed by the 5'-incision of an abasic site. DNA glycosylases recognize the lesion and cleave the N-glycosidic bond by flipping the damaged base out of helical duplex DNA (Fromme et al., 2004). In mammalian cells, eleven DNA glycosylases are identified to recognize and cleave specific damaged DNA bases (Brooks et al., 2013; Wallace, 2014). 8-oxoG DNA glycosylase 1 (OGG1), 3-alkyladenine DNA glycosylase, thymine DNA glycosylase (TDG), and uracil DNA glycosylase (UDG) are the ones that recognize and cleave 8-oxoG, 3meA, G-T mismatch, and U, respectively. The DNA glycosylases can be further classified into two groups based on whether they possess both glycosylases activity and AP lyase activity or glycosylases activity alone. The glycosylases with glycosylases activity alone are known as monofunctional DNA glycosylases. These enzymes can only remove the damaged base to

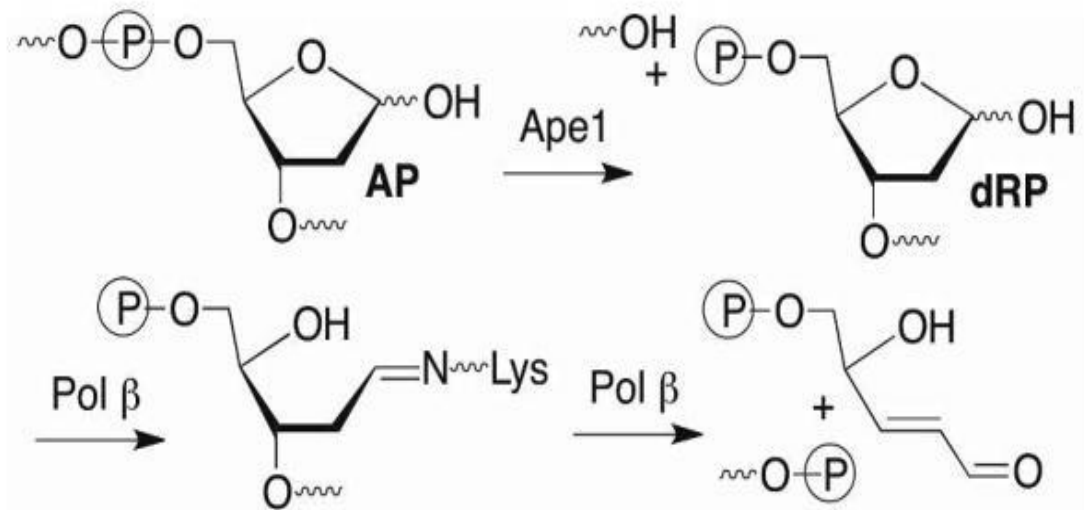


Figure 2.1. The dRP lyase mechanism of pol β . Pol β dRP lyase activity removes a native sugar from the 5'-end of the abasic side to create a 1 nt gap intermediate.

create an abasic site. Bifunctional DNA glycosylases have both glycosylases and AP lyases activity and therefore, they can make a cleavage at AP sites and create a single-strand break. However, the AP lyase activity is much weaker than the glycosylase activity. Thus, AP sites are predominantly incised by APE1 at the 5'-side resulting in a 1 nt gap with 5'-deoxyribose phosphate (dRP) group (Masuda et al., 1998; Wilson et al., 1995) for further BER enzymatic processing (Li and Wilson, 2014). The dRP residue is directly removed by pol β dRP lyase activity. Pol β then fills in the gap using its polymerase activity and generates a nick that is ligated by a DNA ligase completing the repair (*Figure 2.1*). Depending on the number of nucleotides synthesized during repair and cofactors involved, BER is divided into two subpathways (Biade et al., 1998; Fortini et al., 1998; Frosina et al., 1996; Klungland and Lindahl, 1997; Liu and Wilson, 2012). A native sugar is removed by pol β dRP lyase activity leaving 1 nt-gap that is subsequently filled in by the polymerase generating a nick, which

is sealed by DNA ligases. In this scenario, only one nucleotide is synthesized during base lesion repair. This subpathway is called short patch BER (SP-BER) or single-nucleotide BER (SN-BER) (*Figure 2.2*). A modified sugar such as oxidized or reduced sugar that is resistant to pol β dRP lyase activity has to be removed through the long-patch BER (LP-BER) subpathway, where two or more nucleotides are synthesized by pol β generating a 5'-sugar containing flap (*Figure 2.2*). The LP-BER is further classified into pol β /FEN1-mediated LP-BER ("Hit and Run," 2-nucleotide patch) and strand-displacement-mediated LP-BER (3 or more-nucleotide patch) (*Figure 2.2*) (Liu and Wilson, 2012). The removal of the 5'-dRP group during SP-BER is accomplished by β -elimination through the formation of a Schiff base (Beard and Wilson, 2006). The resulted 1 nt gap is filled by pol β gap-filling synthesis creating a nick that is ligated by LIG I or LIG III-XRCC1 completing damage repair (Wilson and Kunkel, 2000). The LP-BER is used to remove an oxidized or reduced sugar, as stated above (Liu and Wilson, 2012). The removal of the modified sugars relies on a flap's cleavage with the 5'-sugar phosphate by FEN1 (*Figure 2.2*), a member of the 5'-end/exonuclease superfamily that plays a crucial role in DNA replication by removing the Okazaki fragments during lagging strand maturation. In the pol β /FEN1-mediated subpathway of BER, pol β fills in the gap creating a short flap with the 5'-dRP group cleaved by FEN1 (*Figure 2.2*). FEN1 cleavage results in another 1 nt gap. Pol β synthesis activity fills in the gap creating a nick that is ligated by DNA ligases (Liu et al., 2005). In the case of strand-displacement-mediated LP-BER, pol β , pol ϵ , and pol δ displace the downstream strand

creating a long flap that will be cleaved by FEN1 at

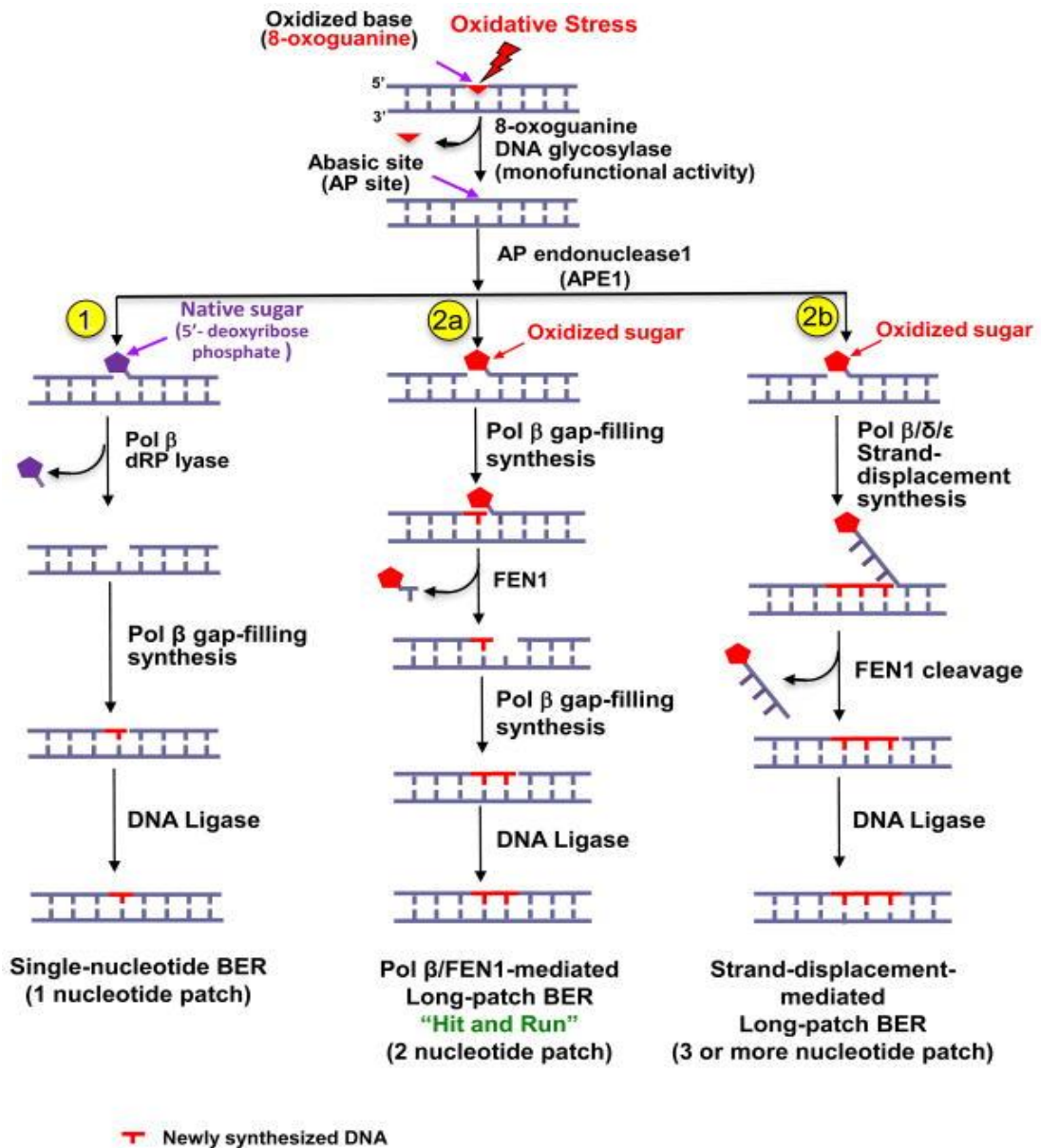


Figure 2.2. Base excision repair pathway.

BER repairs oxidative base lesions through two subways. DNA glycosylases incise 5'-side of the damaged creating a single strand break. SP-BER removes the 5'-dRP group that contains a native sugar. LP-BER removes a modified sugar through the coordination between pol β and FEN1.

the junction of the bottom of the flap (*Figure 2.2*) (Liu and Wilson, 2012). FEN1 cleavage creates a nick that DNA ligases will seal to complete the repair. In this scenario 3 or more nucleotides are inserted (*Figure 2.2*) (Liu and Wilson, 2012). The LP-BER is accomplished by sequential coordination of the BER

enzymes, known as the “passing the baton” mechanism (Wilson and Kunkel, 2000). The SP-BER subpathway appears to be more efficient than LP-BER and is the major subpathway that repairs DNA base lesions. However, in certain DNA sequences, such as repeated DNA sequences, the LP-BER is forced to proceed. This is because DNA slippage results in multinucleotide gap-filling synthesis by pol β (Liu et al., 2009). BER may also shift from SP-BER to LP-BER if the repair is stalled at the excision step following the removal of the lesion. In this scenario, the coordination between the BER enzymes and cofactors is required for effective lesion repair.

Efficient BER is essential to ensure that DNA base lesions are removed effectively to prevent the accumulation of DNA damage and development of diseases such as cancer, aging, neurodegenerative diseases, among others. Efficient BER is mediated by the coordination between BER core enzymes and cofactors (Dianov and Hubscher, 2013; Liu et al., 2007; Liu and Wilson, 2012). For instance, APE1 can stimulate pol β polymerase activity and dRP lyase activity (Bennett et al., 1997; Wong and Demple, 2004). APE1 can also stimulate OGG1 activity by dislodging the enzyme from the AP site after the damaged base is removed, thereby increasing OGG1 turnover (Hill et al., 2001). APE1 also stimulates FEN1 and LIG I catalytic activity during LP-BER (Ranalli et al., 2002). It is believed that the disordered regions of BER enzymes mediate their interaction and coordination (Wallace, 2014). On the other hand, FEN1 can stimulate pol β DNA synthesis during LP-BER by interacting with the BER cofactor PARP1 that also serves as nick surveillance protein (Prasad et al., 2000; Prasad et al., 2001). The results demonstrate the coordination between the core BER enzymes and BER cofactors. PARP1 can also serve as

a flag for the recruitment of LP-BER proteins if the SP-BER is stalled at the excision step (Prasad et al., 2001). Other BER cofactors such as PCNA stimulate BER by serving as a scaffolding protein for all the BER core enzymes (Kedar et al., 2002; Levin et al., 2000; Liu and Wilson, 2012; Tom et al., 2000). XRCC1 promotes LIG III by interacting with pol β and the ligase physically (Cappelli et al., 1997; Dianova et al., 2004; Nash et al., 1997). Another BER cofactor, HMGB1, can stimulate pol β synthesis and FEN1 enzymatic activities during LP-BER (Liu and Wilson, 2012; Prasad et al., 2007).

BER may be impaired due to the deficiency of the repair proteins resulted from the mutations or downregulation of the proteins by epigenetic effects such as overexpression of miRNAs. Upregulation of miRNAs that target DNA repair proteins can downregulate the level of the repair proteins and cause insufficiency of BER capacity. On the other hand, BER may cause adverse effects by inducing mutations and single-strand break intermediates during repair and lesion bypass of oxidized lesions such as 8-oxoG, cyclo-deoxy purines (cPus). In addition, DNA polymerases can also incorporate and misincorporate the damaged bases from the nucleotide pool to induce DNA base damage through BER.

3. Cyclo-deoxypurines (cdPus) and Their Impact on RNA and DNA Metabolism

cPus are the smallest tandem purine oxidative base lesions that exist as 5',8-cyclo-2'-deoxyadenosine (cdA) and 5',8-cyclo-2'-deoxyguanosine (cdG). The lesions are present in the genome in S and R diastereomeric forms for both A (S/R-cdA) and G (S/R-cdG) (*Figure 3.1*). The lesions are generated by the

abstraction of the hydrogen from the 5th carbon

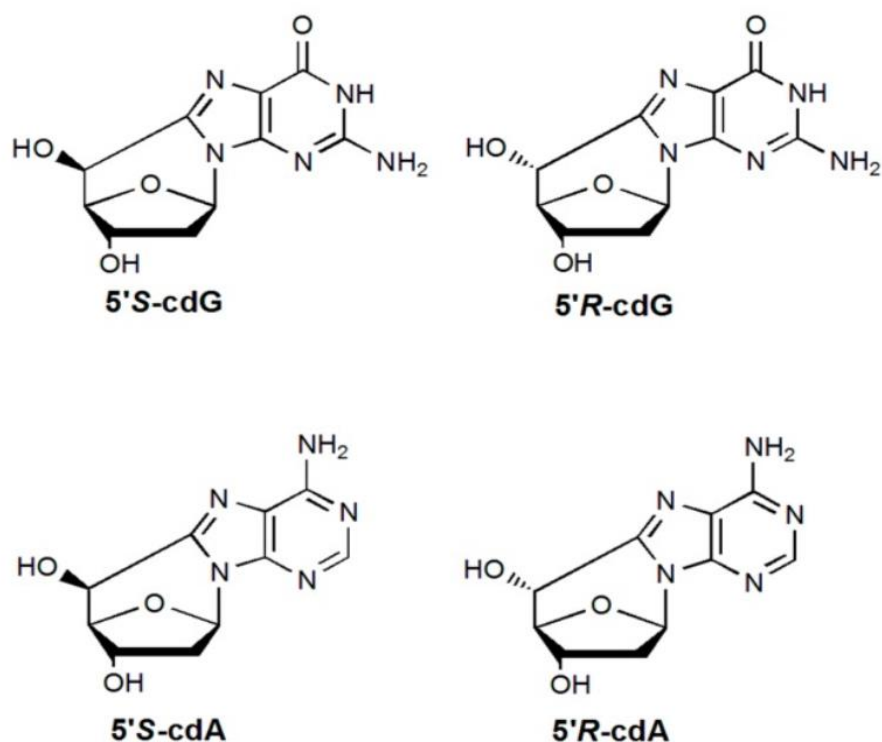


Figure 3.1 The Diastereomeric Cyclo-Deoxy Purine Lesions (cdPu). Cyclo-deoxyadenosine and guanosine in two diastereomeric forms are generated by hydroxyl radicals. cdPus contain an additional covalent bond between the 5th carbon of the deoxyribose and the 8th carbon of the purine bases.

of the 2-deoxyribose moiety by the HO radical followed by intramolecular cyclization of the C5 of the carbon and C8 of the base resulting in additional covalent bond between the base and the sugar. cdPus can inhibit DNA and RNA polymerases causing mutations, DNA strand breaks, and termination of DNA replication and gene transcription. Unlike other oxidized DNA base lesions, cyclodeoxypurine (cdPu) lesions cannot be repaired by the DNA base excision repair pathway (Brooks et al., 2000; Kropachev et al., 2014; Kuraoka et al., 2000). This results in the accumulation of the lesions in the genomic DNA and distorts the DNA backbone initiating the nucleotide excision repair (NER) pathway (Brooks et al., 2000; Kropachev et al., 2014; Kuraoka et al., 2000).

However, NER repairs cdPu lesions at low efficiency compared to its repair of other bulky DNA lesions (Brooks et al., 2000; Kropachev et al., 2014; Kuraoka et al., 2000), thereby resulting in the accumulation of cdPu lesions in DNA. When DNA and RNA polymerases encounter the lesions during DNA replication and repair and gene transcription, they have to bypass the lesions to complete the biological processes (*Figure 3.2*). Studies have shown that repair DNA polymerases such as pol β and translesion DNA polymerases pol η and ι , and ζ can bypass cyloxyadenosine (cdA) (Kuraoka et al., 2001; Xu et al., 2014; You et al., 2013a). Also, cdA lesions can be bypassed by an RNA polymerase (Brooks et al., 2000; Walmacq et al., 2015). A study from the Kuraoka group found that *E. Coli* DNA polymerase I (pol I) can incorporate 5'R and 5'S isomers of cdA (Kamakura et al., 2012b).

The Kuraoka group has found that *E. Coli* pol I large protein fragment, the Klenow fragment, which lacks 5'-3' exonuclease (Klenow and Henningsen, 1970), can incorporate 5'R and 5'S stereoisomers of cdATP at a different efficiency (Kamakura et al., 2012b). The incorporation of a 5'RcdATP and 5'ScdATP to basepair with a dTMP by the pol I fragment is about 17000-fold and 750-fold less efficient than that of dATP. The rate of the incorporation of a 5'ScdATP and 5'RcdATP opposite to dTMP by the Klenow fragment is $25.6 \mu\text{M}^{-1} \text{min}^{-1}$ and $1.13 \mu\text{M}^{-1} \text{min}^{-1}$, respectively. The extension of a cdA by the pol I fragment is only slightly inhibited by the two isomers of cdA, although 5'ScdATP is more readily incorporated and extended by the Klenow fragment (Kamakura et al., 2012b). Pol I Klenow fragment incorporates a 5'ScdATP more efficiently than a 5'RcdATP. This is because the active site of the Klenow fragment binds to 5'R and 5'ScdPu with a different affinity due to the

stereospecific difference between the two isomers (Kamakura et al., 2012b). By superimposing 5'R and 5'ScdATP on the incoming dATP, the interaction between the Klenow fragment and the

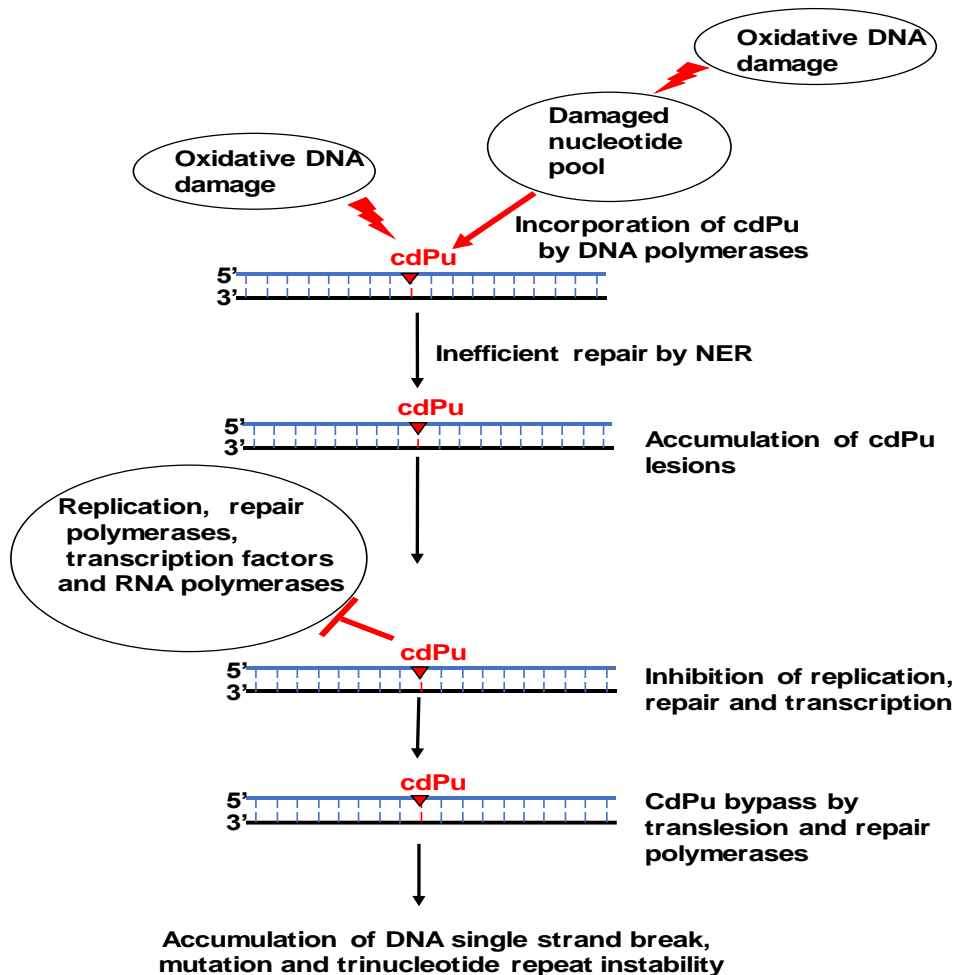


Figure 3.2. Mechanisms of cdPu accumulation and their impact on DNA and RNA metabolism. Accumulation of cdPus Disrupts DNA Replication, Repair and Gene Transcription Leading to Lesion Bypass, Mutations and Genome Instability.

cdA lesions is revealed (Kamakura et al., 2012b). It is found that the 5'-phosphate group of the 5'RcdA is turned away from the active site of the polymerase. In contrast, the 5'-phosphate of the 5'ScdA turns toward the active site (Kamakura et al., 2012b). Thus, compared to 5'ScdATP, the 5'RcdATP can barely form a hydrogen bond with dTMP through the transition from an opened

to a closed conformation in the active site of the polymerase. This results in low efficiency of its incorporation. Interestingly, both stereoisomers of cdATP can also be incorporated by the polymerase to basepair with dCMP. Moreover, 5'RcdATP preferentially base pairs with dCMP rather than dTMP suggesting that 5'RcdATP is more error-prone than 5'ScdATP.

A cdA lesion can also inhibit the binding of TATA box binding protein (TBP) (Marietta et al., 2002) and RNA polymerase II to the CMV promoter that regulates the luciferase reporter gene (Brooks et al., 2000), resulting in reduced synthesis of RNA that further decreases the luciferase report gene expression (Brooks et al., 2000; Marietta et al., 2002; Walmacq et al., 2015). It has been shown that XP cells with NER deficiency transfected with plasmids containing a single 5'ScdA lesion located at the second "A" in the TATA box of the CMV promoter exhibit a reduced luciferase gene expression by 75% (Marietta et al., 2002). In a study that has also tested the effects of a 5'ScdA on the transcriptional activity of RNA polymerase II, XP cells were transfected with a plasmid carrying a single 5'ScdA lesion in the transcribed region of the luciferase reporter gene. The results show that XP cells transfected with plasmids containing the lesion still exhibit 20-30% of the luciferase activity in the XP cells with the plasmids without a lesion (Brooks et al., 2000). This indicates that a 5'ScdA does not entirely abolish the activity of RNA polymerase II, further suggesting that RNA polymerase can partially bypass a 5'ScdA in the template, and the bypass of a cdA by RNA pol II can result in full-length transcribed products. It has been found that yeast RNA pol II bypasses a cdA by preferentially incorporating UTP that base pairs with a cdA although it also misincorporates rA, rG, and rC to base pair with the lesion with low efficiency

(Walmacq et al., 2015). In the presence of ATP alone, yeast RNA pol II can efficiently incorporate it to base pair with a cdA but with a much lower rate than its incorporation of UTP. To continue to extend the nucleotide that basepair with a cdA, RNA pol II can incorporate an rA opposite a dA next to the lesion (Walmacq et al., 2015). Besides, a transcription initiation/elongation factor TFIIIF can stimulate the activity of RNA pol II of bypassing a cdA lesion without affecting its fidelity indicating that the cis and trans factors can also affect the efficiency of the bypass of a cdPu lesion by RNA pol II (Walmacq et al., 2015).

A cdPu lesion can alter the activity of DNA polymerases. It has been reported that the DNA synthesis activities of calf thymus replicative DNA polymerase, pol δ , and bacterial phage DNA polymerase, T7 DNA polymerase are entirely inhibited by 5' RcdA and 5' ScdA lesions resulting in replication fork stalling (Kuraoka et al., 2000). The primer extension activity of calf thymus pol δ is abolished at a 5'R- or 5'ScdA lesion site in the template strand, whereas T7 DNA polymerase can manage to extend the primer at the cdPu lesions (Kuraoka et al., 2000). This indicates that the DNA synthesis of the pol δ ceases before the cdPu lesions while T7 DNA polymerase can bypass 5'S and 5'RcdA by incorporating additional nucleotide. T7 DNA polymerase bypasses a 5'RcdA more efficiently than a 5'ScdA. The results indicate that cdPu lesions can lead to DNA replication stall by inhibiting the activities of replication DNA polymerases further suggesting that the lesions have to be bypassed by translesion DNA synthesis in cells to resolve the stalled replication fork and restart DNA replication.

The Basu group has further identified a translesion DNA polymerase that can bypass a cdPu lesion in *E. Coli*. They demonstrate that cdPus, 5'ScdA, and 5'ScdG strongly block *E. coli* replicative and repair DNA polymerases including pol II, Klenow fragment, pol IV, pol V, and Dpo4 (Jasti et al., 2011; Pednekar et al., 2014). Through the gene knockout of pol II, pol IV, and pol V in the SOS-induced or uninduced *E. coli* strains, the group has found that pol V is the one that is responsible for bypassing a cdPu, 5'ScdA or 5'ScdG inserted in a plasmid through translesion DNA synthesis in *E. coli*. In contrast, pol II and pol IV do not play a role in bypassing the lesions (Jasti et al., 2011; Pednekar et al., 2014). This is further supported by the results showing that the *E. Coli* strain with pol V deficiency that bears the plasmids containing a 5'ScdA or 5'ScdG cannot survive (Jasti et al., 2011; Pednekar et al., 2014). This demonstrates that pol V is required for the bypass of 5'ScdA and 5'ScdG in *E. Coli*. However, *in vitro* biochemical characterization has shown that *E. Coli* Klenow fragment, pol IV, and Dpo4 can incorporate nucleotides to base-pair with 5'ScdA or 5'ScdG (Pednekar et al., 2014). Specifically, the Klenow fragment preferentially incorporates dTTP and dCTG to basepair with 5'ScdA and 5'scdG, respectively (Pednekar et al., 2014). On the other hand, pol IV incorporates dTTP and dCTP to basepair with 5'ScdA and dCTP with 5'ScdG. Dpo4 can insert dTTP and dGTP to basepair with 5'scdA. However, it preferentially inserts dTTP over dCTP to basepair 5'ScdG (Pednekar et al., 2014). This may be due to a more opened and less rigid active site in Dpo4 polymerase that can tolerate distorted and bulky DNA lesions. These results indicate that Klenow fragment, pol IV, and Dpo4 may also play an important role in bypassing the cdPu lesions in *E. Coli*. The results further indicate that pol IV and Dpo4 are more error-prone

than the Klenow fragment by performing nucleotide misincorporation to bypass a cdPu lesion.

In eukaryotic cells, cdPu lesions can also be readily bypassed by several human and yeast translesion DNA polymerases, pol η , pol ι , and pol ζ , but not pol κ . These DNA polymerases can incorporate different nucleotides to basepair with a 5'ScdA and 5'ScdG (You et al., 2013b). For example, pol ι can incorporate dTTP, dGTP, dATP to basepair with 5'ScdA, whereas it incorporates dCTG, dATP, dGTP to basepair with 5'ScdG (You et al., 2013b). In contrast, human pol η usually incorporates a correct nucleotide to basepair with 5'ScdA or 5'ScdG (Swanson et al., 2012b), whereas yeast pol η can also misincorporate dTTP opposite to 5'ScdG (Swanson et al., 2012b). Among these DNA polymerases, pol η and pol ζ can extend the nucleotides incorporated opposite a 5'ScdPu lesion (Swanson et al., 2012b; You et al., 2013b). Human pol η can only extend a matched nucleotide that basepairs with a cdPu lesion. However, yeast pol η can extend both matched and mismatched nucleotides that basepair with the lesions (Swanson et al., 2012b). It is proposed that human pol η and pol ι , and pol ζ cooperate to bypass cdPu lesions during DNA replication and repair. Cell-based mutation analysis has further demonstrated that the bypass of cdPu lesions through these translesion DNA polymerases results in a wide spectrum of mutations indicating the misincorporation of nucleotides through a bypass of cdPu lesions in cells (You et al., 2013b).

A recent study from the Yang group has further revealed the molecular basis underlying the bypass of a 5'ScdA by human pol η using the cocrystals of pol η and the DNA substrates containing a 5'ScdA lesion (Weng et al., 2018b). The

crystal structures indicate that the C8-C5' covalent bond of cdA distorts the backbone of the DNA template by shifting the sugar toward the minor groove. This further results in the change of the width of duplex DNA and pushes the adenine of the cdA to be tilted toward the 3'-direction leading to the disruption of the base stacking between the damaged nucleotide and the adjacent base. The structural study further reveals that ~ 60% of adenines from the damaged nucleotide are shifted into the major groove, thereby preventing the formation of hydrogen bond between the damaged nucleotide and dTTP. In addition, the presence of a different type of metal ions can also alter the configuration of the active site, either facilitate the incorporation of dTTP opposite to cdA or preventing the formation of the hydrogen bonds between cdA and dTTP. The effect is also mediated through the opening of the finger domain of pol η to accommodate the DNA backbone distortion. Since cdA is shifted to the major groove, this protects it from forming the hydrogen bonds with dT at the 3'-end. Instead, this allows cdA to make only van der Waals interaction with the dT preventing the formation of a new base pair of the incoming nucleotide and primer extension. Thus, as a result, pol η fails to extend the dT opposite cdA lesion. The study provides novel insights into the structural basis underlying the nucleotide incorporation by pol η in bypassing a cdA lesion (Weng et al., 2018b).

Similar to the Y family translesion DNA polymerases, pol β , a central component of DNA BER (Beard and Wilson, 2006, 2014), can also bypass a cdA lesion (Jiang et al., 2015b). Pol β can readily bypass both 5'RcdA and 5'ScdA located in the substrates mimicking DNA replication and BER intermediates (Jiang et al., 2015b). It has been shown that pol β wild-type

mouse embryonic fibroblast (MEF) cell extracts can generate a significant amount of DNA synthesis products resulting from the bypass of a 5'RcdA and 5'ScdA lesion located in an open template, DNA substrate containing a 1 nt-gap or 1 nt-gap with a sugar-phosphate residue (Jiang et al., 2015b). However, pol β knockout MEF cell extracts generate only a tiny amount of the lesion bypass products on all the substrates (Jiang et al., 2015b). The results suggest that pol β also plays an essential role in bypassing a cdPu lesion during DNA replication and repair in mammalian cells. Further biochemical analysis has shown that pol β mainly incorporates a dT to basepair with a 5'RcdA, but can also misincorporate dA, dG, and dC to basepair with the damaged nucleotide at low efficiency. Pol β only inserts a dT opposite a 5'ScdA lesion. Moreover, the polymerase can readily extend the dT opposite a 5'RcdA but fails to extend the dT opposite a 5'ScdA (Jiang et al., 2015b) indicating that pol β stalls at a 5'ScdA following its incorporation of a dT. This further inhibits the ligation of the nick by DNA ligase I (LIG I), allowing FEN1 to cleave nucleotides resulting in the accumulation of gaps and single-strand DNA break intermediates (Jiang et al., 2015b). Thus, pol β bypass of a 5'RcdA can lead to nucleotide misincorporation, causing mutations. In contrast, its bypass of a 5'ScdA can cause the accumulation of DNA strand break intermediates that in turn results in recombination and genome instability (Jiang et al., 2015b).

Interestingly, although pol β stalls at a 5'ScdA that is located in the random sequences (Jiang et al., 2015b), it can efficiently extend a dT opposite to a 5'ScdA located in trinucleotide repeats such as CAG repeats. This further results in CTG repeat deletion through BER (Xu et al., 2014). It has been found that this is because both 5'R and 5'S isomers of cdA located on the template

strand induce the formation of a CAG repeat loop in the template the substrates that mimic the intermediates formed during maturation of lagging strand and BER (Xu et al., 2014). This is likely due to the distortion of the backbone of the repeats, which subsequently induces the G:C self-base pair in the CAG repeats. Since pol β preferentially skip over a hairpin or loop structure (Lai et al., 2016; Xu et al., 2013), the loop structure in CAG repeats induced by a cdA lesion can also be readily bypassed by pol β , thereby leading to the displacement of the downstream repeat strand into a flap during DNA lagging strand maturation and BER (Xu et al., 2014). Subsequently, the flap is captured and cleaved efficiently by FEN1, resulting in CTG repeat deletion (*Figure 3.3*). This is further supported by the fact that the locations of a gap relative to that of a cdA lesion in the CAG repeat template can govern the deletion of CTG repeats. A gap that is located at the upstream or opposite the lesion can result in

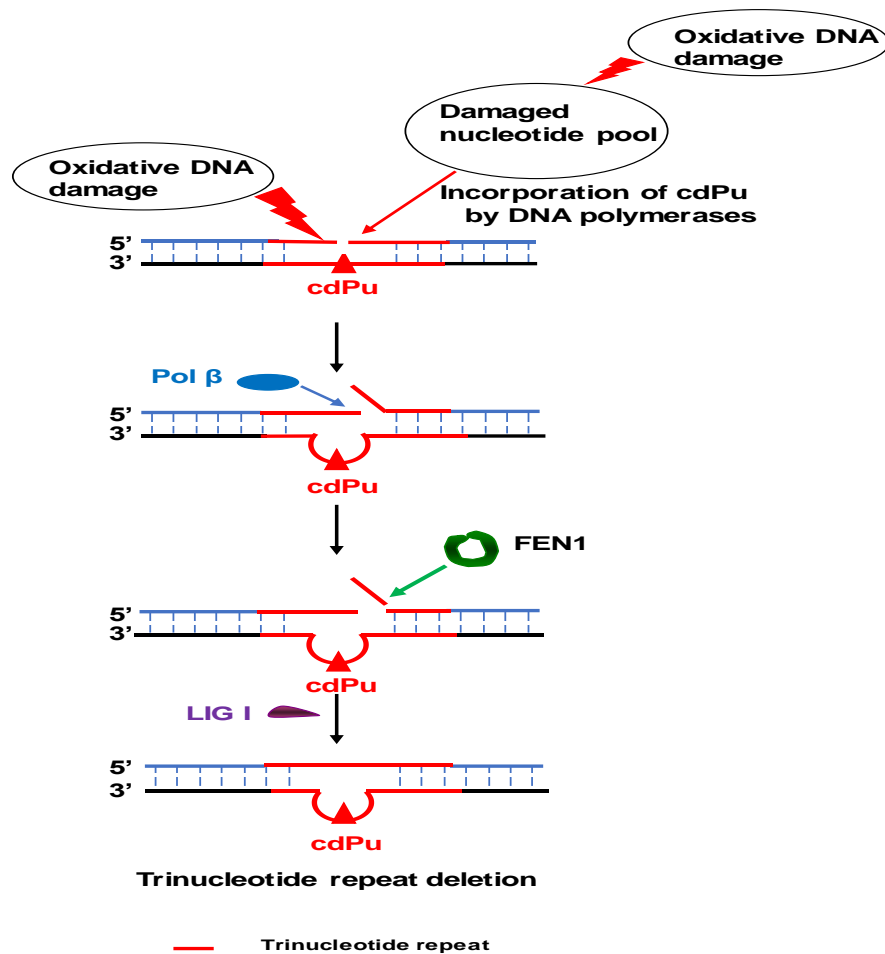


Figure 3.3. A cdA Located at DNA Repeat Sequences Induces Repeat Instability Through Pol β Bypass of a Loop Structure. cdA in CAG repeats induces the formation of a repeat-containing loop leading to repeat deletion via BER.

CTG repeat deletion through the pol β bypass of a CAG repeat loop structure. However, a gap located downstream of the cdA that does not involve pol β loop bypass fails to cause repeat deletion (Xu et al., 2014). These findings further demonstrate the essential role of pol β bypass of a loop structure containing a cdPu lesion in mediating trinucleotide repeat deletion.

Although a study provides mechanistic insight into incorporating cdATP by the Klenow fragment using superimposing modeling, crystallography-based structural studies on the Klenow fragment and other replication and repair

polymerases and translesion DNA polymerases, especially eukaryotic DNA polymerases, are needed to understand the molecular mechanisms underlying cdPu incorporation in DNA. Because DNA replication and repair polymerases often coordinate with their cofactors during DNA replication and repair, the effects of the coordination on the bypass of a cdPu lesion and their impact on cellular function remain to be elucidated. Moreover, the impact of cdPu lesions on the instability of repeated DNA sequences including mono-, di-, tri-, tetra-, and hexanucleotide repeats through DNA replication and repair and the crosstalk among different DNA metabolic pathways and the underlying mechanisms need to be explored.

4. RNA-Templated/Guided DNA Repair

The central dogma of genetics is DNA replicates to preserve its genetic information. The information of DNA is transcribed into mRNA, and the message from mRNA is translated into protein (Crick, 1970; Crick, 1958). However, RNA transcripts synthesized from DNA have sequence homology with the non-template DNA strand. Thus, it is conceivable that cells could potentially utilize the sequence homology of RNA transcripts to guide the repair of DNA damage in the template strand in case of a shortage of homologous DNA sequences and the formation of a DNA-RNA hybrid. RNA can act as a template for DNA synthesis in the reverse transcription of retroviruses and retrotransposons (Baltimore, 1985) and telomeres' elongation (Autexier and Lue, 2006; Blackburn, 1992). It has also been found that DNA polymerase γ (pol γ) can perform DNA synthesis using an RNA template to exhibit reverse transcriptase activity (Gallo et al., 1970; Murakami et al., 2003b; Robert-Guroff

and Gallo, 1977). In budding yeast *Saccharomyces cerevisiae*, RNA can indirectly mediate DNA recombination through a cDNA intermediate (Derr and Strathern, 1993; Nevo-Caspi and Kupiec, 1997), and RNA transcripts can mediate the precise repair of its source DNA (Keskin et al., 2016). Yeast pol δ and pol α can also synthesize DNA across RNA template (Storici et al., 2007). In mammals, the long interspersed elements (LINE1) retrotransposons can prime retrotranscription from 3'-end breaks of DNA to repair DNA (Morrish et al., 2002). Moreover, DNA damage-induced long non-coding RNAs (dilncRNAs) and small DNA damage response RNAs (DDRNs) are present at DSB sites to promote double-strand break DNA repair (DSBR) (Francia et al., 2012; Michelini et al., 2017). It is proposed that dilncRNAs are produced to form DNA-RNA hybrids at DSBs leading to the recruitment of BRCA1, BRCA2, RAD51, and MRE11 to the locations of DSB (D'Alessandro et al., 2018; Francia et al., 2016; Lu et al., 2018; Ohle et al., 2016). In addition, it has been found that the N⁶-methyladenosine (m6A) in RNA induced by UV can recruit pol κ to facilitate nucleotide excision repair and translesion synthesis-mediated SSB repair (Xiang et al., 2017). A recent study also demonstrated that RAD51 and BRCA1 are recruited to the site of DNA damage by METTL3-m6A-YTHDC1 axis to mediate homologous recombination (HR)-mediated repair (Zhang et al., 2020). Most recently, it is found that the human pol θ exhibits reverse transcriptase activity to mediate non-homologous end joining during repair of double-strand break (DSB) repair (Chandramouly et al., 2021). Also, it has been shown that DNA repair proteins are recruited to the R-loops containing DNA:RNA hybrid (Wang et al., 2018a). All these findings suggest that RNA can serve as a template for DNA repair. The roles of DNA repair proteins in

mediating DNA repair in the context of DNA:RNA hybrid and the molecular mechanism how DNA polymerases repair DNA using RNA as a template needs to be explored for understanding of the crosstalk between DNA and RNA in mediating DNA repair.

5. DNA Damage and Modulation of miRNA Expression

MicroRNAs (miRNAs) are short non-coding RNAs that play a major role in posttranscriptional gene regulation through RNA-mediated gene silencing. They are transcribed by RNA polymerase II and processed by DROSHA and DICER, the RNase III ribonucleases, to generate mature miRNA that can be loaded into Argonaut (AGO) protein. This results in an RNA-induced silencing complex (RISC) (Figure 5.1). miRNAs are made up of 18-22 nucleotides in length and can bind to the 3'-untranslated regions of the target mRNAs, thereby causing gene silencing either by causing mRNA

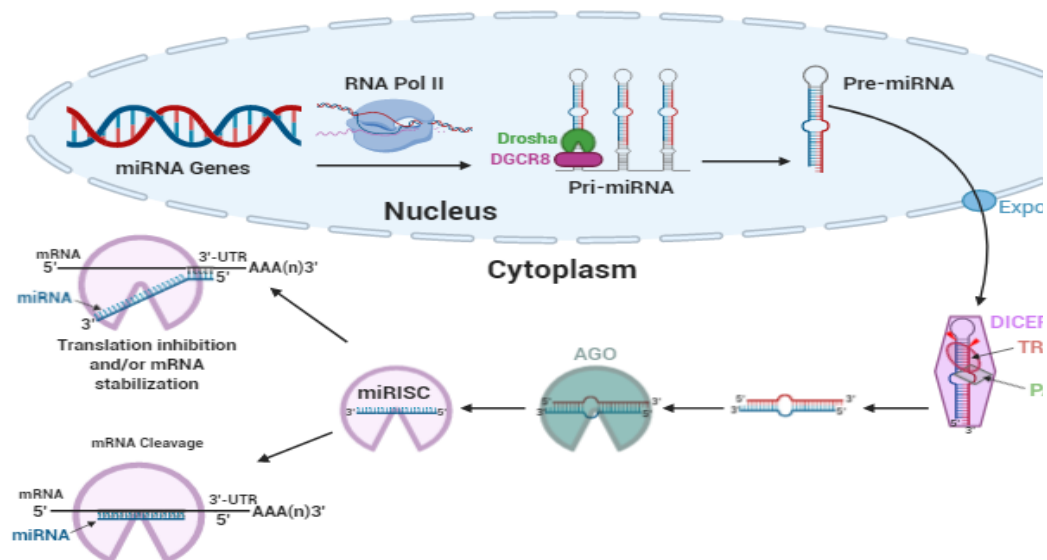


Figure 5.1. miRNA Biogenesis. RNA polymerase II transcribes miRNA from their respective genes. Drosha processes the primary miRNA transcript (Pri-miRNA) within the nucleus to generate pre-miRNA. Pre-miRNA leaves the nucleus via exporting-5 and is subject to Dicer processing to mature miRNA that will be uploaded to AGO to induce RISC.

cleavage when there is perfect complementarity or translation inhibition when there is imperfect complementarity with their target mRNA (*Figure 5.1*) (Bartel, 2004b). miRNAs are involved in several biological processes. It has been found that deregulation of miRNA expression is associated with cancer and neurodegenerative diseases (Carthew and Sontheimer, 2009; Wang and Taniguchi, 2013). Several classes of miRNAs are associated with the regulation of the genes of replication progression, cell cycle, and DNA damage repair (*Figure 5.2*). Usually, miRNAs are deregulated by DNA damage (Bai et al., 2016; He et al., 2016; Wang and Taniguchi, 2013; Zhang et al., 2011). The expression of miRNA in response to DNA damage is thought to be cell-type specific as the alteration of miRNA in different normal cell lines responded IR treatment differently (Wang and Taniguchi, 2013). This is further supported by the fact that tumor cell lines treated with IR exhibit DNA damage response by altering a different set of miRNAs (Wang and Taniguchi, 2013), although some miRNAs are common to specific cell lines. Cells also respond differently to various DNA damaging agents, such as IR, H₂O₂, etoposide, and 5-flourouracile by altering a unique set of miRNA, although they share some miRNAs (Wang and Taniguchi, 2013). It has been found that the miRNAs involved in cell cycle control can be upregulated by E2F (Bueno et al., 2010). miRNAs that are deregulated by DNA damage include miR-34a, -34b, and -34c. These mRNAs belong to the miR-34 family and are upregulated in response to DNA damage. They are also the regulators of the expression of the checkpoint genes, such as E2F, CDK4, CDK6, and cyclin E2 (Huang et al., 2011; Wang and Taniguchi, 2013). In addition, miR-145a and miR-146b that

target the tumor suppressor, BRCA1, are also upregulated upon double-strand DNA breaks (Garcia et al., 2011; Wang and Taniguchi, 2013). miR-155 and miR-21 that target mismatch repair proteins are upregulated in normal human fibroblasts during cellular responses to oxidative DNA damage induced by hydrogen peroxide and radiation (Valeri et al., 2010; Wang and Taniguchi, 2013). miR-155 is decreased in THP-1 human monocytic cell line treated with polystyrene and ARS labeled Titanium dioxide nanoparticles (Hu and Palic, 2020). These results support the notion that miRNAs are cell-specific and respond differently to different DNA damaging agents. On the other hand, miR-16 and mir-15 a/b

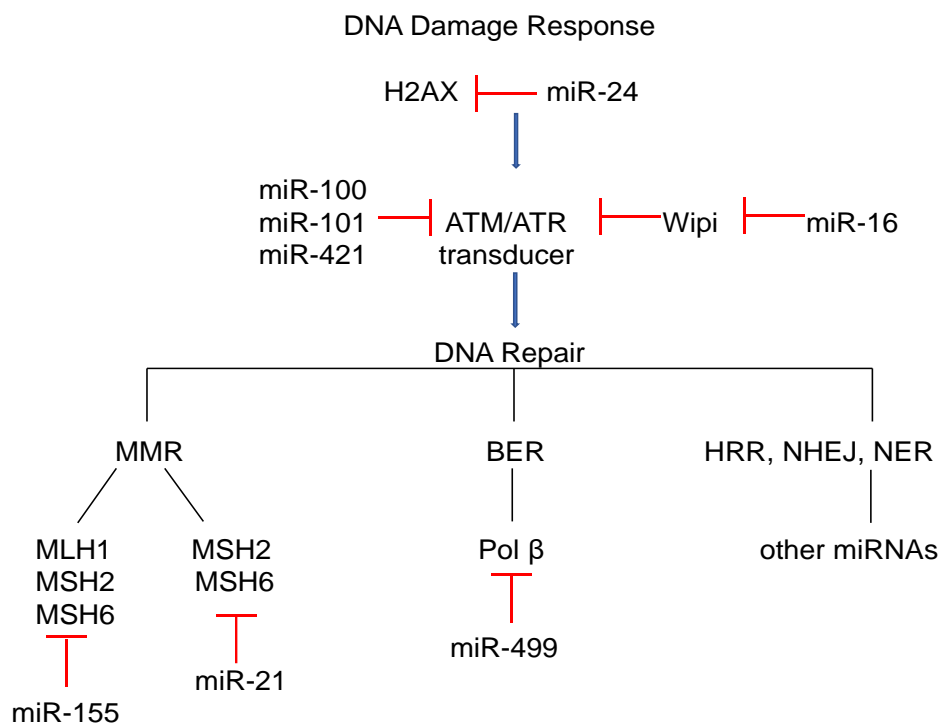


Figure 5.2. miRNAs associated with DNA damage and response.

Several classes of miRNAs are associated with DNA damage and DNA damage response proteins. Depending on which protein they target, miRNAs can negatively or positively influence DNA damage and response.

that target the down regulators of checkpoint proteins, Cdc25a and Wip1, are also upregulated upon DNA damage. The Let-7 family miRNAs, *let-7i*, *mir-15b-16-2*, and *mir-106b-25*, can also be induced by E2F. The miRNAs in this family are involved in limiting S phase entry as a result of genome stress, thereby preventing mutagenesis (Bueno et al., 2010). Also, miRNAs can downregulate MCM2-7 in a *Trp53*-dependent manner (Bai et al., 2016). Thus, overexpression of miRNA that targets DNA repair enzymes can potentially impair DNA repair by downregulating the repair enzymes. The molecular mechanism DNA damage alters miRNA expression and crosstalk among oxidative DNA damage, DNA repair pathways and the miRNAs associated with the DNA repair proteins needs to be explored to develop miRNA-mediated effective treatment for diseases, such as cancer and neurodegenerative diseases and to discover miRNA biomarkers of DNA damage and diseases that facilitate early detection of complications.

OVERVIEW

Endogenous and exogenous DNA damaging agents constantly attack the Mammalian genome. More than 10,000 base lesions are generated per cell per day. Oxidative base lesions are generated by oxidative stress and are among the most frequently produced DNA damage that occurs in the mammalian genome. Majority of oxidative base lesions are efficiently repaired by the BER pathway. However, a bulky oxidized DNA base, 5',8-cyclopurine-2'-deoxynucleosides (cdPus) with an additional covalent bond between the 5th

carbon of deoxyribose and 8th carbon, fail to be repaired by BER and can only be repaired by NER with low efficiency. Consequently, this leads to the accumulation of the lesions in the genome. cdPu lesions may also be introduced by incorporation of cdPu triphosphate generated by oxidation of the nucleotide pool. However, it remains elusive whether DNA polymerases can play a role in the accumulation of the lesions by incorporating the lesions from oxidized nucleotide pool during DNA replication and repair. More studies have shown that cells can utilize their RNA to perform RNA-template/guided DNA synthesis to facilitate DNA strand break repair. Yet, it remains to be elucidated how RNA-templated/guided DNA synthesis by human DNA polymerases can mediate DNA repair. Interestingly, it has been shown that oxidative DNA damage can upregulate miRNAs that are associated with DNA repair. However, the molecular mechanism underlying the upregulation of the miRNAs induced by oxidative DNA damage remains to be elucidated. To address the knowledge gaps, in this dissertation, I have explored the role of DNA polymerases in accumulating damaged bases in the genome, the role of RNA-templated/guided DNA base lesion repair and the underlying molecular mechanism for the modulation of miRNAs associated with DNA repair proteins in response to oxidative DNA damage. In **Chapter I**, I examined the incorporation of cdAs by human DNA repair polymerases, pol β , and pol η during BER determined the efficiency of cdA incorporation using steady-state kinetics. I found that pol β and pol η incorporated cdAs opposite dT and misincorporated opposite dC. The incorporated cdAs were readily extended and ligated into duplex DNA. Molecular docking analysis showed that the 5',8-covalent bond in cdA disrupted its hydrogen bonding with a template base.

Chapter II explored the molecular mechanisms of RNA-templated/guided DNA synthesis by repair DNA polymerases and their roles in repairing a DNA base lesion. The results showed that pol β , pol κ , and pol λ only inserted one nucleotide at the 1 nt-gapped with an RNA template. In contrast, the translesion DNA polymerases, pol η , pol ν , and pol θ performed efficient RNA-templated/guided DNA synthesis with both 1 nt-gapped and open template intermediates. In **Chapter III**, I explored the molecular mechanism underlying the oxidative DNA damage-induced upregulation of miR-499-5p that targets pol β . The results showed that oxidative DNA damage resulting from KBrO_3 upregulated the miRNA in an OGG1-dependent manner. The results further demonstrated that the upregulation of miR-499-5p downregulated pol β expression. These results indicate that oxidative DNA damage deregulates the levels of miRNAs to alter the expression of DNA repair proteins. This may further result in the accumulation of DNA damage leading to carcinogenesis.

1. CHAPTER I. INCORPORATION OF 5',8-CYCLO-2'DEOXYADENOSINES BY DNA REPAIR POLYMERASES VIA BASE EXCISION REPAIR

1.1. ABSTRACT

5',8-cyclo-2-deoxy nucleosides (cPus) are the smallest tandem purine lesions including 5',8-cyclo-2'-deoxyadenosine (cdA) and 5',8-cyclo-2'-deoxyguanosine (cdG). They can inhibit DNA and RNA polymerases, causing mutations, DNA strand breaks, and DNA replication, and gene transcription termination. cPus can be removed by nucleotide excision repair with low efficiency allowing them to accumulate in the genome. Recent studies suggest that cPus can be induced in damaged nucleotide pools and incorporated into the genome by DNA polymerases. However, it remains unknown if and how DNA polymerases can incorporate cPus. In this study, we examined the incorporation of cdAs by human DNA repair polymerases, DNA polymerases β (pol β), and pol η during base excision repair. We then determined the efficiency of cdA incorporation by the polymerases using steady-state kinetics. We found that pol β and pol η incorporated cdAs opposite dT and dC with low efficiency, and incorporated cdAs were readily extended and ligated into duplex DNA. Using molecular docking analysis, we found that the 5',8-covalent bond in cdA disrupted its hydrogen bonding with a template base suggesting that the phosphodiester bond between the 3'-terminus nucleotide and the α -phosphate of cdATP were generated in the absence of hydrogen bonding. The enzyme kinetics analysis further suggests that pol β and pol η increased their substrate binding to facilitate the enzyme catalysis for cdA incorporation. Our study

reveals unique mechanisms underlying the accumulation of cPu lesions in the genome resulting from nucleotide incorporation by repair DNA polymerases.

1.2. INTRODUCTION

The human genome is constantly damaged by endogenous and exogenous agents (Lindahl, 1993). Among them, reactive oxygen species (ROS) are the most common form of DNA damaging agents that can result in various oxidized DNA base lesions (Cadet et al., 1999; Dizdaroglu, 1992). These include 5', 8-cyclo-2'-deoxyadenosine (cdA) and 5', 8-cyclo-2'-deoxyguanosine (cdG), which are referred to as 5', 8-cyclopurines (cPus) (Brooks, 2008; Chatgililoglu et al., 2007; Jaruga and Dizdaroglu, 2008; Wang, 2008). cdA and cdG contain a covalent bond between C5' of the 2'-deoxyribose and C8 of adenine and guanine (Chatgililoglu et al., 2007) that adopts 5'-R or 5'-S diastereoisomer. The additional covalent bond between the sugar backbone and base of cPus can distort DNA structure (Cadet et al., 2003; Chatgililoglu et al., 2011; Dizdaroglu, 1992) and prevent the base excision repair (BER) enzyme, DNA glycosylases, from removing the lesions (Brooks et al., 2000; Das et al., 2012). A significant amount of cPu lesions are detected in the mammalian genome. The lesions are stable compared with other oxidatively generated DNA adducts and cannot be artificially produced during DNA isolation (Chatgililoglu et al., 2011; Dizdaroglu et al., 2001; Jaruga and Dizdaroglu, 2008).

Unlike other oxidized DNA base lesions repaired by BER, cPu lesions are repaired by nucleotide excision repair (NER) (Brooks et al., 2000; Kropachev et al., 2014; Kuraoka et al., 2000). However, NER repairs cdPu lesions two to four-fold less efficiently than other types of bulky DNA adducts (Kropachev et

-strand breaks (Jiang et al., 2015a). On the other hand, RNA polymerase II and pol β can also cause multi-nucleotide deletion and repeat deletion to bypass cdAs during transcription and BER (Walmacq et al., 2015; Xu et al., 2014). Thus, the accumulation of cPu lesions in the human genome can result in mutations and genome instability associated with pathological conditions, including aging, inflammation, carcinogenesis, and neurodegeneration (Brooks, 2008; Jaruga and Dizdaroglu, 2008; Kirkali et al., 2009; Wang et al., 2012; Wang et al., 2011).

Endogenous and exogenous ROS can damage DNA bases in the genome and the nucleotide pool (Kamiya and Kasai, 1995; Rai, 2010). It is implicated that the nucleotide pool is more susceptible to ROS than the genomic DNA. Previous studies have shown that ROS induces more 8-oxoGTP and 2-hydroxy adenosine triphosphate than 8-oxoG and oxidized adenosine generated in the genomic DNA (Kamiya and Kasai, 1995; Kasai and Nishimura, 1984; Rai, 2010). This further suggests a possibility that DNA polymerases may incorporate oxidized nucleotides triphosphate to create DNA damage during DNA replication and repair. It has been found that DNA polymerases incorporate an 8-oxoG to basepair with A and C efficiently (Macpherson et al., 2005). The incorporated damaged nucleotide can be further extended, allowing the damaged base to be integrated into the genomic DNA (Macpherson et al., 2005; Whitaker et al., 2017). The findings indicate that DNA polymerases can compromise genome integrity by incorporating incorrect and/or damaged nucleotides such as 8-oxoG from the damaged nucleotide pool. Since cPus can

also be generated in the nucleotide pool, we hypothesized that human DNA polymerases can incorporate cPu triphosphate into DNA during DNA repair. To test our hypothesis, we examined the incorporation of cdA triphosphate by human repair DNA polymerases during BER and determined the catalytic efficiency of cdA incorporation using steady-state kinetics. For the first time, we found that human repair DNA polymerases incorporated cdATP into duplex DNA. We showed that pol β and translesion DNA polymerase, pol η , incorporated 5'-RcdA and 5'-ScdA to basepair with dT. However, both polymerases also misincorporated cdA to basepair with dC more efficiently than with dT, suggesting that the incorporation of cdAs by repair DNA polymerases can introduce cPu lesions in genomic DNA while it preferentially causes mutations. Using molecular docking analysis, we demonstrated that in the active sites of pol β and pol η , cdA exhibited a distorted configuration that disrupted its hydrogen bonding with template bases. The results suggest that the phosphodiester bond between cdA and the 3'-terminus nucleotide of the primer was created by the nucleophilic attack from the 3'-hydroxy group to the α -phosphate of cdATP in the absence of the hydrogen bonds. The enzyme kinetics analysis suggests that the repair DNA polymerases managed to increase the catalysis for cdA incorporation by improving their substrate binding. The results further revealed the structural and functional basis underlying the incorporation of cdA by repair DNA polymerases and the mutagenic effects resulting from cdA incorporation.

1.3. MATERIALS AND METHODS

1.3.1. Materials

5'R- and *5'S*-diastereoisomers of 5', 8-cyclo-2'-deoxyadenosine and their triphosphates were synthesized and purified by DEAE-Sephadex and reverse-phase HPLC according to the procedures described previously (Chatgialloglu et al., 2019). Oligonucleotides were synthesized by Integrated DNA Technologies (IDT, Coralville, IA, USA). Radionucleotide, ³²P-ATP (6000 μCi/mmol), was purchased from PerkinElmer Inc (Boston, MA, USA). Micro Bio-Spin 6 chromatography columns were from Bio-Rad (Hercules, CA, USA). Human pol β and DNA ligase I (LIG I) were purified as described previously (Beaver et al., 2015). Human Pol η (polymerase domain) was provided by Dr. Wei Yang at National Institute of Diabetes and Digestive and Kidney Diseases (NIDDK)/National Institutes of Health (NIH) (Weng et al., 2018b). All other standard chemical reagents were from Sigma–Aldrich (St. Louis, MO, USA) and Thermo Fisher Scientific (Pittsburgh, PA, USA).

1.3.2. Oligonucleotide Substrates

Oligonucleotide substrates containing a 1 nt-gap were designed to mimic the 1 nt-gap intermediates formed during BER for testing the incorporation of cdAs and extension of the incorporated cdAs by DNA polymerases. The substrates were constructed by annealing the upstream primer (22 nt) without or with a cdA at the 3'-terminus and the downstream primer (23 nt) containing either a 5'-phosphate or 5'-phosphorylated tetrahydrofuran (THF) residue, an analog of

deoxyribose phosphate (dRP) with the 46 nt template strand containing a dT or dC located at the 23rd or 24th nucleotide counted

Table 1.1. Oligonucleotides sequence

Oligonucleotides	nt	Sequence (5'-3')
<u>Upstream Strand</u>		
U1	22	GTCCTAATAAGGACTTAGATTG
U2	23	GTCCTAATAAGGACTTAGATTGA
U3	23	GTCCTAATAAGGACTTAGATTGG
U4	23	GTCCTAATAAGGACTTAGATTGX
<u>Downstream strands</u>		
D1	23	pGAAAGACCGCCCCCTCTGAGAAG
D2	23	pFGAAAGACCGCCCCCTCTGAGAAG
<u>Template Strands</u>		
T1	46	CTTCTCAGAGGGGGCGGTCTTTCTCAATCTAAGTCCTTATTAGGAC
T2	46	CTTCTCAGAGGGGGCGGTCTTTCCAATCTAAGTCCTTATTAGGAC

^aThe nucleotide opposite to the one nt gap is in boldface. X, 5'RcdA or 5'ScdA. F, tetrahydrofuran.

from the 3'-end. The molar ratio of the upstream primer, downstream primer, and the template is 1:2:2. The substrates were radiolabeled at the 5'-end of the upstream primer. To construct the substrates for testing the extension and ligation of incorporated cdAs, the upstream primer with a cdA at the 3'-terminus was generated by incubating 100 nM 1 nt-gap substrate containing a THF or phosphate at the 5'-end of the downstream primer with 50 nM pol β or pol η in the presence of 200 μ M cdA in BER buffer containing 50 mM Tris-HCl, pH 7.5, 50 mM KCl, 0.1 mM EDTA, 0.1 mg/ml bovine serum albumin, and 0.01% Nonidet P-40 at 37°C for 30 min. The upstream primer was then subject to gel purification using 15% urea-denaturing polyacrylamide gel electrophoresis. The purified upstream primer with a 3' terminus cdA was annealed to the

downstream primer and the template strand at a molar ratio of 1:2:2, creating a nicked substrate.

1.3.3. Enzymatic Activity Assays

The incorporation of cdAs by the DNA polymerases with the 1 nt-gap substrate was measured by incubating 25 nM substrates with increasing concentrations of DNA polymerases in the presence of 200 μ M cdA or a fixed concentration of the DNA polymerases in the presence of increasing concentrations of cdA. The enzymes were incubated with the substrate at 37 °C for 30 minutes in 10 μ l reaction mixture containing 50 mM Tris-HCl, pH 7.5, 50 mM KCl, 0.1 mM EDTA, 0.1 mg/ml bovine serum albumin, and 0.01% Nonidet P-40. To test if an incorporated cdA can be further extended by DNA polymerases leading to a ligation product, the upstream primer with a 3'-terminus cdA at the substrate was then incubated with various concentrations of DNA polymerases at 37°C for 30 min in BER buffer containing 50 mM Tris-HCl, pH 7.5, 50 mM KCl, 5 mM Mg^{2+} , 0.1 mM EDTA, 0.1 mg/ml bovine serum albumin, and 0.01% Nonidet P-40. To further examine if an incorporated cdA can be ligated at a nick by LIG I during BER, we incubated the nicked substrate containing a 3'-terminus cdA with increasing concentrations of LIG I in BER buffer containing 5 mM Mg^{2+} and 1 mM ATP at 37 °C for 30 minutes. Substrates and products were separated by 15% urea-denaturing polyacrylamide gel and detected by a phosphorimager. All experiments were repeated at least three times.

1.3.4. Steady-State Kinetics of Incorporation and Extension of cdAs by pol β and pol η

The steady-state kinetics of the incorporation and extension of cdA opposite dT and dC by pol β and pol η were determined using various concentrations of 1 nt-gapped substrates ranging from 5 nM to 50 with a fixed concentration of pol β or pol η in the presence of 200 μ M cdA for its incorporation, and 50 μ M dG for cdA extension. The cdA incorporation and extension products at different time intervals from 0 to 10 or 15 min were determined and quantified, and the velocity of the polymerases at various substrate concentrations was obtained. The velocity and substrate concentrations were then analyzed using the enzyme kinetics module of Prism-GraphPad, version 6.03. The Michaelis-Menten constants, K_m , V_{max} , and k_{cat} values were obtained.

1.3.5. Molecular Docking of cdA in the Crystal Structures of pol β and pol η

Protein structures were obtained from the protein data bank. The X-ray crystal structures of the pol β (PDB ID 5TBB) and pol η (PDB ID 4J9N) were chosen for the molecular docking analysis because of their high resolution (Reed et al., 2017; Zhao et al., 2013). In addition, since pol β structure (PDB ID 5TBB) illustrates the interaction of the enzyme with a 1nt-gap substrate, it can be used as a platform for molecular simulation of the incorporation of cdA with the 1 nt-gap substrate in our study. For the dT template of pol β structure, the 6th base was replaced with dT. Autodock vina (Trott and Olson, 2010) was used to dock the 5'R-cdA and 5'S-cdA to the pol β and pol η . The structures were rendered using PyMol 2.1 (L).

1.4. RESULTS

1.4.1. cdA can be Incorporated into DNA by pol β and pol η

The repair polymerases, pol β , and translesion polymerases such as pol η play an essential role in mediating DNA lesion bypass (Crespan et al., 2013; Vaisman and Woodgate, 2017a) during DNA replication and repair. Pol β can also incorporate an 8-oxoG to DNA during BER (Caglayan et al., 2017). On the other hand, replication DNA polymerases have high fidelity of DNA synthesis and possess the 3'-5' exonuclease activity for its proofreading. We reason that pol β and translesion DNA polymerases can incorporate a cdA into DNA through their gap-filling synthesis during BER. To test this, we initially determined if DNA polymerases can incorporate cdAs by examining the incorporation of 5'R- and 5'-ScdA in the presence of increasing concentrations of pol β , pol η , pol θ , pol ν , and the replication polymerase, pol δ with the 1 nt-gap substrate without or with a 5'-phosphorylated THF. We found that pol β and pol η incorporated a comparable amount of cdAs with the substrate. However, pol ν , and Pol δ failed to incorporate cdAs. Thus, we further characterized the cdA incorporation by pol β and pol η on the 1 nt-gap substrate with or without a dRP that is represented by THF. The substrates represent the 1 nt gap intermediates formed before and after the dRP group is removed by pol β dRP lyase activity during BER. They were employed to test if the dRP group can affect the efficiency of cdA incorporation. We initially examined the incorporation of a 5'R- or 5'S-cdA by pol β on the 1-nt gap substrates containing a template dT with a 5'-phosphate or 5'-phosphorylated THF residue in the downstream primer (*Figure 1.2*). The results showed that increasing

concentrations of pol β (10 nM-100 nM) incorporated 5'S-cdA and 5'R-cdA (200 μ M) to fill in the 1 nt gap on the substrates with low efficiency (*Figure 1.2A lanes 2-5, 7-10, 12-15, 17-20*). Pol β incorporated more cdA on the substrate containing a THF than the one without a THF (*Figure 1.2A, compare lanes 2-5, 7-10 with lanes 12-15, 17-20*). Pol β exhibited poor incorporation of 5'S-cdA on the gapped substrates generating only up to 5% and 1% incorporation product on the substrate with or without THF (*Figure 1.2A, compare lanes 2-5 with lanes 7-10*). The incorporation of 5'R-cdA by high concentrations of pol β also generated a small amount of a 2 nt insertion product on the substrates (*Figure 1.2A, lanes 9-10 and 19-20*), indicating that pol β extended 5'R-cdA leading to the incorporation of the nucleotide that was base paired with the template dC. To determine if the concentration of cdA may also affect the efficiency of its incorporation, we examined cdA incorporation by pol β (50 nM) on the substrates in the presence of increasing concentrations of cdA (*Figure 1.2B*). The results showed that increasing concentrations of 5'S-cdA and 5'R-cdA (50 μ M-500 μ M) significantly stimulated the pol β incorporation of the nucleotides on the 1 nt-gapped THF substrate (*Figure 1.2B, lanes 2-5 and lanes 7-10*). On the 1 nt-gapped substrate, increasing concentrations of cdA enhanced the pol β incorporation of 5'R-cdA (*Figure 1.2B, lanes 17-20*) but not the incorporation of 5'S-cdA (*Figure 1.2B, lanes 12-15*). In addition, at high concentrations of 5'R-cdA, pol β extended an inserted cdA to generate a cdA:C mismatch (*Figure 1.2B, lanes 10, 18-20*). The results indicate that pol β incorporated 5'R-cdA more efficiently than it inserted 5'S-cdA. The results also indicate that the 5'-sugar-phosphate significantly stimulated pol β

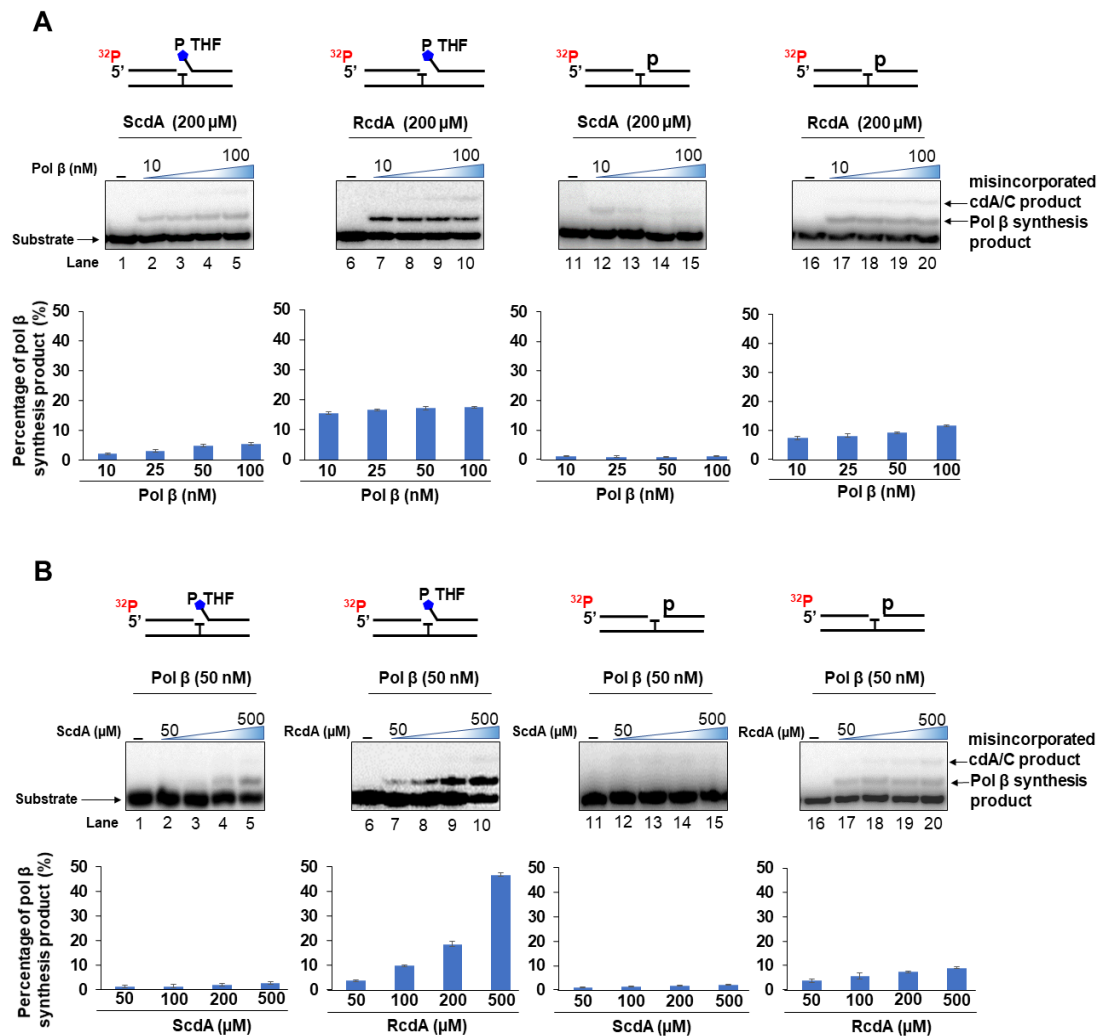


Figure 1.2. The incorporation of cdA by pol β during BER.

(A) The incorporation of cdA by pol β was determined in the presence of increasing concentrations of pol β (10, 25, 50, and 100 nM). Lanes 2-6 show the incorporation of 5'S-cdA by pol β 1 nt-gap substrate containing a tetrahydrofuran (THF) residue in the downstream primer. Lanes 8-12 illustrate the incorporation of 5'R-cdA by pol β with the substrate containing a THF residue at the downstream strand. Lanes 14-18 represent the incorporation of 5'S-cdA by pol β with the substrate having a phosphate at the 5'-end of the downstream primer. Lanes 20-24 indicate the incorporation of 5'R-cdA by pol β with the substrate containing a phosphate at the 5'-end of the downstream primer. (B) The incorporation of cdA by pol β in the presence of increasing concentrations of cdA (50, 100, 200, and 500 μ M). Lanes 2-6 represent the incorporation of 5'S-cdA by pol β with the 1 nt-gap substrate containing a THF residue in the downstream primer. Lanes 8-12 indicate the incorporation of 5'R-cdA by pol β with the substrate having a THF residue in the downstream primer. Lanes 14-18 illustrate the incorporation of 5'R-cdA by pol β with the substrate containing a phosphate at the 5'-end of the downstream primer. Lanes 20-24 represents the incorporation of 5'R-cdA by pol β with the substrate containing a phosphate at the 5'-end of the downstream primer. Lane 1, 7, 13, and 19 represents substrate alone. All experiments were done at least in triplicate. The quantification of the results is shown

below the gels. The percentage of the products is illustrated as average \pm SD in the bar charts.

incorporation of cdA (Figure 1.2A and Figure 1.2B, compare lanes 2-5 with lanes 12-15 and lanes 7-10 with lanes 17-20). We then examined if pol η can also incorporate cdA to fill the 1 nt gap. We found that increasing concentrations of pol η (1 nM-50 nM) generated a significant amount of 1 nt insertion product from 5'R-cdA and 5'S-cdA on the substrates with or without a THF (Figure 1.3A, lanes 2-6, 8-12, 14-18, and 20-24). Moreover, we found that high concentrations of pol η inserted multiple cdA to misbasepair with the template nucleotides on the 1 nt-gapped substrates (Figure 1.3A, lanes 5-6, 11-12, 17-18, and 23-24). The results indicate that pol η extended an inserted cdA and continued to incorporate cdA to misbasepair with the template nucleotides. Similarly, increasing concentrations of 5'R-cdA and 5'S-cdA significantly stimulated the insertion of the damaged nucleotides in the presence of 20 nM pol η (Figure 1.3B, lanes 2-6, 8-12, 14-18, and 20-24). High concentrations of 5'S-cdA and 5'R-cdA also resulted in the extension of an inserted cdA and nucleotide misinsertion by pol η (Figure 1.3B, lanes 5-6, 11-12, 17-18, and 24). Interestingly, pol η did not show a significant difference in its incorporation of cdA on the substrate with or without THF (Figure 1.3A and 3B, compare lanes 2-6, 8-12 with lanes 14-18, lanes 20-24), indicating that the translesion DNA polymerase did not exhibit a preference for the 5'-sugar phosphate group. The results suggest that pol η accommodated cdA lesions more efficiently in its active site than pol β , thereby facilitating the efficient incorporation of the damaged nucleotide. The results are also consistent with previous studies showing that pol η can readily bypass cdA lesions (Chatgililoglu et al., 2019; Swanson et al., 2012a; You et al., 2013a)

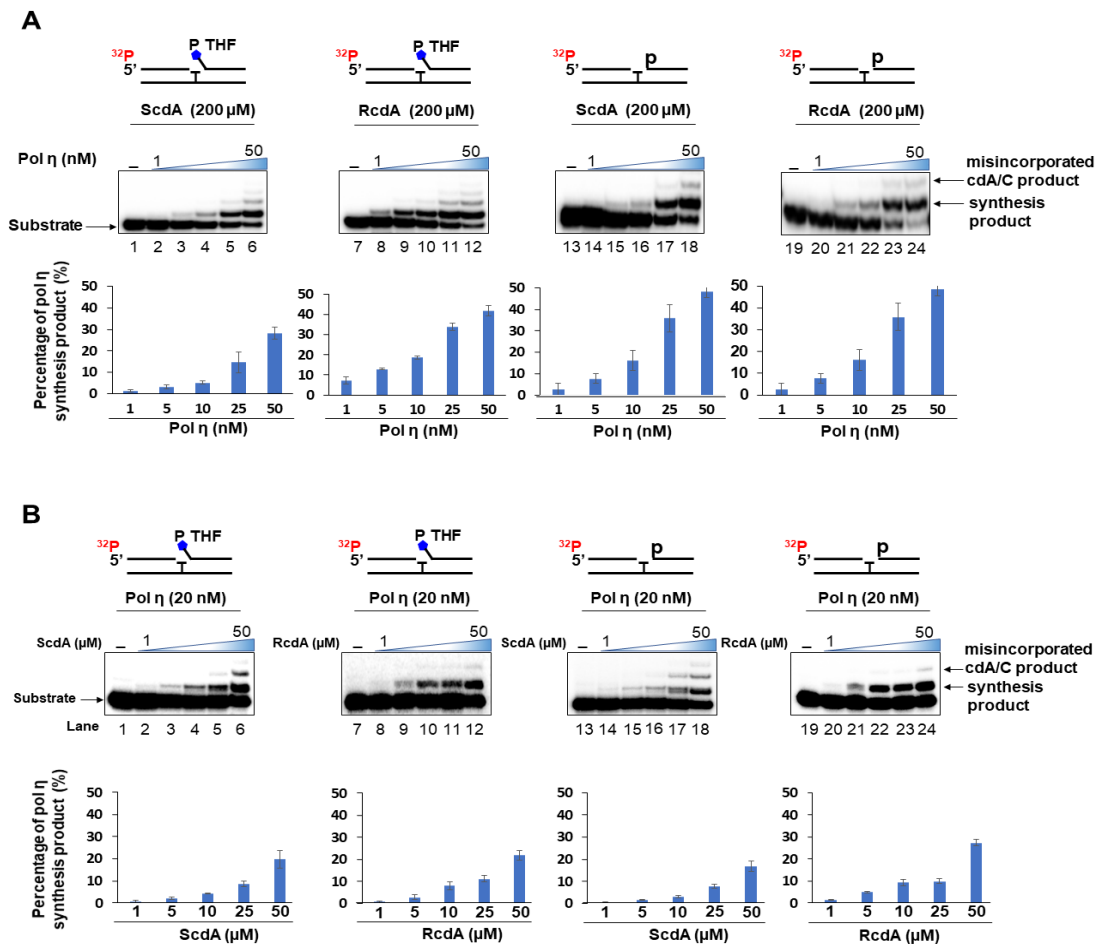


Figure 1.3. The incorporation of cdA by pol η during BER.

(A) The incorporation of cdA by pol η was determined in the presence of cdA (200 μ M) and increasing concentrations of pol η (1, 5, 10, 25, and 50 nM). Lanes 2-6 illustrate the incorporation of 5'S-cdA by pol η with the 1 nt-gap substrate containing a THF in the downstream primer. Lanes 8-12 represent the incorporation of 5'R-cdA by pol η with the substrate containing a THF in the downstream primer. Lanes 14-18 indicate the incorporation of 5'S-cdA by pol η with the substrate containing a phosphate at the 5'-end of the downstream primer. Lanes 20-24 represent the incorporation of 5'R-cdA by pol η with the substrate containing a phosphate at the 5'-end of the downstream primer. (B) The incorporation of cdA by pol η (20 nM) in the presence of increasing concentrations of cdA (1, 5, 10, 25, and 50 μ M). Lanes 2-6 represent the incorporation of 5'S-cdA by pol η with the substrate containing a THF residue in the downstream primer. Lanes 8-12 illustrate the incorporation of 5'RcdA by pol η with the substrate containing a THF residue in the downstream primer. Lanes 14-18 indicate the incorporation of 5'S-cdA by pol η with the substrate containing a phosphate at the 5'-end of the downstream primer. Lanes 20-24 represent the incorporation of 5'R-cdA by pol η with the substrate containing a phosphate at the 5'-end of the downstream primer. Lane 1, 7, 13, and 19 represents substrate alone. All experiments were performed at least in triplicate. The quantification of the results is illustrated below the gels. The percentage of the products is illustrated as average \pm SD in the bar charts.

1.4.2. Pol β and pol η can misincorporate cdA opposite a template dC during BER.

It is reported that pol β and pol η can bypass oxidized DNA bases during DNA replication and BER (Jiang et al., 2015a; Weng et al., 2018b; You et al., 2013a). However, the polymerases can perform nucleotide misinsertion during lesion bypass (Chatgialiloglu et al., 2019; Jiang et al., 2015a; Swanson et al., 2012b; You et al., 2013a). Since we found that pol β and pol η were able to extend 5'R- and 5'S-cdA, creating a cdA:dC mismatch at high concentrations of the polymerases or the nucleotides (*Figure 1.2A, lanes 4-5, 9-10, and 19-20, Figure 1.2B, lanes 9-10 and 19-20, Figure 1.3, lanes 5-6, 11-12, 17-18, and 23-24*), we then validated the incorporation of 5'R-cdA and 5'S-cdA to basepair with a template dC by pol β and pol η (*Figure 1.4A, Figure 1.4B*). The results showed that with 200 μ M cdATP, increasing concentrations of pol β at 1 nM-50 nM resulted in 5-60% of incorporation of 5'R-cdA and 5'S-cdA that base-paired with a dC on the substrates with or without a THF (*Figure 1.4A, lanes 2-5, 7-10, 12-15, and 17-20*). Similarly, in the presence of the same concentration of cdATP, 1-50 nM pol η led to the incorporation of 5-80% cdATP that base-paired with dC on the substrate with or without the THF residue (*Figure 1.4B, lanes 2-6, 8-12, 14-18, and 20-24*). We also found that pol β and pol η failed to incorporate cdATP to basepair with a dG. The results indicate that pol β and pol η preferentially created a cdA:dC mismatch that may potentially lead to a transition mutation *in vivo*.

1.4.3. Incorporated cdA can be extended by repair DNA polymerases leading to the formation of the ligated repair product.

We then asked if an incorporated cdA can be further extended by pol β and pol η , thereby leading to the repair product and preventing DNA strand breaks during BER. We initially examined the extension of an incorporated cdA by pol β and pol η using a nicked substrate containing 5'R-cdA or 5'S-cdA at the 3'-end of the upstream primer. We found dG that base paired with the following template nucleotide, especially

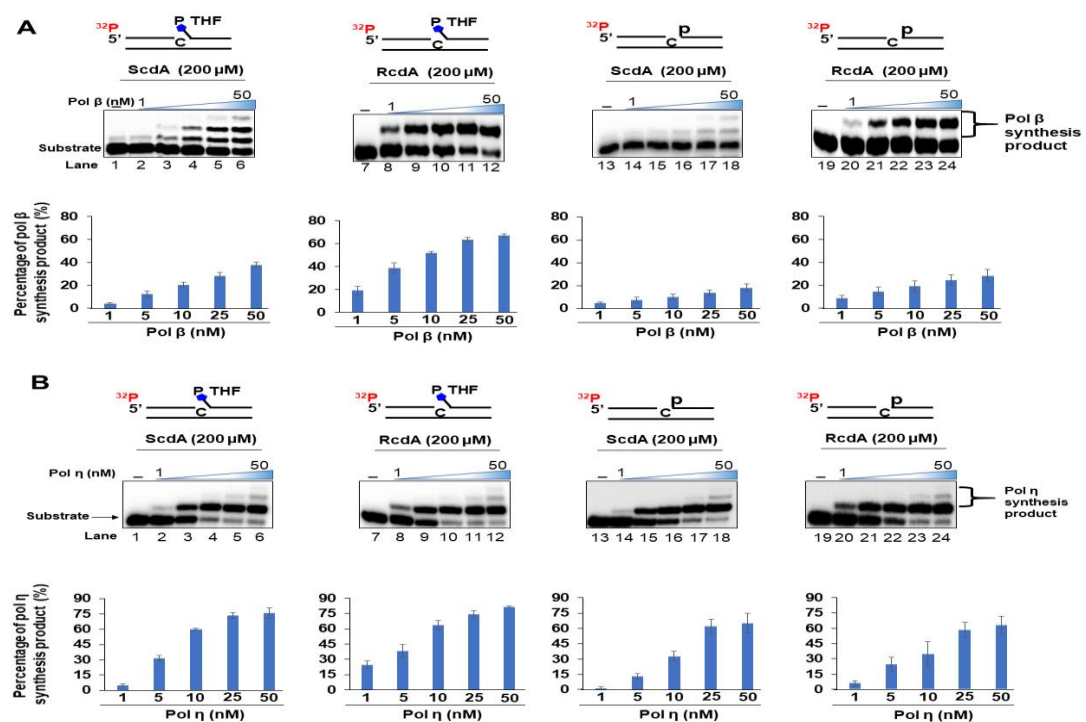


Figure 1.4. The misincorporation of cdA with a dC by pol β and pol η during BER.

(A) The misincorporation of cdA by pol β in the presence of a fixed concentration of cdA (200 μ M) and increasing concentrations of pol β (1, 5, 10, 25, and 50 nM). Lanes 2-6 represent the misincorporation of 5'S-cdA by pol β with the 1 nt-gap substrate containing a THF residue at the downstream primer. Lanes 8-12 illustrate the misincorporation of 5'R-cdA by pol β with the substrate containing a THF in the downstream primer. Lanes 14-18 represent the misincorporation of 5'S-cdA by pol β with the substrate containing a phosphate at the 5'-end of the downstream primer. Lanes 20-24 indicate the misincorporation of 5'R-cdA by pol β with the substrate containing a phosphate at the 5'-end of the downstream primer. (B) The

misincorporation of cdA by pol η was determined in the presence of a fixed concentration of cdA (200 μ M) and titrated concentration of pol η (1, 5, 10, 25, 50 nM). Lanes 2-6 represent the misincorporation of 5'S-cdA by pol η with the substrate containing a THF residue in the downstream primer. Lanes 8-12 illustrate the misincorporation of 5'RcdA by pol η with the substrate containing a THF residue in the downstream primer. Lanes 14-18 indicate the misincorporation of 5'R-cdA by pol η with the substrate containing a phosphate at the 5'-end of the downstream primer. Lanes 20-24 illustrate the misincorporation of 5'S-cdA by pol η with the substrate containing a downstream 5'-phosphate. Lane 1, 7, 13, and 19 represents substrate alone. All experiments were performed at least in triplicate. The quantification of the results is illustrated below the gels. The percentage of the products is illustrated as average \pm SD

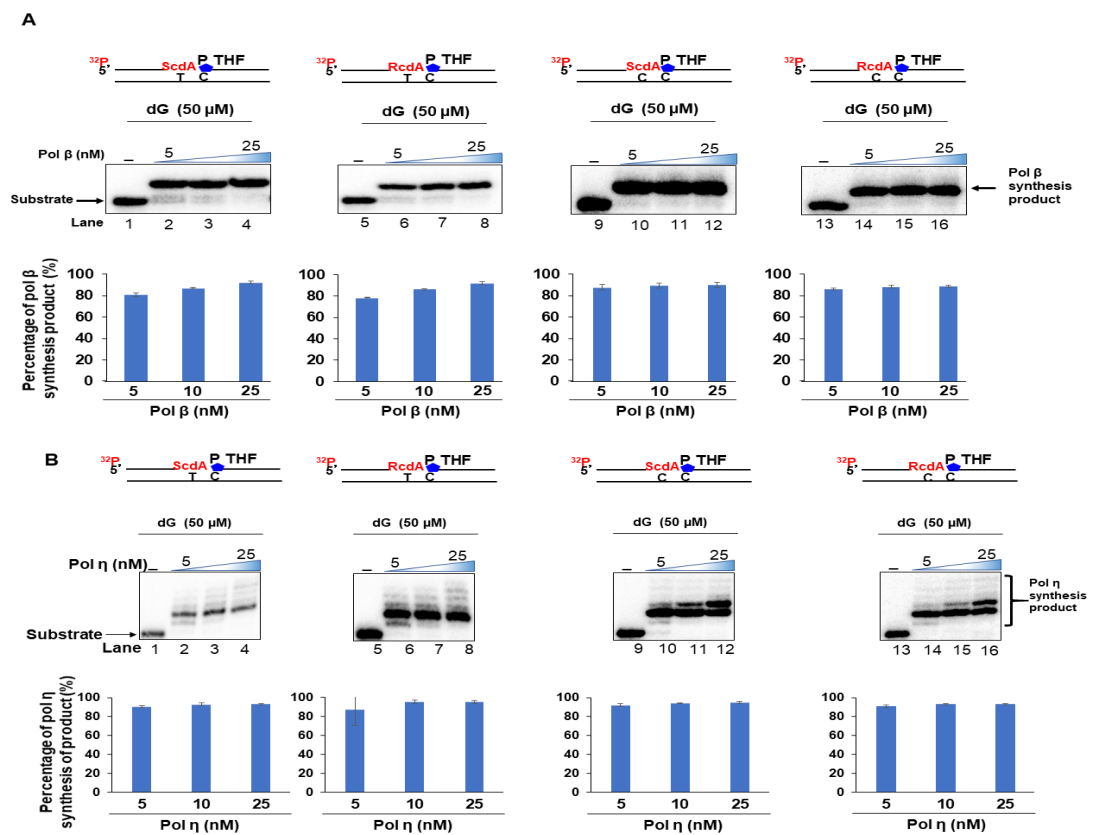


Figure 1.5. Extension of cdA base paired with dT or dC by pol β and pol η

(A) The extension of cdA by pol β was determined in the presence of a fixed concentration of dG (50 μ M) and increasing concentrations of pol β (5, 10, and 25 nM). Lanes 2-4 represent the extension of 5'S-cdA base-paired with dT by pol β with the 1 nt-gap substrate containing a THF residue at the downstream primer. Lanes 6-8 illustrate the extension of 5'R-cdA base-paired with dT by pol β with the substrate containing a downstream 5'-THF residue. Lanes 10-12 represent the extension of 5'S-cdA base-paired with dC by pol β with substrate containing a downstream 5'-THF residue. Lanes 14-16 indicate the extension of 5'R-cdA base-paired with dC by pol β with the substrate containing a downstream 5'-THF residue. (B) The extension of cdA by pol η was determined in the presence of a fixed concentration of dG (50 μ M) and increasing concentrations of pol η (5, 10, and 25 nM). Lanes 2-4 represent the extension of 5'S-cdA base-paired with dT by pol η with the 1 nt-gap substrate

containing a 5'-THF residue. Lanes 6-8 illustrate the extension of the 5'R-cdA base-paired with dT by pol η with the THF-containing substrate. Lanes 10-12 represent the extension of the 5'S-cdA base-paired with dC by pol η with the THF-containing substrate. Lanes 14-16 indicate the extension of the 5'R-cdA base paired with dC by pol η with the THF-containing substrate. Lane 1, 5, 9, and 13 represents substrate alone. All experiments were performed at least in triplicate. The quantification of the results is illustrated below the gels. The percentage of the products is illustrated as average \pm SD in the bar charts.

with the substrates containing a THF (*Figure 1.5B, lanes 11-12 and 14-16*). The results further indicated that pol β and pol η not only incorporated cdA but also readily extended the lesions and created nucleotide misincorporation facilitating the integration of cdA lesions into the genomic DNA. Since the integration of cdPu lesions in DNA may also be accomplished through the direct ligation of incorporated cdAs, which is the essential step for the completion of BER, next, we tested if a nick generated from the incorporated cdAs can be ligated by LIG I (*Figure 1.6*), the DNA ligase that can be involved in both single-nucleotide and long-patch BER subpathway. We tested this by incubating the nicked substrate containing 5'S-cdA or 5'R-cdA at the 3' end of the upstream primer with increasing concentrations (5 nM-25 nM) of LIG I. We found that LIG I at 5 nM-25 nM resulted in 40%-90% ligation product (*Figure 1.6, lanes 2-4, 6-8, 10-12, and 14-16*), which was comparable with the ligation product resulting from dA (87-93%) and dG (92%-97%) (*Figure 1.6*) indicating that LIG I efficiently ligated the nick generated from the incorporated 5'R-cdA and 5'S-cdA. Our results suggest that cdA lesions can be incorporated into the human genome by repair DNA polymerases through BER.

1.4.4. Steady-state kinetics of pol β and pol η

To gain the new insights into the molecular mechanisms underlying the incorporation and extension of cdAs by pol β and pol η , we further performed

the steady-state kinetic studies on the incorporation and extension of cdAs with different template nucleotides by pol β and pol η and determined the K_m , k_{cat} , and catalytic efficiency, k_{cat}/K_m for the enzymatic reactions (*Table 1.2 and Table 1.3*). The results showed that pol β incorporation of 5'R-cdA opposite dT on the substrates without and with a THF exhibited a low K_m of $3.5\text{-}8.0 \times 10^{-2} \mu\text{M}$ with a low k_{cat} ranging from 7.0 to $23 \times 10^{-4} \text{S}^{-1}$ (*Table 1.2*). The results led to the k_{cat}/K_m of $2.0\text{-}2.9 \times 10^{-2} \mu\text{M}^{-1} \text{s}^{-1}$ for pol β 5'R-cdA incorporation (*Table 1.2*). The k_{cat}/K_m for 5'R-cdA incorporation on the substrate with a THF is ~ 1.5 -fold of that without the residue (*Table 1.2*). However, the K_m and k_{cat} for incorporation of 5'-ScdA on the substrates could not be obtained because the enzyme exhibited extremely low nucleotide incorporation activities (*Table 1.2*). Pol β exhibited

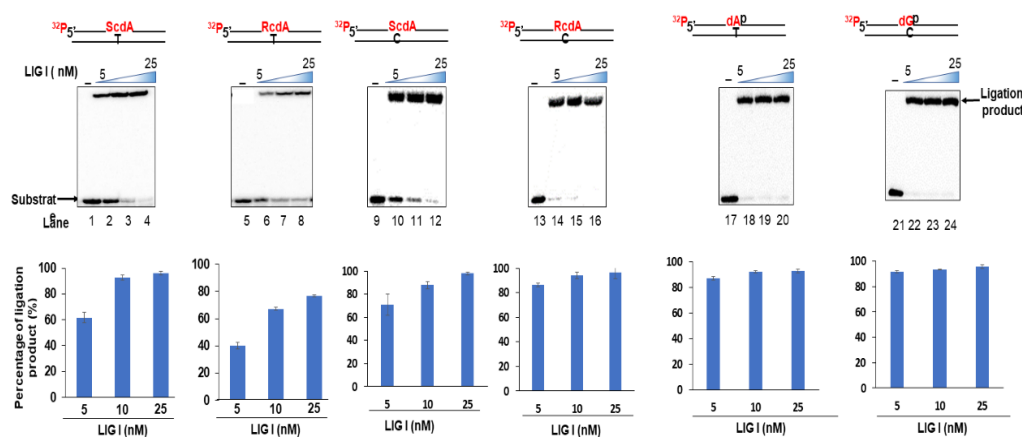


Figure 1.6. Ligation of cdA by DNA Ligase I. Ligation of cdA base-paired with dT or dC by Ligase I.

The ligation of cdA by Ligase I was measured in the presence of increasing concentrations of Ligase I (5, 10, and 25 nM). Lanes 2-4 represent the ligation of 5'S-cdA base-paired with dT with the nicked substrate containing a 5'-phosphate at the downstream primer. Lanes 6-8 illustrate the ligation of 5'R-cdA base-paired with dT with the nicked substrate. Lanes 10-12 represent the ligation of 5'S-cdA base-paired with dC with the nicked substrate. Lanes 14-16 indicate the ligation of 5'R-cdA base-paired with the nicked substrate. Lanes 18-20 represent ligation of normal dA with dT. Lanes 22-24 represent ligation of normal dG with dC. Lane 1, 5, 9, 13, 17 and 21 represents substrate alone. All experiments were performed at least in triplicate. The quantification of the results is illustrated below the gels. The percentage of the products is illustrated as average \pm SD in the bar charts.

a lower K_m ($1.2-5.8 \times 10^{-2} \mu\text{M}$) and higher catalytic efficiency ($3.3-6.7 \times 10^{-2} \mu\text{M}^{-1} \text{s}^{-1}$) in incorporating cdAs opposite dC than dT (*Table 1.2*) The catalytic efficiency for pol β 5'R-cdA and 5'S-cdA incorporation opposite dC were ~ 1.5 - and 3-fold of that with template dT (*Table 1.2*). The enzyme exhibited similar efficiency in extending 5'R- and 5'S-cdA opposite dT (*Table 1.2*). The efficiency for extension of the nucleotide opposite dC was 7-8-fold higher than that for template dT (*Table 1.2*). The results indicate that pol β managed to incorporate 5'R-cdA opposite dT on the 1 nt gap substrates with higher catalytic efficiency on the substrate with a THF, and the enzyme preferentially incorporated 5'R- and 5'S-cdA opposite dC. The results further suggest that the incorporation of cdA during BER can simultaneously introduce the damaged nucleotides and mismatches to cause DNA damage and mutagenesis *in vivo*. On the other hand, pol η did not exhibit a significant difference in incorporating 5'R- and 5'S-cdA opposite dT and dC with catalytic efficiency of $4.6-10 \times 10^{-2} \mu\text{M}^{-1} \text{s}^{-1}$ with varying K_m ($1.3-4.4 \times 10^{-2} \mu\text{M}$) and k_{cat} ($10-31 \times 10^{-4} \mu\text{M s}^{-1}$) (*Table 1.3*). Similar to pol β , pol η also exhibited a higher efficiency of incorporating 5'R- and 5'S-cdA on the substrate with a THF compared with the one without the residue (*Table 1.3*). However, pol η exhibited a high k_{cat} ($160-1600 \times 10^{-4} \text{s}^{-1}$) and catalytic efficiency ($131-167 \times 10^{-2} \mu\text{M}^{-1} \text{s}^{-1}$) in extending both 5'R- and 5'S-cdAs. The catalytic efficiency for the enzyme to extend cdA is 16-35-fold of that for its nucleotide incorporation (*Table 1.3*). The catalytic efficiency of pol η in incorporating cdA was slightly higher than that of pol β . However, the efficiency of pol η in extending cdA opposite dT and dC was 57-89-fold and 7-9-fold of that of pol β (compared the results in *Table 1.3* with those in *Table 1.2*). The

results indicate that pol η incorporated cdAs and its resulted mismatches into DNA more efficiently than pol β .

1.4.5. Repair DNA polymerases accommodate cdA lesions in their active sites to facilitate the phosphodiester bond formation and nucleotide incorporation

To further gain the mechanistic insights into how pol β and pol η incorporated cdA, creating a mismatch during BER, we then conducted a molecular docking analysis on the structures of the DNA polymerases (pol β , PDB5TBB (Reed et al., 2017), pol η PDB4J9N (Zhao et al., 2013) that were docked with cdA using Autodock vina and PyMOL 2.1. We found that in the active site of pol β , the base of 5'R-cdA was orientated facing dT or dC compared with dA:dT and dG:dC base pair (Figure 1.7 A, B, panels a-b). In contrast, 5'S-cdA exhibited a distorted configuration that pulled out the base away from the template dT and dC (Figure 1.7B, panels a-b, bottom). However, our docking analysis failed to predict any hydrogen bond formation between cdA and the template dT or dC. The results are consistent with those showing that pol β performed the incorporation of 5'R-cdA and poor incorporation of 5'S-cdA (Figures 1.2 and 1.4). At pol η active site, only 5'S-cdA was oriented to face toward the template dT (Figure 1.7C, panel a, bottom). 5'R-cdA and 5'S-cdA were pulled out away from the template dT and dC (Figure 1.7C, panels a-b). No hydrogen bonds were predicted between cdA and the template bases. Overlay of cdATP on dA opposite a template dT in pol β revealed that the base of 5'R-cdATP was aligned well with that of A (Figure 1.7D, panel a). However, the phosphate groups failed to align with the 5'-phosphate and pyrophosphate from dATP

(Figure 1.7D, panel a). The base and phosphate groups of 5'S-cdATP were turned away from dATP (Figure 1.7D, panel a). 5'R- and 5'S-cdATP in pol η were positioned away from the base of dATP. However, their γ - and β -phosphates were aligned well with the pyrophosphates released from dATP (Figure 1.7D, panel b). We then looked into the amino acid residues involved in facilitating the

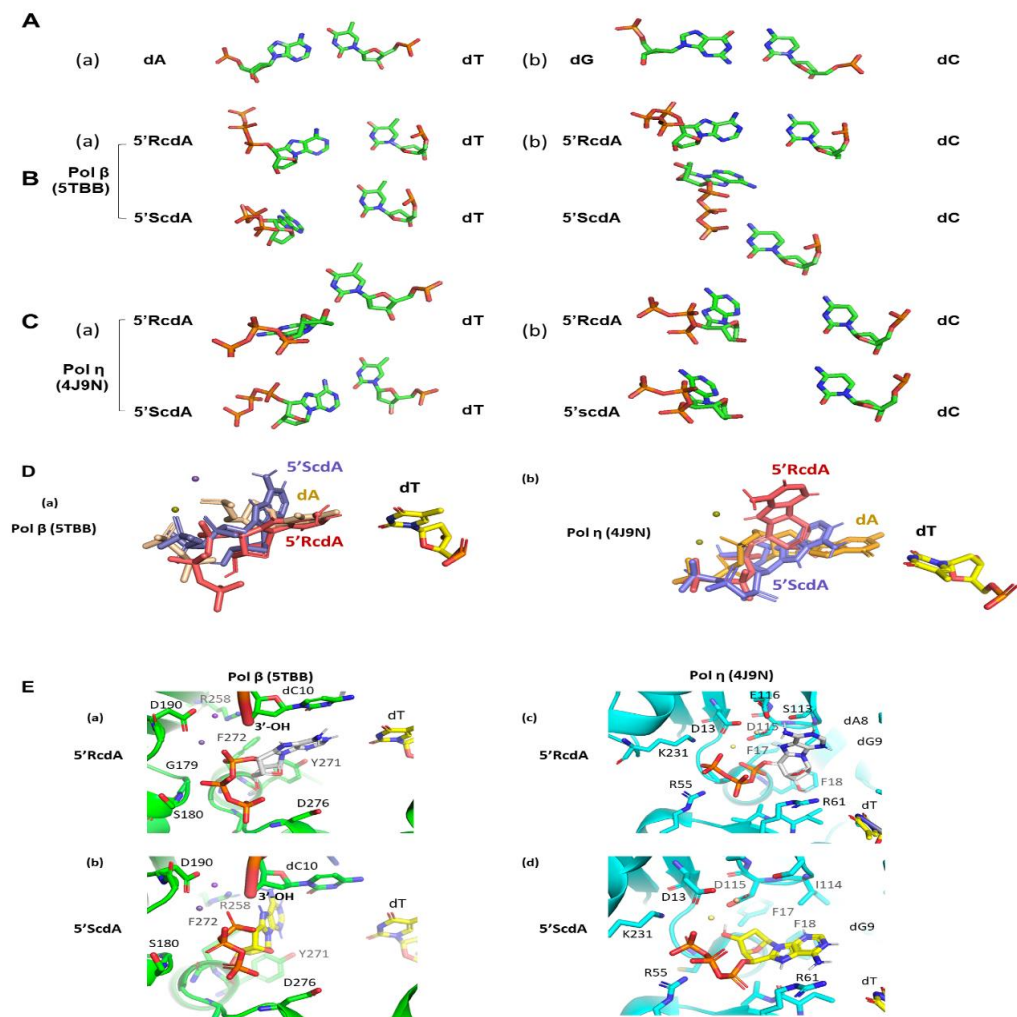


Figure 1.7. The molecular docking analysis on the interaction between pol β and pol η and cdAd

(A) (a) The docked structure of dA:dT basepair. (b) The docked structure of dG against dC. (B) (a) The docked structure of pol β with 5'R- or 5'S-cdA opposite a template dT. (b) The docked structure of pol β with 5'R- and 5'S-cdA opposite a template dC. (C) (a) The docked structure of pol η with 5'R- and 5'S-cdA opposite a template dT. (b) The docked structure of pol η with 5'R- and 5'S-cdA opposite a template dC. (D) (a) The superimposed docking structure of pol β with dA, 5'R-cdA, and 5'S-cdA opposite

dT. (b) The superimposed docking structure of pol η with dA, 5'R-cdA, and 5'S-cdA opposite dT. (E) (a) The amino acids surrounding 5'R-cdA opposite to dT in the active site of pol β . (b) The amino acids that were around 5'ScdA opposite to dT in the active site of pol β . (c) The amino acids that were around 5'R-cdA opposite dT in the active site of pol η . (d) The amino acids that are around 5'S-cdA opposite dT in the active site of pol η .

Table 1.2. The steady state kinetics of the incorporation of cdA by Pol β

Substrate	K_m ($10^{-2} \mu\text{M}$)	V_{max} ($10^{-5} \mu\text{M s}^{-1}$)	k_{cat} (10^{-4}s^{-1})	k_{cat}/K_m ($10^{-2} \mu\text{M}^{-1} \text{s}^{-1}$)
RcdA : dT	3.52 ± 0.70	1.76 ± 0.16	7.03 ± 0.67	2.00
RcdA : dT (THF)	7.96 ± 1.60	5.85 ± 0.40	23.39 ± 1.50	2.94
ScdA : dT	ND	ND	ND	ND
ScdA : dT (THF)	ND	ND	ND	ND
RcdA : dC	1.91 ± 0.72	1.62 ± 0.26	6.50 ± 1.03	3.40
RcdA : dC (THF)	2.97 ± 0.61	3.50 ± 0.58	14.01 ± 2.32	4.71
ScdA : dC	5.83 ± 1.40	2.01 ± 0.52	18.83 ± 3.30	3.23
ScdA : dC (THF)	1.21 ± 0.49	4.90 ± 0.83	8.03 ± 2.10	6.64
RcdA : dT extension	0.81 ± 0.17	5.6 ± 0.11	2.25 ± 0.45	12.78
ScdA : dT extension	4.17 ± 2.40	1.93 ± 0.44	7.73 ± 1.77	11.85
RcdA : dC extension	2.02 ± 0.59	1.96 ± 0.34	39.10 ± 6.73	19.40
ScdA : dC extension	3.67 ± 0.96	2.86 ± 0.44	57.10 ± 8.88	15.60

THF: a tetrahydrofuran residue with a phosphate group at the 5'-end of the downstream primer of the substrates

ND: Measurable enzyme kinetic parameters were not obtained due to the extremely low percentage of 5'S-cdA incorporation products.

The results represented average \pm SD and were obtained from at least three independent experiments.

Table 1.3. The Steady State Kinetics of the Incorporation of cdA by pol η

Substrate	$K_m(10^{-2} \mu\text{M})$	$V_{\text{max}}(10^{-5} \mu\text{M s}^{-1})$	$k_{\text{cat}}(10^{-4} \text{s}^{-1})$	$k_{\text{cat}}/K_m(10^{-2} \mu\text{M}^{-1} \text{s}^{-1})$
RcdA : dT	1.32 ± 0.21	2.58± 0.21	10.33 ± 0.85	7.83
ScdA : dT	2.16 ± 1.12	2.41± 0.16	9.63 ± 0.63	4.46
RcdA : dC	1.82 ± 0.33	4.41± 0.53	17.64 ± 2.12	9.69
ScdA : dC	4.39 ± 0.08	7.63± 0.47	30.53 ± 1.87	6.95
RcdA:dT extension	1.21 ± 0.01	3.95± 0.02	197.30 ± 10.60	163.10
ScdA:dT extension	1.00 ± 0.36	3.17± 0.25	158.60 ± 12.70	158.60
RcdA:dC extension	12.5 ± 1.93	32.5± 5.49	1622.30±275.10	129.78
ScdA:dC extension	6.83 ± 1.01	17.7± 3.64	884.80 ± 182.00	± 129.55

The results represented average ± SD and were obtained from at least three independent experiments.

incorporation of 5'R- and 5'S-cdA by pol β and pol η (*Figure 1.7E*). For pol β , F272 and Y271 in the α -helix were positioned parallel or perpendicular to the base of 5'R-cdA and 5'S-cdA (*Figure 1.7E*, panels a-b). G179 was in proximity with the β -phosphate of 5'R-cdA but not with that of 5'S-cdA (*Figure 1.7E*, panels a-b). D190 and R258 appeared to coordinate with two magnesium ions, which interacted with the phosphate groups of cdAs (*Figure 1.7E*, panels a-b). For pol η , F18 was parallel with the sugar and base rings of 5'R-cdA and 5'S-cdA, respectively (*Figure 1.7E*, panels c-d). D115 and D13 were coordinated with magnesium ions, and K231 and R55 were coordinated with the β and γ phosphate groups of cdA (*Figure 1.7E*, panels c-d). The results suggest that the hydrophobic interaction between the bases of cdA and hydrophobic amino

acids, along with the coordinated phosphates and magnesium ions, mediated the cdA incorporation by the repair DNA polymerases.

1.5. DISCUSSION

In this study, for the first time, we discovered that human repair DNA polymerases, pol β and pol η incorporated 5'R-cdA and 5'S-cdA into duplex DNA through BER (Figures 1.2-1.4). We demonstrated that the incorporated cdA lesions were extended by repair DNA polymerases and ligated into duplex DNA (Figures 1.5-1.6). Further analysis on the efficiency of the catalysis for cdA insertion and extension by pol β and pol η showed that K_m for pol β cdA incorporation on the 1 nt gap substrate was 1.5-10-fold and 2.5-17-fold lower than K_{mDNA} and K_{mdCTP} for correct nucleotide insertion (Table 1.2) (Beard et al., 1996; Chagovetz et al., 1997). The K_m of pol η is 15-25-fold lower than K_{mATP} for correct nucleotide insertion and 386-944-fold lower than K_{mdCTP} for incorrect nucleotide insertion (Table 1.3) (Washington et al., 2003). However, our results showed that the k_{cat} and catalytic efficiency, k_{cat}/K_m of pol β was ~350-1000-fold and ~200-300-fold lower than its correct nucleotide insertion (Table 1.2) (Beard et al., 1996). Similarly, k_{cat} and k_{cat}/K_m for pol η cdA incorporation were ~11-18-fold and ~960-1700-fold lower than correct nucleotide insertion (Table 1.3) (Washington et al., 2003). k_{cat} for pol η cdA:dC incorrect nucleotide insertion was ~18-30-fold lower than that of dT:dC (Table 1.3) (Washington et al., 2003). However, the catalytic efficiency, k_{cat}/K_m for cdA:dC was 2-3-fold higher than k_{cat}/K_{mdCTP} for the misincorporation. The results suggest that the polymerases attempted to increase the efficiency of the catalysis of cdA incorporation by lowering K_m . Since our molecular docking results showed that no hydrogen

bond formed between template dT, dC and cdAs in pol β and pol η (Figure 1.7), it is conceivable that the polymerases could adopt a unique conformation to facilitate the catalysis of cdA incorporation but also trap themselves on the substrates.

Analysis on the rate of the extension of the 3'-terminus cdA that base-paired with template T by the polymerases showed that the K_m for pol β extension of cdAs was ~ 2-11-fold and 5~25-fold lower than the extension of dG and an 8-oxoG (Table 1.2) (Whitaker et al., 2017). In contrast, k_{cat} for pol β cdA extension was ~300-1000-fold and ~22-75-fold lower than its extension of dG and 8-oxoGs, leading to the catalytic efficiency that was ~100-156-fold and ~3-5-fold lower than its extension of the undamaged and damaged nucleotides (Table I) (Whitaker et al., 2017). Although the K_m for pol η extension of cdAs was similar to that of pol β (Table 1.2 and Table 1.3), its k_{cat} and catalytic efficiency of pol η was ~25-88-fold and ~58-88-fold higher than that of pol β (Table 1.2 and Table 1.3). The results indicate that pol η promoted the incorporation of cdA lesions in DNA much more efficiently than pol β by extending the damaged nucleotides. Our results further suggest that the accumulation of cdPu lesions in the genome can be aggravated by their incorporation through repair DNA polymerases during BER, along with the low efficiency of their removal by NER (Kropachev et al., 2014). Thus, our results suggest a potential role of repair DNA polymerases in causing the accumulation of cPu lesions in the genome by incorporating oxidized nucleotides.

Surprisingly, our results also showed that the polymerases led to cdA:dC mismatch (Figure 1.2-1.6). This may potentially result in a transition mutation

in vivo. A previous study indicates that *E. Coli* repair DNA polymerase I (Klenow fragment) can incorporate 5'S-cdATP opposite dT. In contrast, it incorporates 5'R-cdATP opposite a template dC (Kamakura et al., 2012a), demonstrating similarity between the bacterial repair DNA polymerase and human DNA repair polymerases in misincorporating cdA into genomic DNA. Our results are consistent with our previous finding showing that high concentrations of pol β can also misincorporate dC to bypass a template cdA (Jiang et al., 2015a). Here, we further demonstrate that the human repair DNA polymerases can also perform nucleotide misinsertion through its direct incorporation of cPus. Our results suggest that the incorporation of cdA by repair DNA polymerases can potentially serve as an alternative mechanism to induce oxidative DNA damage and its-resulted mutations in the genome. Considering the low efficiency of repairing cdPu lesions by NER, the mutagenic effects resulting from cdA:dC misbasepair may lead to more severe adverse biological effects than other types of base lesions.

Our results also showed that pol β and pol η exhibited a difference in incorporating cdA lesions. We found that pol β incorporated much more 5'R-cdA than 5'S-cdA (Figures 1.2 and 1.4A). This suggests that 5'R-cdA adopted a configuration that favored its incorporation by pol β . The results are consistent with those from our previous study showing that the pol β can efficiently bypass a template 5'R-cdA but not 5'S-cdA (Jiang et al., 2015a). Our molecular docking analysis results further provided several structural insights into the underlying mechanisms. First, the base of 5'R-cdA but not 5'-ScdA was oriented to face the template nucleotide in the pol β active site (Figures 1.7B and 1.7D, panel a). Second, although the base of 5'R-cdA did not form hydrogen bonds with

that of the template dT, it was oriented to parallel with the side chain of F272 (Figure 1.7D, panel a), suggesting a hydrophobic interaction between the rings of F272 and adenine of 5'R-cdA. Third, for both 5'R-cdA and 5'S-cdA, Y271 was positioned perpendicular to the base (Figure 1.7E, panels a-b), indicating the loss of its hydrophobic interaction with the cdA base. Fourth, structural overlay suggested that R258, D190, and G179 were responsible for coordinating with magnesium and phosphates to facilitate the catalysis of 5'R-cdA incorporation (Figure 1.7E, panel a). The disappearance of G179 in the presence of 5'S-cdA (Figure 1.7E, panel b) suggested that G179 coordinated with the phosphates to facilitate the nucleophilic attack from the 3'-OH group. On the other hand, in the active site of pol η , the bases 5'R-cdA and 5'S-cdA have turned away from the template dT and dC (Figure 1.7C). Although 5'S-cdA was oriented to face to dT, its incorporation by pol η exhibited little difference from that of 5'R-cdA (Figure 1.3). A structural overlay between the β - and γ -phosphate of cdA and that of dA (Figure 1.7D, panel b) in the active site of pol η suggested that the coordinated phosphates of cdA mediated the catalysis of cdA incorporation. This appeared to be mediated by K231 and R55 and magnesium ions coordinated by D13 and D115 (Figure 1.7E, panels c-d). In addition, the hydrophobic interaction between F18 and the rings of sugar of 5'R-cdA and adenine could also be involved in stabilizing the base and orientation of the phosphates facilitating the catalysis of cdA incorporation. The mechanistic insights can be validated using X-ray crystallography of pol β and pol η with the mutations of critical amino acids in their catalytic sites. The studies will further reveal the enzyme-substrate interaction and catalysis for cdA incorporation of the polymerases.

Our results suggest that the incorporation of cdA by pol β and pol η was mediated by the nucleophilic attack between the 3'-hydroxy group of the last nucleotide of the primer and α -phosphate of cdATP in the absence of hydrogen bonds. It appeared that the hydrophobic interaction between cdA and template bases and base stacking facilitated the proximity between the 3'-hydroxyl group and the α -phosphate, promoting the nucleophilic attack and cdA incorporation. The results suggest that the nucleophilic attack from the 3'-hydroxyl group to the α -phosphate of 5'R- and 5'S-cdA played a predominant role in mediating the incorporation of cdA. However, the cdA:dC misbasepair generated by pol β and pol η (Figure 1.4) further suggesting that the loss of the hydrogen bond between cdA and dT resulted in the mismatches, demonstrating that the hydrogen bonding was essential for maintaining the fidelity of the repair DNA polymerases.

A variety of oxidized nucleotides including cdPus and 8-oxoG among others can be generated in the DNA or the nucleotide pool (Kasai and Nishimura, 1983; Nakabeppu, 2014). However, it remains unknown how much cPus can be generated from the nucleotide pool in human cells. It has been shown that free dGTPs are oxidized with an 8-9-fold higher frequency than dGMP (Kamiya and Kasai, 1995), indicating that dGTP is more susceptible to oxidation than dGMP *in vivo*. It is estimated that the concentration of 8-oxodG ranges from 0.2 to 2 μ M in the nucleotide pool of mitochondria in rat tissues under physiological conditions (Pursell et al., 2008). Considering the bigger size of the nucleus than mitochondria, it is possible that more 8-oxodGTP can be generated in the nucleotide pool of the nucleus. Similar to the cellular production of 8-oxodGTP, it is conceivable that more cdPu triphosphate may also be generated from the

oxidation of the nucleotide pool than from direct oxidation of deoxypurines in double-strand DNA. It has been shown that there are approximately 10,000 8-oxoGs and 180-320 cdPus generated in the genomic DNA of mammalian cells and tissues per day (Randerath et al., 2001). Interestingly, a previous study has shown that pol β incorporates 8-oxodGTP at a low catalytic efficiency, k_{cat}/K_m 8-oxodGTP of $130 \times 10^{-5} \text{ min}^{-1} \mu\text{M}^{-1}$ ($2 \times 10^{-5} \text{ s}^{-1} \mu\text{M}^{-1}$) (Miller et al., 2000). Our result showed that k_{cat}/K_m DNA for pol β and pol η to incorporate cdA is higher than the k_{cat}/K_m 8-oxodGTP for 8-oxodGTP incorporation. Since the Wilson group has shown that K_m DNA of pol β is ~14-fold higher than K_m dNTP (Beard et al., 1996), our results suggest that pol β and pol η exhibited comparable efficiency of incorporating cdA but with lower efficiency of extending cdA than 8-oxodG (Table 1.2 and 1.3) (Whitaker et al., 2017). Thus, we suggest that pol β and pol η can play a significant role in promoting the accumulation of cdA in the genome. The contribution of cdPus lesions in DNA from the oxidized nucleotide pool needs to be further determined by examining the incorporation of cdGTPs and cdATPs by different repair DNA polymerases *in vitro* and *in vivo*. Moreover, since cdPus incorporated by repair DNA polymerases during BER can be recognized and removed by NER (Kropachev et al., 2014), it is possible that BER and NER can crosstalk to govern the incorporation of cdPu lesions. A recent study has shown that cdPu lesions can inhibit the repair of an AP site by BER in mammalian cells (Boguszewska et al., 2021), suggesting that the removal of cdPus by NER can modulate BER efficiency. The coordination between BER and NER pathways governing the accumulation and removal of cdPu lesions and base lesions needs to be further explored in the future.

cdPu lesions are associated with the etiology of breast cancer. This notion is supported by the fact that more cdPu lesions can be induced by oxidative stress in several breast cancer cell lines than normal cells (Nyaga et al., 2007). This is because cancer cells proliferate more quickly than normal cells and can generate a high level of H₂O₂-mediated oxidative stress (Szatrowski and Nathan, 1991). Interestingly, cdPus may also be involved in treating solid tumors by the antitumor drug, Tirapazamine (TPZ) (Birincioglu et al., 2003). In TPZ-treated hypoxic cells, the amount of cdA and cdGs are significantly increased, suggesting that cdPus lesions mediate cancer cell killing of TPZ (Birincioglu et al., 2003). Moreover, since nucleotide analogs are routinely used as drugs for cancer therapy (Gandhi et al., 1995; Prakasha Gowda, 2010; Saif et al., 2009), our discovery of the incorporation of cdA lesions in DNA by repair DNA polymerase suggests that cPus can also be developed into a new nucleotide analog for cancer treatment. This is because, first, a single cdA lesion can efficiently inhibit DNA replication polymerases and RNA polymerase and the DNA binding of the TATA box-binding proteins (Brooks et al., 2000; Kuraoka et al., 2000; Marietta et al., 2002), thereby inhibiting both DNA replication and gene transcription in cancer cells. Second, cPu lesions are poorly repaired by NER, leading to their accumulation in the genome (Brooks, 2008). This may inhibit cancer cell growth and progression. Finally, the misincorporation of cPu lesions in DNA can potentially cause mutations during their incorporation and lesion bypass in cancer cells, thereby attenuating cancer cell survival.

In summary, in this study, we have discovered that the incorporation of cdA lesions by human repair DNA polymerases, pol β , and pol η . We showed that

pol β and pol η not only incorporated the lesions but also created a cdA:dC mismatch. Moreover, the incorporated cdA lesions can be fully extended by pol β and ligated by LIG I, suggesting that the lesion can be readily embedded in the human genome. Using steady-state kinetics and molecular docking analysis, we provided new mechanistic insights into the mechanisms underlying cdA incorporation by pol β and pol η .

2. CHAPTER 2. RNA-GUIDED DNA BASE EXCISION REPAIR VIA DNA POLYMERASE SWITCHING

2.1. ABSTRACT

DNA repair is mediated by DNA synthesis of DNA polymerases in the context of a DNA template. However, recent studies have shown that RNA-guided DNA synthesis by DNA polymerases is also involved in double-strand DNA break repair. Yet, it remains to be elucidated how RNA-guided DNA synthesis by human DNA polymerases can mediate DNA repair. In this study, we explored the molecular mechanisms of RNA-directed DNA synthesis by repair DNA polymerases and its roles in repairing a DNA base lesion and double-strand breaks. We showed that pol β , pol κ , and pol ι only inserted one nucleotide at the 1 nt-gapped with an RNA template. In contrast, the translesion DNA polymerases, pol η , pol ν , and pol θ performed efficient RNA-guided DNA synthesis with both 1 nt-gapped and open template intermediates. We found that pol η exhibited more efficient RNA-directed DNA synthesis than pol β . Using molecular dynamics, we identified a strong hydrogen bonding formed between a dCTP and GTP on an RNA template in pol β in 50 ns and 100 ns and demonstrated the dynamic conformation changes of pol β and misorientation of the triphosphate of the nucleotide to accommodate the formation of hydrogen bonding. We showed that during base lesion repair and strand break repair in the context of an RNA template, the repair DNA polymerases extended the synthesized DNA resulting in a nick within DNA for ligation and completion of repair. Our study suggests the unique crosstalk

between RNA and DNA repair and via the dual role of DNA- and RNA-directed DNA synthesis by repair DNA polymerases.

2.2. INTRODUCTION

Genome integrity and stability must be maintained to allow faithful transfer of genetic information from parental to daughter cells (Crick, 1970; Crick, 1958). However, the genome is constantly damaged by endogenous and environmental stressors (Hoeijmakers, 2001; Lindahl, 1993). Major genome damage includes various DNA damage such as DNA base damage, mismatches, DNA adducts, thymine dimers, single- and double-strand breaks, among others (Hoeijmakers, 2001; Lindahl, 1993; Lopes et al., 2001a). DNA base damage is the most common form among the damage with a rate of $\sim 10^5$ base lesions generated per cell per day (Hoeijmakers, 2009). Double-strand DNA breaks (DSB) are the most severe DNA damage that can cause chromosomal breakage and rearrangement and cell death (Heyer et al., 2010). To combat the adverse effects of DNA damage, cells have evolved different DNA repair pathways to remove various DNA lesions. In response to different types of DNA damage, a specific DNA repair pathway is activated. Moreover, multiple DNA repair pathways can also be simultaneously activated to repair different DNA damage that can be induced by endogenous or environmental stressors.

A critical step of DNA repair is DNA synthesis performed by DNA repair polymerases that is essential for filling in DNA gaps and generating nicks for ligation. Specific DNA polymerases are employed in different DNA repair pathways in cells, although on some occasions, multiple DNA repair

polymerases can cooperate to participate in damage repair (Lai et al., 2016). For example, double-strand DNA breaks can be repaired by both nonhomologous end-joining (NHEJ) and homologous recombination (HR).

RNA can act as a template for DNA synthesis in the reverse transcription of retroviruses and retrotransposons (Baltimore, 1985) and telomeres' elongation (Autexier and Lue, 2006; Blackburn, 1992). Early studies have identified the reverse transcriptase activity of DNA polymerase γ (pol γ) (Gallo et al., 1970; Murakami et al., 2003b; Robert-Guroff and Gallo, 1977). It has been found that yeast DNA polymerase δ and α can perform DNA synthesis using RNA as a template (Storici et al., 2007). Recent studies have further implicated the important roles of RNA in guiding DNA repair (D'Alessandro et al., 2018; Francia et al., 2016; Lu et al., 2018; Xiang et al., 2017). RNA transcripts are synthesized from their DNA templates; therefore, cells may exploit the sequence homology of RNA to repair their DNA templates. It has been shown that in yeast, RNA can indirectly mediate DNA recombination through a cDNA intermediate (Derr and Strathern, 1993; Nevo-Caspi and Kupiec, 1997). RNA transcript can also facilitate the precise repair of its source DNA (Keskin et al., 2016). Mammalian long interspersed elements (LINE1) retrotransposons can prime retrotranscription from DNA strand breaks at the 3'-end to repair DNA (Morrish et al., 2002). DNA Damage induced long non-coding RNAs (dilncRNAs) and small DNA damage response RNAs (DDRNs) are recruited to DSB sites to promote double-strand break DNA repair (DSBR) (Francia et al., 2012; Michelini et al., 2017). It is believed that dilncRNAs could form DNA-RNA hybrids at DSBs, leading to the recruitment of BRCA1, BRCA2, RAD51, and MRE11 to the locations of DSB (D'Alessandro et al., 2018; Francia et al.,

2016; Lu et al., 2018; Ohle et al., 2016). Another study also reported that ultraviolet (UV) irradiation can induce formation of m⁶A RNA modification at single-strand breaks (SSBs) that helps to recruit DNA polymerase κ (pol κ) for nucleotide excision and trans lesion synthesis-mediated SSB repair (Xiang et al., 2017). Most recently, a study has demonstrated that the human translesion DNA polymerase θ (pol θ) exhibits reverse transcriptase activity to mediate non-homologous end joining during repair of double-strand break (DSB) repair (Chandramouly et al., 2021). RNA is also be involved in UV-induced DNA damage repair through RNA methylation, N⁶-methyladenosine (m⁶A) (Xiang et al., 2017) that recruits pol κ to damage sites. A recent study further demonstrates that UV-induced DNA damage activates METTL3 to generate m⁶A on mRNA and lncRNA and recruit RAD51 and BRCA1 to DNA damage sites promoting DSB repair (Zhang et al., 2020). This suggests that RNA may be served as a template for DNA repair and mediating the recruitment of DNA repair proteins.

On the other hand, RNA:DNA hybrids can also promote the accumulation of DNA damage and genome instability during DNA replication and gene transcription (Brambati et al., 2020). In particular, during gene transcription, RNA:DNA hybrids can result in R-loops as the hotspots of DNA damage (Garcia-Muse and Aguilera, 2019). It has been shown that deficiency of the removal of R-loops ultimately results in dsDNA breaks (Garcia-Muse and Aguilera, 2019), suggesting that both the nontemplate and template DNA strand in R-loops can be damaged in cells. Several studies have suggested that DNA repair is involved in repairing DNA damage resulting from RNA:DNA hybrids (Chandramouly et al., 2021; Storici et al., 2007; Xiang et al., 2017). We have

further demonstrated that DNA base excision repair (BER) can repair a DNA base lesion on the non-template DNA strand of an R-loop formed on trinucleotide repeats leading to the resolution of the R-loop and repeat instability (Laverde et al., 2020). However, it remains unknown if oxidative DNA damage in the template DNA strand can be repaired while it is basepaired with RNA or the damage can only be repaired after the RNA strand is removed. Since more and more studies show that RNA can guide DNA synthesis and DNA repair (Chandramouly et al., 2021; Gallo et al., 1970; Robert-Guroff and Gallo, 1977; Storici et al., 2007; Xiang et al., 2017), we hypothesize that RNA can serve as a template to mediate base lesion repair in RNA:DNA hybrids. To test the hypothesis, we initially characterized RNA-guided DNA synthesis activity of replication and repair DNA polymerases. We then examined BER enzymatic activities that are essential steps for the accomplishment and completion of BER. We found that replication DNA polymerases, pol δ and pol ϵ failed to synthesize DNA with an RNA template. DNA polymerase β (pol β), pol I, and the translesion DNA polymerase, pol k only performed 1 nt gap-filling synthesis. The translesion DNA polymerases, pol h, pol q, and pol n, performed not only RNA-guided 1 nt gap-filling synthesis and strand-displacement synthesis but also exhibited reverse transcriptase activity. The steady-state kinetics of pol b and pol h DNA synthesis with the RNA template showed a comparable catalytic efficiency with the synthesis with the DNA template. Using the molecular dynamic simulation, we further revealed the molecular basis underlying the DNA synthesis that mediates RNA-guided BER.

2.3. MATERIALS AND METHODS

2.3.1. Materials

Oligonucleotides were synthesized by Eurofins Genomics (Louisville, KY, USA). Radionucleotide, ^{32}P -ATP (6000 $\mu\text{Ci}/\text{mmol}$), was purchased from PerkinElmer Inc (Boston, MA, USA). Micro Bio-Spin 6 chromatography columns were from Bio-Rad Laboratories (Hercules, CA, USA). Pol β and DNA ligase I (LIG I) were purified as described previously (Beaver et al., 2015). Pol η , pol δ , pol θ , and pol ν were purified and provided by the Yang Laboratory as described previously (Weng et al., 2018a). Pol κ , pol λ , and pol ϵ were purchased from ENZYMAX (Lexington, KY, USA). All other standard chemical reagents were from Sigma–Aldrich (St. Louis, MO, USA) and ThermoFisher Scientific (Pittsburgh, PA, USA).

2.3.2. Oligonucleotide substrates

An open template substrate with a DNA primer and RNA template was designed to mimic the substrate to test the reverse transcription activity of DNA polymerases. Substrates containing 1 nt-gap were designed to test RNA-guided DNA repair. The substrates for testing DNA polymerases reverse transcriptase activity were constructed by annealing and 19 nt-upstream DNA primer with a 36 nt-RNA template with random sequence or a 30 nt-RNA template containing the RNA sequence of COVID-19 spike protein. The open template substrate for testing the reverse transcription activity of HCV was constructed by annealing an 18 nt-upstream DNA primer with a 30 nt RNA

template containing HCV RNA sequence. The substrates for testing RNA-guided DNA repair were constructed by annealing the 19 nt-upstream

Table 2.1. Oligonucleotides sequence

Oligonucleotides	nt	Sequence (5'-3')
<u>Upstream Strand</u>		
U1	19	CTTTCCTTTTACGTCATCC
<u>Downstream strands</u>		
D1	16	pGGGGCAGACTGGGTGG
D2	16	pFGGGCAGACTGGGTGG
D3	17	pGGGGCAGACTGGGTGG
<u>Template Strands</u>		
T1	36	CCACCCAGUCUGCCCCCGGAUGACGUAAAAGGAAAG
T2 (HCV)	30	GUGGUACUGCCUGAUAGGGUGCUUGCGAGU
T3 (Covid19)	30	GGUGUUGGUUACCAACCAUACAGAGUAGUA

^aThe nucleotide opposite to the one nt gap is in boldface. F, tetrahydrofuran.

DNA primer and 16 nt-downstream DNA primer containing either a 5'-phosphate or 5'-phosphorylated tetrahydrofuran (THF) residue with the 36 nt-RNA template containing dC opposite to the 1 nt gap. The substrates were assembled by annealing the upstream and downstream primers with the template strand at a molar ratio of 1:2:3. The substrates were radiolabeled at the 5'-end of the upstream DNA primer. The substrate for the reconstituted BER was constructed by annealing the 19 nt DNA primer with a 17 nt downstream DNA primer and the 36 nt-RNA template. A nicked substrate was also created to test DNA ligase activity with an RNA template. The sequences of the oligonucleotides are listed in *Table 2.1*.

2.3.3. Enzymatic activity assays

RNA-guided DNA synthesis activity of various DNA polymerases were measured by incubating 25 nM substrates with fixed or increasing

concentrations of the DNA polymerases in the presence of 50 μ M dNTPs at 37 °C for 30 minutes in reaction mixture (10 μ l) that contained BER buffer with 50 mM Tris-HCl, pH 7.5, 50 mM KCl, 5 mM Mg²⁺, 0.1 mM EDTA, 0.1 mg/ml bovine serum albumin, and 0.01% Nonidet NP-40. Substrates and products were separated by 15% urea-denaturing polyacrylamide gel and detected by Pharos FX Plus PhosphorImager (Bio-Rad, Hercules, CA, USA). All experiments were repeated at least three times independently.

2.3.4. Steady-state kinetics of RNA-guided DNA synthesis.

The steady-state kinetics of DNA synthesis by pol β and pol η was determined by incubating fixed concentration of the DNA polymerases with increasing concentrations of the DNA:RNA hybrid substrates in the presence of 50 μ M dG for the 1 nt gap substrate and 50 mM dNTPs or increasing concentrations of deoxyribonucleotide triphosphate (25 μ M-500 μ M) for the 1 nt gap substrates and open template substrate (50 nM) at 37 °C at different time intervals ranging from 0 to 15 minutes in the reaction mixture (10 μ l) that contained BER buffer with 50 mM Tris-HCl, pH 7.5, 50 mM KCl, 5 mM Mg²⁺, 0.1 mM EDTA, 0.1 mg/ml bovine serum albumin, and 0.01% Nonidet NP-40. The reaction was stopped using 2x stopping buffer containing 95% formamide and 10 mM EDTA, 0.05% (w/v) bromophenol blue, Sigma-Aldrich (St. Louis, MO, USA) and 0.05% (w/v) xylene cyanol, Sigma-Aldrich (St. Louis, MO, USA) followed by incubation at 95°C for 5 minutes. Substrates and products were separated by 15% urea-denaturing polyacrylamide gel and detected by Pharos FX Plus PhosphorImager (Bio-Rad, Hercules, CA, USA). The apparent Michaelis-

Menten constants, V_{\max} , K_m , and k_{cat} values were calculated using the Enzyme Kinetics module of the Prism-GraphPad software, version 6.03.

2.3.5. Molecular dynamics simulation of the ternary complexes of pol β with a 1 nt gap containing RNA template.

Protein structures were obtained from the data bank. The X-ray crystal structure of pol β (PDB ID 5TBB) was chosen for molecular dynamics simulation for its high resolution (Reed et al., 2017). Besides, the complex structure suits our objective as it illustrates the interaction of pol β with 1 nt-gap substrate.

2.4. RESULTS

2.4.1. Translesion DNA polymerases can perform DNA synthesis with an RNA template.

DNA polymerases play an important role in DNA replication, repair, and DNA lesion bypass to maintain genome integrity and stability. However, repair DNA polymerases can exhibit structural flexibility to tolerate and bypass damaged and distorted bases. It is possible that repair DNA polymerase may tolerate the effects of sugar pucker in an RNA template to perform DNA synthesis, i.e., reverse transcriptase activity to govern DNA damage repair. To test this, we initially examined the DNA synthesis activity of replication, repair, and translesion DNA polymerases, pol β , pol λ , pol η , pol κ , pol θ , pol ν , and pol ι using an open template substrate containing RNA (*Figure 2.1 and Figure 2.2*). The results showed that pol δ , pol β , and pol ι failed to perform DNA synthesis with the RNA template, although they exhibited processive DNA synthesis with

a DNA template (*Figure 2.1*, lane 2, 3, 5, 17, 18, and 20). On the other hand, pol η , pol ν , and pol θ readily performed DNA synthesis on the RNA

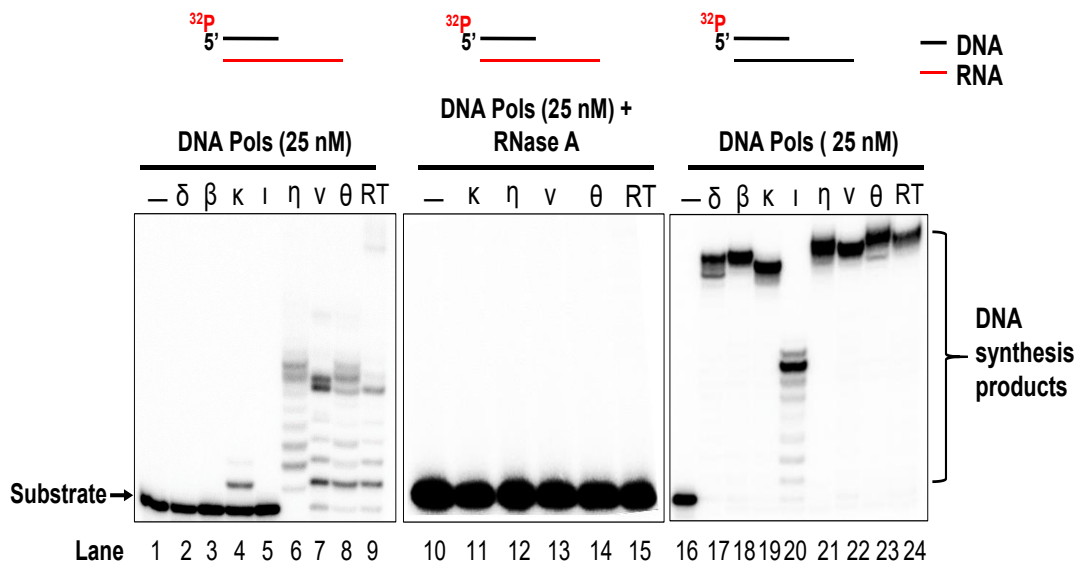


Figure 2.1. RNA and DNA template-dependent DNA synthesis by DNA polymerases.

RNA and DNA-dependent DNA synthesis by DNA polymerase were tested using DNA primer annealed to a template RNA and DNA. Lanes 2-8 represent RNA template-dependent DNA synthesis by 25 nM of DNA polymerases. Lanes 11-14 represent RNA-dependent DNA synthesis by 0.5 nM of DNA polymerases in the presence of RNase A. Lanes 17-23 represent DNA template-dependent DNA synthesis by 25 nM of DNA polymerases. Lanes 9, 15 and 24 represent RT synthesis. Lanes 1, 10, and 16 represent substrate only.

template (Figure 2.1, lanes 4, 6, 7, and 8). The results further suggest that replication and repair DNA polymerases were inhibited by the sugar pucker of

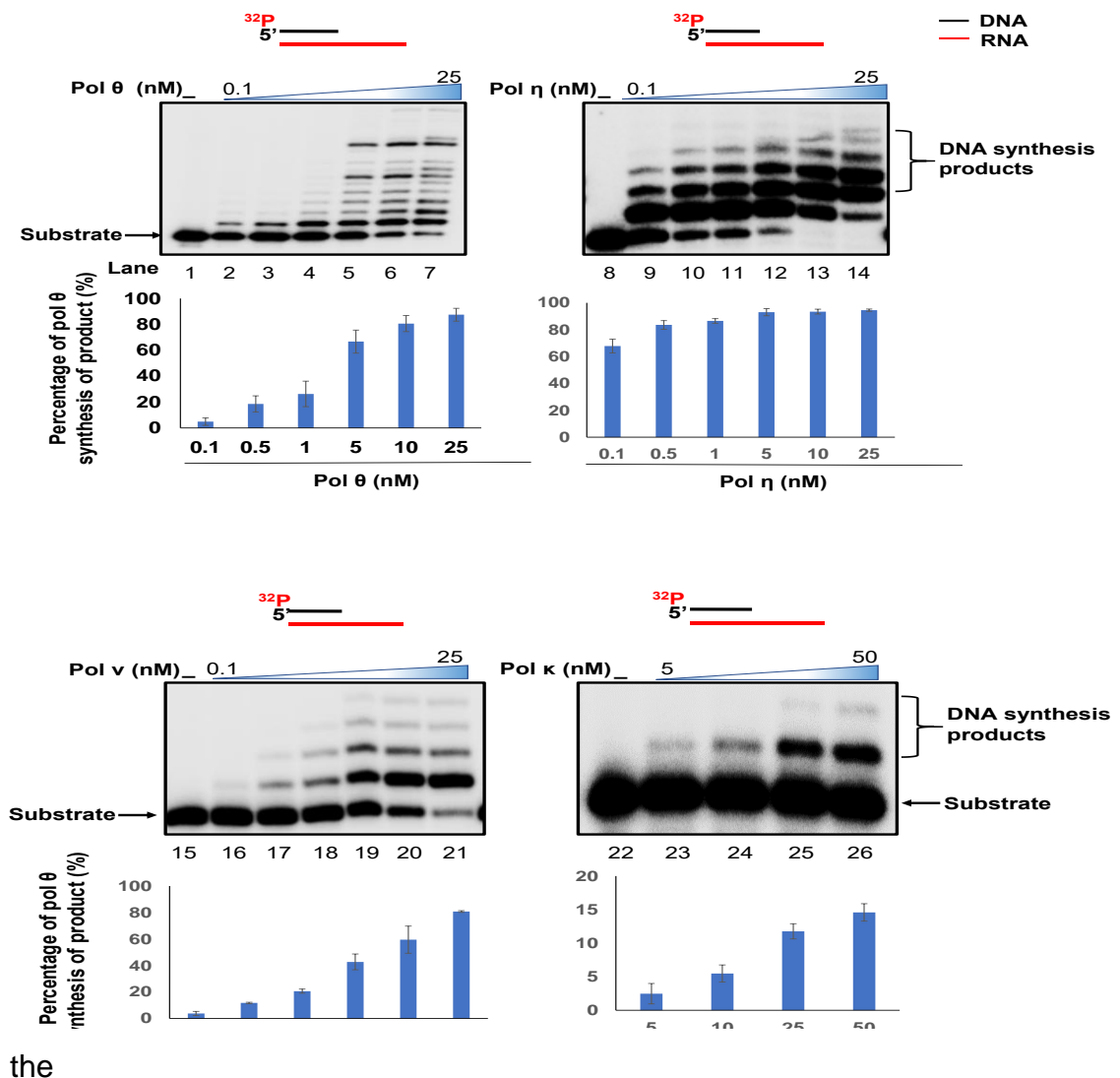


Figure 2.2. RNA dependent DNA synthesis by DNA polymerases.

RNA dependent DNA synthesis by DNA polymerases using a substrate containing RNA as a template and DNA primer in the presence of a fixed concentration of dNTPS (50 μM) and increasing concentrations of the DNA polymerases (0.1, 0.5, 1, 5, 10, and 25 nM for pol θ, pol η and pol ν and 5, 10, 25, and 50 nM for pol κ). Lanes 2-7 represent DNA synthesis by pol θ. Lanes 9-14 represent DNA synthesis by pol η. Lanes 16-21 represent the DNA synthesis by pol ν. Lanes 23-26 represent the DNA synthesis by pol κ. Lanes 1, 8, 15 and 22 represent substrate only. All experiments were done in triplicate.

RNA template. However, translesion DNA polymerase managed to accommodate the sugar configuration of the RNA template to synthesize DNA. Moreover, the translesion DNA polymerase exhibited distributive DNA synthesis (*Figure 2.1*, lane 4, lanes 6-8) with the RNA template but processive DNA synthesis with a DNA template (*Figure 2.1*, lanes 21-24). We then tested if the DNA synthesis products were RNA-dependent by detecting the DNA synthesis in the presence of RNase A (*Figure 2.2*, lanes 11-15). We found that no DNA synthesis products were detected, demonstrating the RNA-dependence of the DNA synthesis. We then examined the RNA-dependent DNA synthesis at the open template substrate by translesion DNA polymerases under various concentrations (*Figure 2.2*). The results indicated that pol η , pol ν , and pol θ performed distributive DNA synthesis on the RNA template at concentrations ranging from 0.1 nM-25 nM (*Figure 2.2*, lanes 2-7, 9-14, 16-21). However, pol κ at 5 nM-50 nM mainly synthesized one nucleotide (*Figure 2.2*, lanes 23-26). Similar results were obtained with the DNA synthesis by pol η , pol ν , and pol θ on the open template substrates containing the RNA sequences of COVID-19 spike protein and hepatitis C virus RNA (*Figure 2.3*).

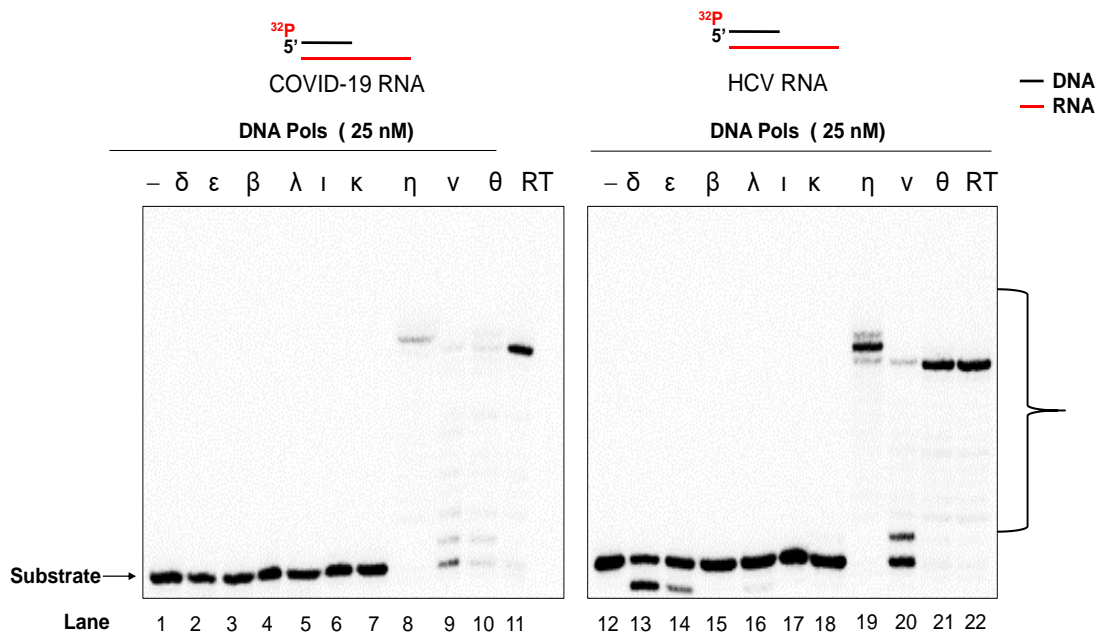


Figure 2.3. DNA synthesis on viral RNA by DNA polymerases.

RNA-dependent DNA synthesis by DNA polymerase was tested using DNA primer annealed to COVID-19 and HCV template RNA. Lanes 2-11 represent COVID-19 RNA template-dependent DNA synthesis by 25 nM of DNA polymerases. Lanes 13-22 represent HCV RNA-dependent DNA synthesis by 25 nM of DNA polymerases. Lanes 1 and 12 represent substrate only.

This indicates that the RNA-guided DNA synthesis by the polymerases is independent of the sequences of RNA templates. The distributive nucleotide synthesis on the RNA template substrate suggests that the translesion DNA polymerases mediate in RNA-guided DNA repair.

2.4.2. DNA polymerases can perform RNA-guided gap-filling and strand-displacement synthesis during base lesion repair on a DNA template

We then asked if the repair and translesion DNA polymerases can mediate base excision repair (BER) using an RNA template. We tested this by characterizing RNA-guided DNA synthesis on the 1 nt-gap substrate with or

without a deoxyribose phosphate (dRP) residue that was represented by a tetrahydrofuran (THF) (*Figure 2.4* and *Figure 2.5*). The substrates mimic the BER intermediates before and after the sugar phosphate residue is removed by pol β dRP lyase activity. Similar to the results from the open template substrate, Pol δ and pol ι failed to synthesize DNA on the 1 nt gap substrates with the RNA template (*Figure 2.4*, lanes 2 and 5). In contrast, pol β , pol λ , pol κ , pol η , pol ν , and pol θ performed DNA synthesis on the template RNA (*Figure 2.4*, lanes 3, 4, 6, 7, 8 and 9 and *Figure 2.5*). Pol β , and pol λ only synthesized one nucleotide with the substrates (*Figure 2.5A* and *2.5B*, lanes 2-6 and lanes 8-13). Pol β at 0.5 nM-25 nM resulted in up to 40% 1 nt gap-filling product with the substrate containing the THF residue (*Figure 2.5A*, lanes 2-6 and bar chart below the gel), whereas the same concentrations of the enzyme generated up to 60% synthesis product from the substrate without THF (*Figure 2.5 B*, lanes 2-6 and bar chart below the gel). Compared with pol β , pol λ exhibited weaker RNA-guided 1 nt gap-filling synthesis on the substrates (*Figure 2.5A*, lanes 8-11 and *Figure 2.5 B*, lanes 8-13, and bar charts below the gels). The enzyme at 0.1 nM-25 nM only generated up to 20% and 60% of products with the substrates (*Figure 2.5A* and *2.5B*, bar charts below the gels).

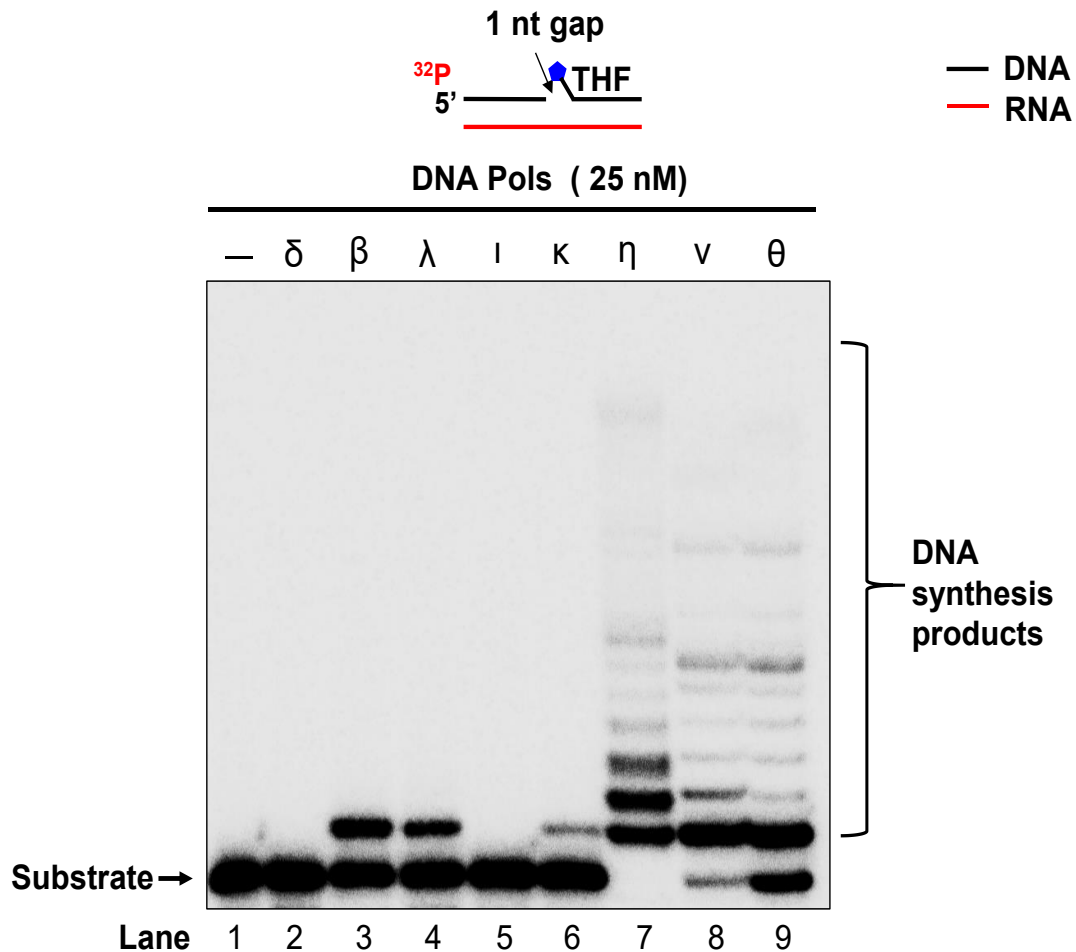


Figure 2.4. RNA template-dependent DNA repair.

RNA-dependent DNA repair synthesis by DNA polymerases using a one nucleotide gap substrate containing RNA as a template, DNA primer, and a THF residue in the downstream primer in the presence of a fixed concentration of dNTPs (50 μM) and fixed concentrations of DNA polymerases (25 nM).

Pol η , pol ν , and pol θ predominantly synthesized one nucleotide with the substrates while they managed to synthesize multiple nucleotides by strand-displacing the downstream primer (*Figure 2.5A*, lanes 13-18, 20-25, and 27-32, *Figure 2.5 B*, lanes 15-20, 22-27 and 29-34). Increasing concentrations of the polymerases (0.1 nM-25 nM) resulted in up to 80% of RNA-guided DNA synthesis products (*Figure 2.5 A* and 2.5 B, bar charts below the gels). The results indicated that pol β and pol λ performed 1 nt gap-filling synthesis. Pol η ,

pol ν , and pol θ performed both 1 nt gap-filling synthesis and strand-displacement synthesis. This notion was further supported by the results showing that pol β failed to synthesize DNA on the nick substrate (*Figure 2.6*, panel A), and pol η generated strand-displacement synthesis products on the nick substrate (*Figure 2.6*, panel B). The results further indicated that the RNA-guided DNA synthesis of pol β and pol λ was reduced by the presence of THF (compare *Figure 2.5 A*, lanes 2-6 and lanes 8-11 with *Figure 2.5 B*, lanes 2-6 and lanes 8-13) suggesting the 5'-deoxyribose phosphate can inhibit the DNA synthesis of the polymerases on the RNA template.

2.4.3. Steady-state kinetics of the RNA-guided DNA synthesis of repair and translesion DNA polymerases

To compare the catalytic efficiency of RNA-guided DNA synthesis on the 1 nt-gap substrates and open template substrates of pol β and pol η we performed the steady-state kinetics to determine the rate of RNA-guided DNA synthesis by pol η and pol β by varying the concentrations of dGTP (Table 2.2 and Table 2.3). The results indicated that pol β exhibited K_m , V_{max} , and k_{cat} for the 1 nt gap substrate without THF was $31.4 \pm 0.1 \times 10^{-2} \mu\text{M}$, $12.0 \pm 2.4 \times 10^{-11} \text{ M s}^{-1}$, and $1.2 \times 10^{-2} \text{ s}^{-1}$. For the substrate with THF, K_m , V_{max} , and k_{cat} were $33.5 \pm .03 \times 10^{-2} \mu\text{M}$, $7.0 \pm 0.0 \times 10^{-11} \text{ M s}^{-1}$, and $0.8 \times 10^{-2} \text{ s}^{-1}$ (Table 2.2). The catalytic efficiency, k_{cat}/K_m of pol β on the substrate without THF was 1.6-fold higher than

that with THF (Table 2.2). Pol η exhibited K_m , V_{max} , and k_{cat} of $5.8 \pm 0.9 \times 10^{-2} \mu\text{M}$, $13.2 \pm 0.4 \times 10^{-11} \text{ M s}^{-1}$, and $13.2 \times 10^{-2} \text{ s}^{-1}$ for the substrate without

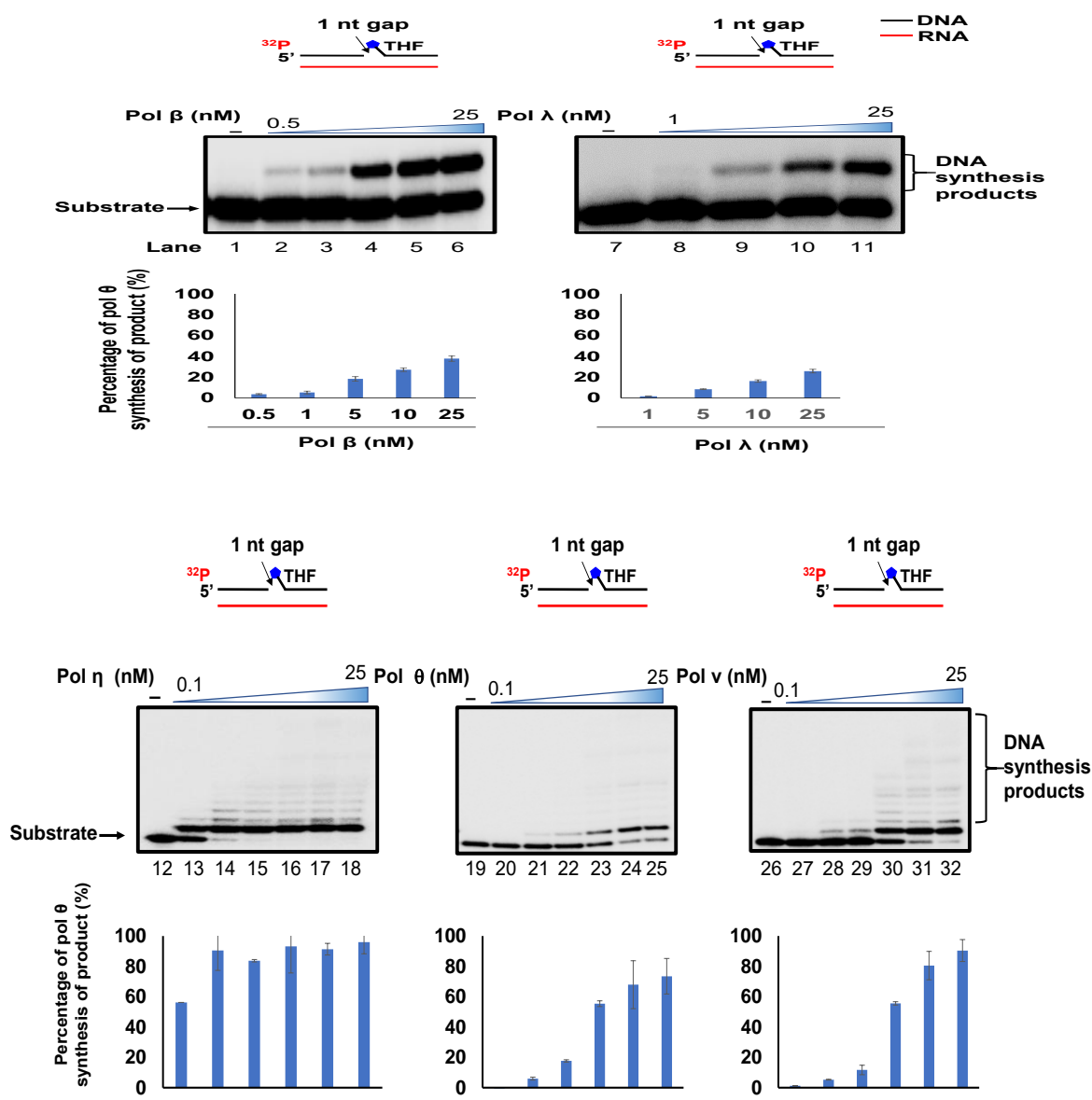


Figure 2.5. A. RNA dependent DNA repair.

RNA dependent DNA repair synthesis by DNA polymerases using a one nucleotide gap substrate containing RNA as a template, DNA primer and a THF residue in the downstream primer in the presence of a fixed concentration of dNTPS ($50 \mu\text{M}$) and increasing concentrations of the DNA polymerases (0.5, 1, 5, 10, and 25 nM for pol β , 1, 5, 10 and 25 nM for pol λ , and 0.1, 0.5, 1, 5, 10, and 25 nM for pol η , pol θ and pol ν). Lanes 2-6 represent the DNA synthesis by pol β . Lanes 7-11 represent the DNA synthesis by pol λ . Lanes 12-18 represent DNA synthesis by pol η . Lanes 19-25 represent DNA synthesis by pol θ . Lanes 26-32 represent DNA synthesis by pol ν . Lanes 1, 7, 12, 19 and 26 represent substrate only. All experiments were done in triplicate.

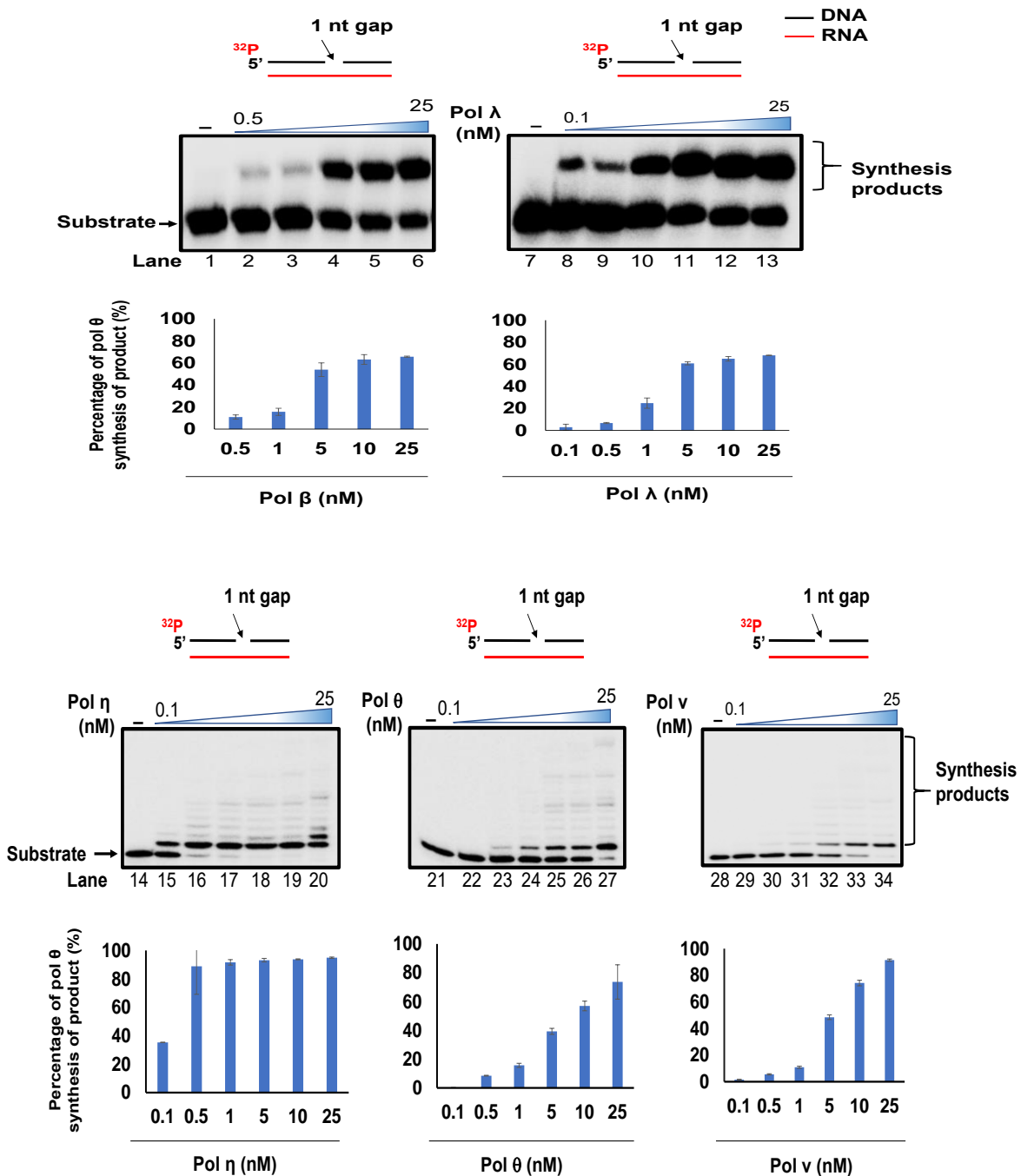


Figure 2.5 B. RNA-dependent DNA repair.

RNA dependent DNA repair synthesis by DNA polymerases using one nucleotide gap substrate containing RNA as a template, DNA primer, and phosphate at the 5'-end of the downstream primer in the presence of a fixed concentration of dNTPs (50 μM) and increasing concentrations of the DNA polymerases (0.5, 1, 5, 10, and 25 nM for pol β and 0.1, 0.5, 1, 5, 10, and 25 nM for pol λ , pol η , pol θ and pol ν). Lanes 2-6 represent the DNA synthesis by pol β . Lanes 7-13 represent the DNA synthesis by pol λ . Lanes 14-20 represent the DNA synthesis by pol η . Lanes 21-27 represent the DNA synthesis by pol θ . Lanes 28-34 represent the DNA synthesis by pol ν . Lanes 1, 7, 14, 21, and 28 represent substrate only. All experiments were done in triplicate.

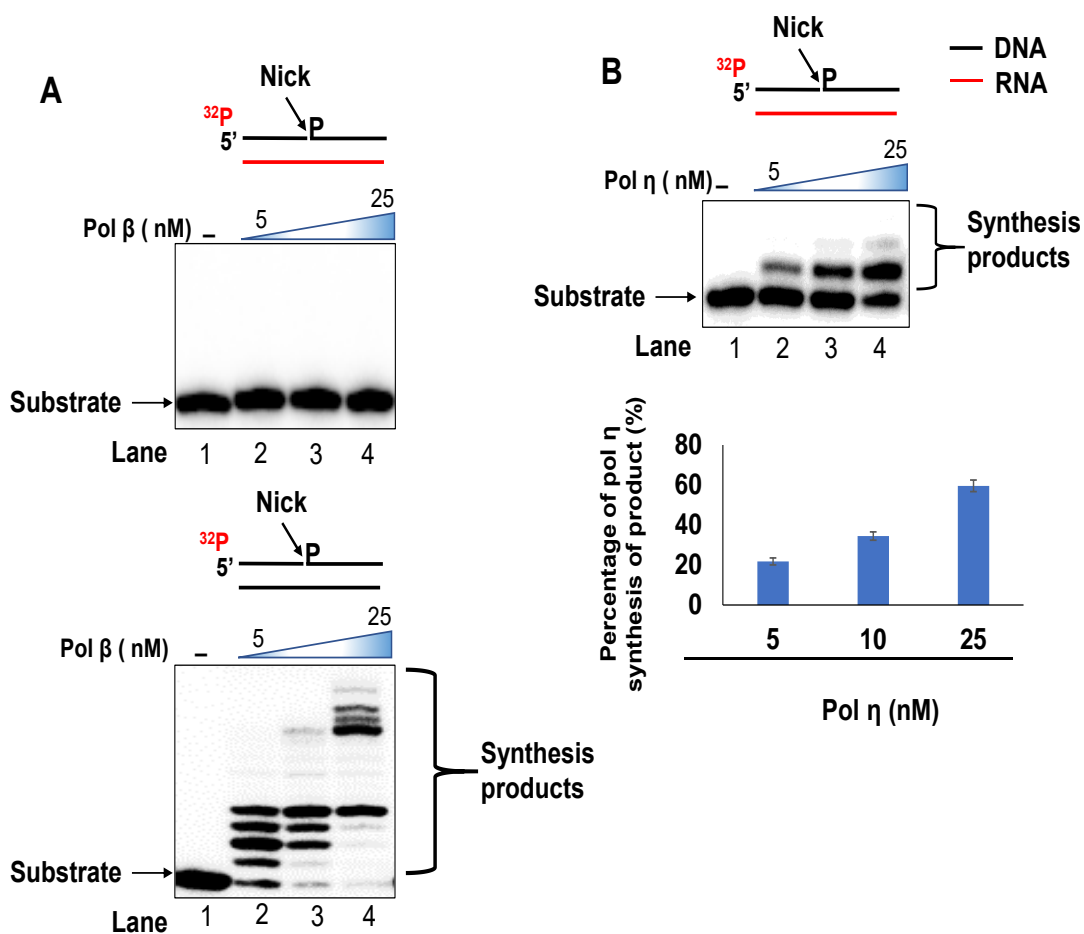


Figure 2.6. DNA synthesis on RNA-templated nick substrate.

RNA-dependent DNA repair synthesis by DNA polymerases using a nick substrate containing RNA as a template. **(A)** Lanes 2-4(top) represent no synthesis product on RNA template by pol β, and lanes 2-4 (bottom) represent synthesis product on template DNA. **(B)** Lanes 2-4 represent the synthesis product on RNA template by pol η.

THF and $4.1 \pm 1.3 \times 10^{-2} \mu\text{M}$, $15.6 \pm 1.4 \times 10^{-11} \text{M s}^{-1}$, and $15.6 \times 10^{-2} \text{s}^{-1}$ for the substrate with THF (Table 2.3). The catalytic efficiency, $k_{\text{cat}}/K_{\text{m}}$ of pol η for the substrate without and with THF was $22.7 \times 10^5 \text{M}^{-1} \text{S}^{-1}$ and $39 \times 10^5 \text{M}^{-1} \text{S}^{-1}$. In contrast to pol β, the catalytic efficiency of pol η for the substrate with THF was 1.7-fold higher than the substrate without THF (Table 2.3). The catalytic efficiency of pol η for the substrate without and with THF was 60-fold and 163-fold of pol β, respectively. The catalytic efficiency of pol η for the open template

was about 10-fold higher than that of the 1 nt gap substrate (Table 2.3). We also conducted steady-state kinetic experiments by varying the concentrations of the RNA template substrates. The results were consistent with those from varying concentrations of dGTP. The K_m , V_{max} , and k_{cat} for pol β on the substrate without THF was $1.7 \pm 0.1 \times 10^{-2} \mu\text{M}$, $2.9 \pm 0.1 \times 10^{-11} \text{ M s}^{-1}$, and $0.29 \times 10^{-2} \text{ s}^{-1}$, and those for the substrate with THF were $6.8 \pm 4.5 \times 10^{-2} \mu\text{M}$, $1.6 \pm 0.7 \times 10^{-11} \text{ M s}^{-1}$, and $0.16 \times 10^{-2} \text{ s}^{-1}$ (Table 2.4). The results led to 8-fold higher of catalytic efficiency, k_{cat}/K_m with the substrate without THF than with the residue (Table 2.4). For pol η , $10.1 \pm 2.6 k_{cat}$ from the substrate without THF were $3.4 \pm 0.5 \times 10^{-2} \mu\text{M}$, $15.2 \pm 1.2 \times 10^{-11} \text{ M s}^{-1}$, $15.2 \times 10^{-2} \text{ s}^{-1}$ that are comparable to those of $3.1 \pm 0.4 \times 10^{-2} \mu\text{M}$, $22.2 \pm 1.5 \times 10^{-11} \text{ M s}^{-1}$, and from the substrate with THF (Table 2.5). However, pol η exhibited K_m , V_{max} , and k_{cat} of $10.1 \pm 2.6 \times 10^{-2} \text{ s}^{-1}$, $53.9 \pm 9.8 \times 10^{-11} \text{ M s}^{-1}$, $53.9 \times 10^{-2} \text{ s}^{-1}$ on the open template substrate (Table 2.5). The catalytic efficiency, k_{cat}/K_m of pol η with the substrates are comparable with $44.9 \times 10^5 \text{ M}^{-1} \text{ s}^{-1}$, $70.5 \times 10^5 \text{ M}^{-1} \text{ s}^{-1}$, and $53.9 \times 10^5 \text{ M}^{-1} \text{ s}^{-1}$ for the 1 nt-gap substrate without or with THF and open template substrate (Table 2.5). The catalytic efficiency of pol η with 1 nt gap substrate without or with THF is 28-fold and 352-fold higher than that of pol β (Table 2.4 and 2.5). The results suggest that RNA-guided pol β gap-filling DNA synthesis was much less efficient than that of pol η . The pol β DNA synthesis was inhibited by the 5'-deoxyribose phosphate. In contrast, 5'-sugar-phosphate did not affect the RNA-guided gap-filling synthesis by Pol η exhibited comparable catalytic efficiency with both 1 nt-gap substrates and open-template substrate. The difference in the catalytic efficiency of the DNA polymerases may be attributed to the structural flexibility of pol η leading to a more open catalytic center than pol β .

Table 2.2. Table 2.3, Table 2.4, Table 2.5. Steady-state Kinetics of RNA guided DNA synthesis by pol β , η

Table 2.2 Steady-state kinetics of RNA-guided DNA synthesis by pol β

Substrate	K_M (10^{-2} μ M)	V_{max} (10^{-11} M S^{-1})	k_{CAT} (10^{-2} S^{-1})	k_{CAT}/K_M ($\times 10^5$ (M^{-1} S^{-1}))
1 nt gap dGTP	31.4 ± 1.3	12.0 ± 2.4	1.2	0.38
1 nt gap-THF dGTP	33.5 ± 0.3	8.0 ± 0.4	0.8	0.24
1 nt gap dGTP-DNA	13.5 ± 0.0	7.0 ± 0.0	70.0	51.8

Table 2.3 Steady-state kinetics of RNA-guided DNA synthesis by pol η

Substrate	K_M (10^{-2} μ M)	V_{max} (10^{-11} M S^{-1})	k_{CAT} (10^{-2} S^{-1})	k_{CAT}/K_M ($\times 10^5$ M^{-1} S^{-1})
1 nt gap dGTP	5.8 ± 0.9	13.2 ± 0.4	13.2	22.7
1 nt gap THF dGTP	4.1 ± 1.3	15.6 ± 1.4	15.6	39.0
Open template	0.4 ± 0.1	12.7 ± 0.4	12.7	317

The kinetic experiments for table I and II were performed by varying the concentrations of dGTP. All results are from at least three independent experiments.

Table 2.4 Steady-state kinetics of RNA-guided DNA synthesis by pol β

Substrate	K_M (10^{-2} μ M)	V_{max} (10^{-11} M s^{-1})	k_{CAT} (10^{-2} s^{-1})	k_{CAT}/K_M (10^5 M^{-1} s^{-1})
1 nt gap	1.7 ± 0.1	2.9 ± 0.1	0.29	1.6
1 nt gap-THF	6.8 ± 4.5	1.6 ± 0.7	0.16	0.2

Table 2.5 Steady-state kinetics of RNA-guided DNA synthesis by pol η

Substrate	K_M (10^{-2} μ M)	V_{max} (10^{-11} M s^{-1})	k_{CAT} (10^{-2} s^{-1})	k_{CAT}/K_M (10^5 M^{-1} s^{-1})
1 nt gap	3.4 ± 0.5	15.2 ± 1.2	15.2	44.9
1 nt gap-THF	3.1 ± 0.4	22.2 ± 1.5	22.2	70.5
Open template	10.1 ± 2.6	53.9 ± 9.8	53.9	53.1

The kinetic experiments for table III and IV were performed by varying the concentrations of the RNA template substrates. All results are from at least three independent experiments.

2.4.4. Molecular dynamic simulation reveals the mechanisms underlying RNA-dependent DNA synthesis by repair and translesion DNA synthesis polymerases

Employing the molecular dynamic simulation, we further explored the dynamic interaction between pol β and an RNA template and dCTP in 5 ns and 100 ns

(*Figure 2.7*). The molecular simulation at 100 ns revealed the dynamics illustrating a structural change from open to close polymerase conformation upon the occupancy of dCTP at the enzyme catalytic center (*Figure 2.7A*). The conformational change was demonstrated by the changes of the distance (A) between Arg40 and Asp276 and Try36 located at the α helix in the finger domain and Gua6 (*Figure 2.7A*). The results showed that the distance of Arg40-Asp276 and Try36-Gua6 started to decrease from 15A and reached 2.5 A or 0A at 22.5 ns indicating the polymerase used the α helix to close the catalytic center to hold dCTP. The closed conformation was sustained to 50 ns, and the distance between the residues was increased again to 15A and fluctuated between 5A to 7.5A indicating the opening of the enzyme. The open conformation of the polymerase lasted 22.5 ns and then went back to closed conformation (*Figure 2.7A*). The results indicate that pol β underwent a dynamic transition between closed and open conformation to accommodate the changes induced by the RNA template. Further analysis of the dynamic changes of the catalytic center of the polymerase indicated three hydrogen bonds formed between dCTP and dG on the RNA template (*Figure 2.7B*). However, the configuration of triphosphate of dCTP was orientated opposite to that on the DNA template (*Figure 2.7B*). The results suggest that the misorientation of the triphosphate significantly reduced the efficiency of the nucleotide incorporation.

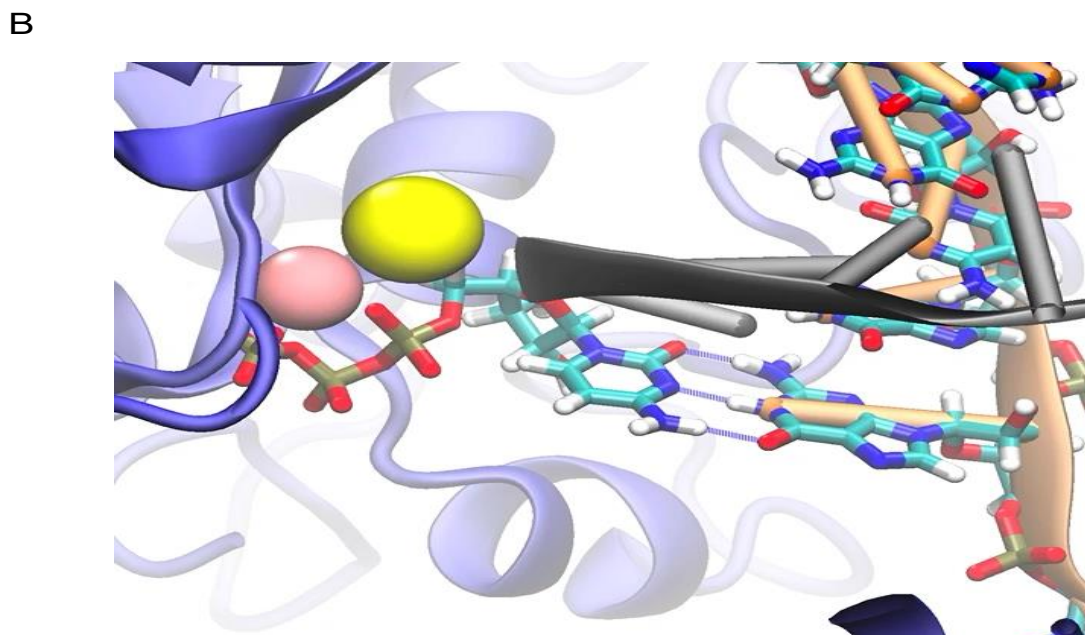
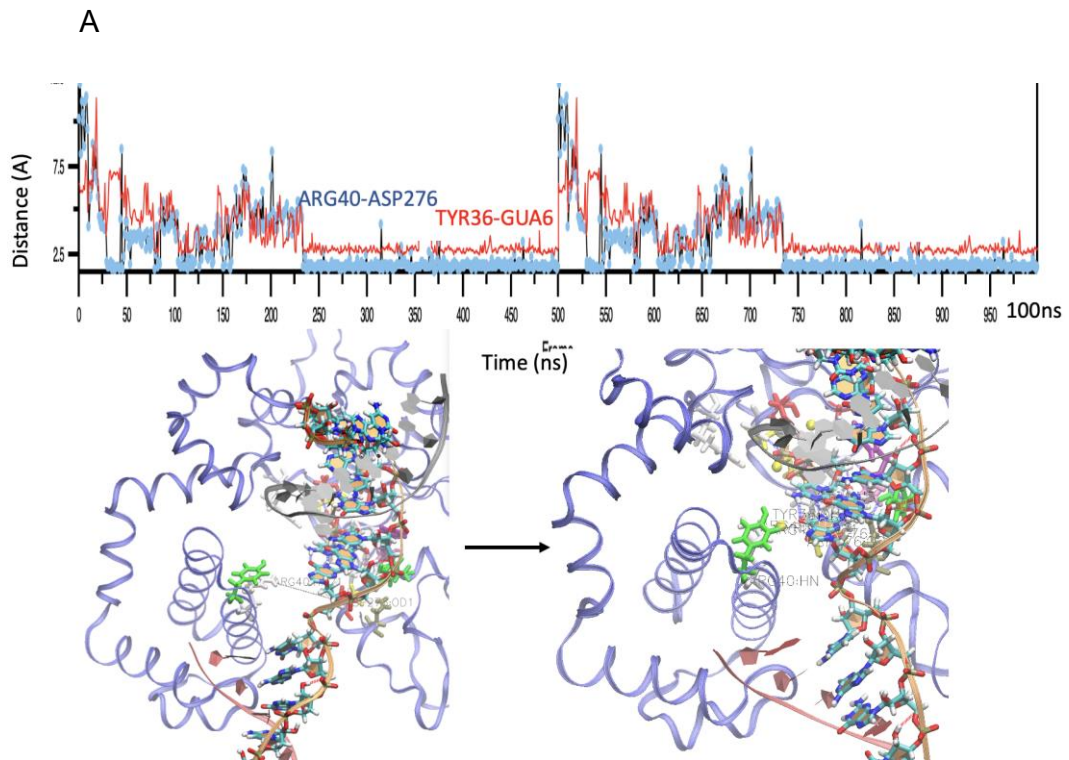


Figure 2.7. Molecular dynamics simulation of the ternary complexes of pol β with a 1 nt gap.

(A) Molecular simulation of pol β , 1 nt gap duplex DNA, and dCTP showing distance changes in angstrom (\AA) from open to close conformation (top). Structural change of the ternary complex from open to closed conformation (bottom). **(B)** Ternary structure of the complex showing the hydrogen bonds between the template dG and incoming dC.

2.4.5. A DNA nick on an RNA template is translocated into duplex DNA to be sealed by a DNA ligase

Since the completion of BER is accomplished by ligation of a nick, we then asked if the nick that is generated in the context of an RNA template can be ligated by DNA ligases. We examined the ligation of a DNA nick on an RNA template by DNA ligase I (LIG I) and DNA ligase III β (LIG III β) (*Figure 2.6*). We found that LIG I failed to seal the nick even at a high concentration of 50 nM (*Figure 2.8A*). However, LIG III β at 50 nM resulted in a small amount of ligation product (*Figure 2.8B*, lane 8). We further demonstrated that ligation only occurred at the double-strand DNA regions with at least six nucleotides away from an RNA template (*Figure 2.8D*). The results indicate that a DNA nick in the context of an RNA template was weakly ligated by LIG III β . The results further suggest that BER in the context of an RNA template is mainly accomplished by the ligation of a nick that is translocated into duplex DNA.

2.5. DISCUSSION

In this study, we characterized RNA-guided DNA synthesis by human DNA polymerases and discovered a new pathway of RNA-guided base lesion repair. Our results showed that pol β , pol λ , and pol κ only filled in 1 nt with an RNA template, whereas translesion DNA polymerases, pol η , pol θ , and pol ν performed DNA synthesis on the open RNA template and gap-filling and strand-displacement synthesis on the 1 nt gap substrates (*Figure 2.1-Figure 2.4*). The results indicated that DNA synthesis mediated RNA-guided base lesion repair

via gap-filling synthesis and strand-displacement synthesis. We found that pol η exhibited much higher efficiency to perform gap-filling and strand-displacement synthesis on the RNA template. However, our result also showed LIG I and LIG III β did not ligate RNA templated nicked DNA effectively (*Figure 2.8A and B*). The ligation of DNA nick only occurred at the regions of double-stranded DNA that was at least 6 nucleotides away from the RNA template (*Figure 2.8D*). The results indicated that nick had to be

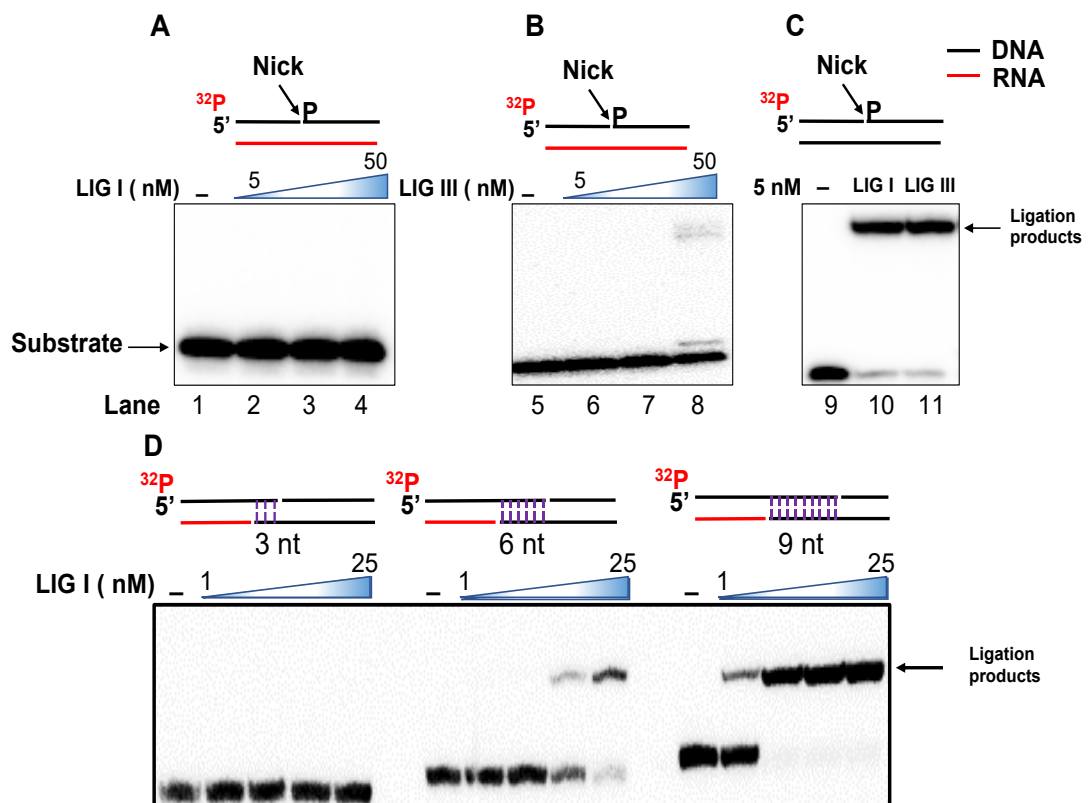


Figure 2.8. Ligation of RNA templated nick using titrated concentration of DNA ligases.

(A) Lig I cannot ligate DNA nick opposite RNA template, lanes 2 -4. (B) Lig III generate small ligation products at high concentration of the enzyme, lane 8. (C) Ligation products of Lig I and Lig III on DNA template, lanes 10 and 11. (D) DNA ligation of s nicked DNA downstream of the template RNA. Lanes 2 -5 show no ligation products of a nick translocated 3 nt to the duplex DNA. Lanes 12-15 shows ligation products translocated 9 nt to the duplex DNA. Lanes 7-10 shows ligation products translocated 6 nt to the duplex DNA.

translocated into the downstream region with a DNA template by strand-displacement synthesis of the DNA polymerases. Our results suggest that the completion of base lesion repair on the DNA template strand of an R-loop can be accomplished by the translation of a nick through RNA-guided strand-displacement synthesis mediated by translesion DNA polymerases to the double-strand DNA regions. Thus, our results support a model during which a DNA base lesion such as an abasic (AP) site on the DNA template strand of an R-loop is converted to 1 nt gap. Pol β fills the gap, switches with translesion DNA polymerases such as pol η , and dissociates from the RNA template. Subsequently, pol η performs strand-displacement synthesis leading to the formation of a nick-flap in regions with a DNA template that is removed by flap endonuclease 1 (FEN1). The resulted nick is then ligated by DNA ligases (*Figure 2.9*). Alternatively, pol η or other translesion DNA polymerases perform gap-filling synthesis and strand-displacement synthesis and generate a nick-flap in DNA template regions. Subsequently, FEN1 cleaves the flap leading to a nick that is sealed by DNA ligases (*Figure 2.9*)

Our steady-state kinetics results demonstrated that pol β exhibited less efficient gap-filling synthesis in the presence of 5'-THF than in the absence of the residue indicating that pol β DNA synthesis was inhibited by a deoxyribose phosphate residue (Table 2.2). Pol η , on the other hand, showed much more efficient DNA synthesis than pol β on the gap substrates but did not exhibit more efficient DNA synthesis with a THF than without the residue (Table 2.3). The results suggest that pol η exhibited more flexible structures at its catalytic center. The flexibility also confers the ability of the translesion synthesis polymerases to tolerate bulky DNA lesions (Johnson et al., 2000b; Masutani et

al., 1999a; Masutani et al., 1999b; Trincao et al., 2001), thereby accommodating the different configurations of ribonucleotides to execute DNA synthesis. Our results are consistent with the notion that the DNA damage tolerance nature of translesion DNA polymerases may help them synthesize RNA-templated DNA (Waters et al., 2009) and that the mutagenic translesion

DNA synthesis of the translesion DNA polymerase may also be modulated by RNA-guided DNA synthesis and DNA repair.

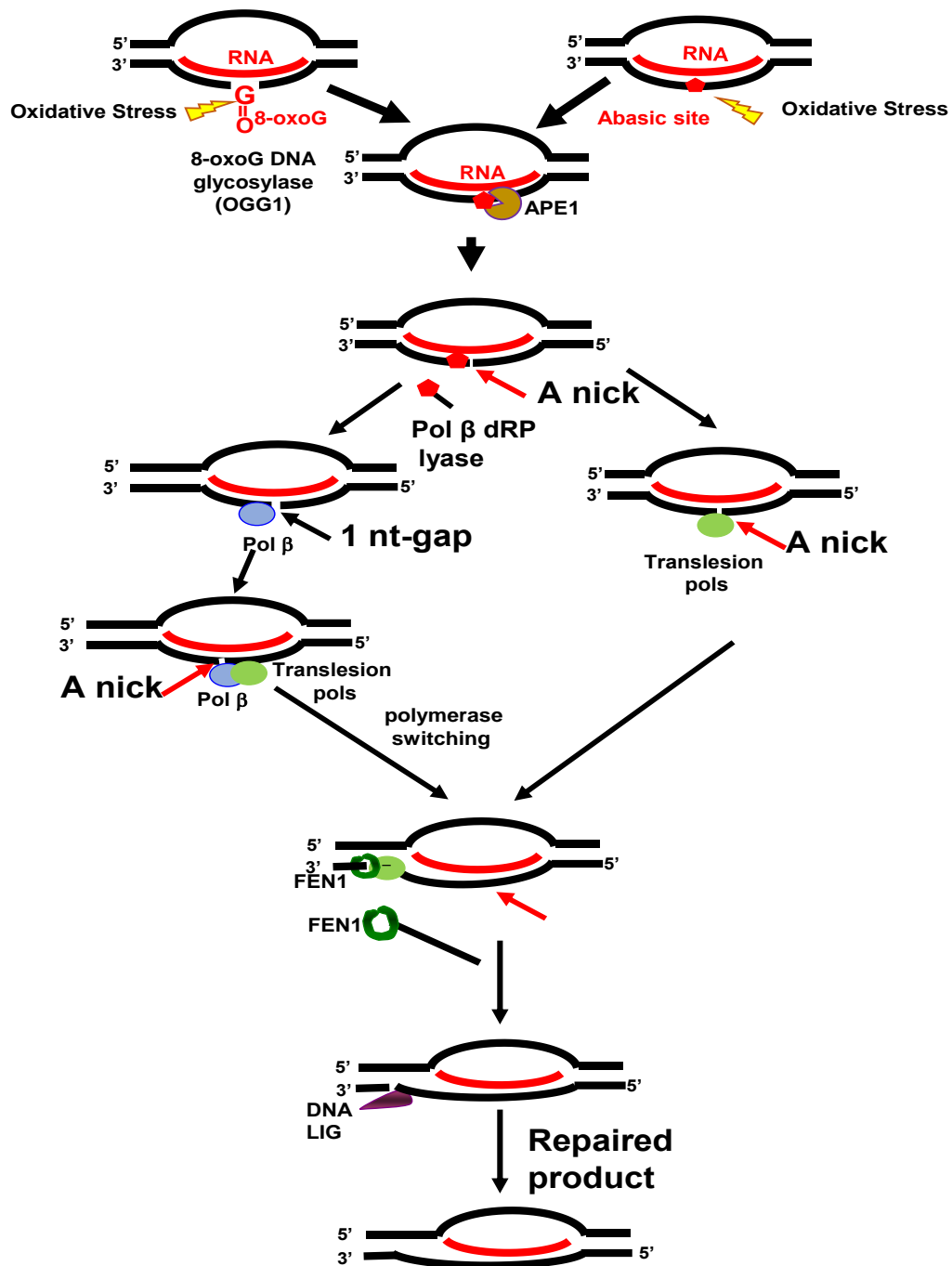


Figure 2.9. Hypothetical model for RNA guided DNA repair.

DNA damage on template DNA on DNA:RNA hybrid can be initiated by inserting one nucleotide by pol β followed by strand displacement by translesion DNA polymerases or strand displacement by translesion DNA polymerases to the region of duplex DNA. FEN 1 cleaves the flap, and DNA ligase ligate the nick.

In this study, we showed that human DNA replication polymerases, pol δ , and pol ϵ failed to synthesize DNA in the context of RNA template. This is in contrast to yeast DNA replication polymerases, which can synthesize RNA-guided DNA synthesis (Storici et al., 2007). The results indicate that the same class of DNA polymerases from different organisms can exhibit different activity on the RNA-guided DNA synthesis. Also, previous studies have demonstrated the ability of pol ι , and pol κ to synthesize DNA on an RNA template (Franklin et al., 2004; Murakami et al., 2003a). However, our results showed that pol ι failed to synthesize DNA using an RNA template (*Figure 2.1* and *Figure 2.3* lane 5). Moreover, we found that pol κ could only mediate RNA templated base lesion repair by predominantly synthesizing a single nucleotide (*Figure 2.1* and *Figure 2.2*, lanes 23-26). The discrepancy of the polymerases on RNA-guided DNA synthesis may be attributed to the difference in the experimental conditions between our study and previous studies.

Cells may potentially utilize the abundant RNA transcripts to repair DNA damage that occurs in RNA:DNA hybrids formed in highly transcribable genes and non-dividing cells to maintain their genome integrity. Our study further revealed how RNA-guided DNA repair is mediated by repair DNA polymerases. The fact that translesion DNA polymerases performed RNA-guided DNA synthesis on the HCV and COVID-19 genomic RNA sequences (*Figure 2.3*) suggests a potential role of translesion DNA polymerases in mediating the reverse transcription of virus genomic RNA and bypass of RNA base lesions, cDNA mutations during viral infection.

Future studies can be conducted to determine the efficiency of DNA synthesis and repair on template RNA by DNA polymerases and find factors that may influence the polymerases DNA synthesis and repair on template RNA.

3. CHAPTER 3. OXIDATIVE DNA DAMAGE ALTERS MIR-49-5P ASSOCIATED WITH DNA POLYMERASE β

3.1. ABSTRACT

MicroRNAs (miRNAs) are small non-coding RNAs, which can bind to mRNAs to promote their degradation leading to gene silencing. The upregulation of several miRNAs that regulate DNA repair proteins is associated with DNA damage, cancer development, and neurodegenerative diseases. However, the roles of the deregulation of these miRNAs in the disorders and the underlying molecular mechanism remain unknown. In this study, using human embryonic kidney 293 (HEK293) cells, we initially determined the modulatory effects of oxidative DNA damage on the level of miR-499a-5p and its-resulted downregulation of pol β . We then explored the mechanisms underlying the modulation of miR-499a-5p by oxidative DNA damage. We found that 5 mM KBrO₃ significantly increased the expression of miR-499a-5p at 12 and 24 hours of the treatment. Its level was decreased following recovery at 24 h and 48 h. In contrast, the level of pol β mRNA significantly reduced at 6 and 12 h and started to increase following 24 h of treatment and recovery. Pol β protein level decreased from 12 h following KBrO₃ treatment to 12 h of recovery. Further analysis on the profiles of DNA base lesions in the promoter region of miR-499a-5p using DNA damage landscape assay showed that dC and dG were the damaged bases at the promoter region of miR-499a-5p. We found that oxidative DNA damage regulates miR-499a-5p through OGG1 without affecting the DNA methylation pattern at the promoter region of the miRNA. We found that inhibition of OGG1 activity significantly reduced the miR-499-5p level

suggesting that OGG1 bound to 8-oxoGs induced by oxidative DNA damage at the promoter region of miR-499-5p, leading to its upregulation. Our results indicate that oxidative DNA damage deregulates the levels of miRNAs to alter the expression of DNA repair proteins. This may further result in the accumulation of DNA damage, promoting mutagenesis and carcinogenesis.

3.2. INTRODUCTION

microRNAs (miRNAs) are a group of short non-coding RNAs involved in RNA-mediated gene silencing and post-transcriptional regulation of gene expression. miRNAs are 18-22 nucleotides in length. They have sequence complementarity with the 3'-end of their targeted mRNAs. Therefore, they can bind to the targeted mRNAs to degrade the mRNAs and inhibit translation of proteins upon whether miRNAs have a perfect or imperfect complementarity with their targeted mRNAs (Bartel, 2004a; Mirihana Arachchilage et al., 2015; Perron and Provost, 2008; Saini et al., 2007). miRNAs are involved in multiple cellular functions. They play important roles in cell proliferation, differentiation, cell cycle progression, cellular stress response, and apoptosis (Leung and Sharp, 2010; Mendell and Olson, 2012; Olejniczak et al., 2018; Simone et al., 2009). Cellular stresses such as disease status, DNA damage, and invasion of pathogens can all affect cellular functions that are regulated by miRNAs through the deregulation of miRNA expression (Olejniczak et al., 2018). Previous studies have shown that the expression of miR-21-5p and miR155-5p that target the mismatch repair proteins, MSH2 and MSH6, and MLH1 are upregulated by oxidative DNA damaging agents such as H₂O₂ and radiation (Simone et al., 2009), suggesting that miRNAs serve as a cellular response to oxidative DNA

damage to regulate cellular DNA repair capacity. However, the upregulation of miRNAs that target BER proteins may lead to the downregulation of the proteins involved in BEE pathway. For example, upregulation of miR-140 represses breast cancer progression by inhibiting FEN1 expression (Lu et al., 2020). Similarly, increased expression of miR-499-5p that targets pol β , the core enzyme of BER, enhances the sensitivity of esophageal cancer cells to cisplatin (Wang et al., 2015). Thus, it is possible to develop an effective treatment for cancer by regulating miRNAs that target DNA repair genes. The complex nature of miRNA expression in tissue and DNA damaging agent-dependent manner makes it challenging to identify universal miRNAs as biomarkers of DNA damage and therapeutic targets of cancer and other diseases (Wang and Taniguchi, 2013). Therefore, extensive studies are required to create a network that illustrates the expression profiles of miRNAs as a response to different DNA damaging agents in a cell and tissue-specific manner. Although previous studies have shown oxidative DNA damage alters the level of several miRNAs, including miRNAs associated with DNA repair and DNA damage response proteins, the underlying molecular mechanisms for the deregulation of miRNAs induced by DNA damage remain unknown. Understanding the mechanisms is crucial for the identification of new therapeutic targets for cancer and other diseases. Because BER is responsible for repairing the most common forms of DNA damage, including base lesions, abasic sites, and single-strand breaks, the BER pathway is crucial to maintain genomic stability (Jobert et al., 2013; Kolodner and Marsischky, 1999; Krokan and Bjoras, 2013; Liu et al., 2017). Thus, the deregulation of miRNAs that target BER enzymes can impact the effectiveness of DNA repair and genomic stability. In this study, we asked if and

how oxidative DNA damage can affect the expression of miRNAs that can target BER proteins. We hypothesize that oxidative DNA damage occurs on the promoter regions of miRNAs to disrupt miR-499-5p expression leading to deregulation of BER proteins. We tested this hypothesis by determining how oxidative DNA damage can alter miRNA expression using human embryonic kidney cells (HEK293H) treated with potassium bromate (KBrO₃). Since KBrO₃ predominantly induce 8-oxoG (Kawanishi and Murata, 2006), and OGG1 can also serve as a transcription factor (Ba and Boldogh, 2018; Pan et al., 2017; Wang et al., 2018b) by binding to 8-oxoG, we further examined if KBrO₃-induced oxidative DNA damage could alter miR-499a-5p expression in an OGG1-dependent manner. We found that KBrO₃ upregulated miR-499-5p level and downregulated pol β expression level. We showed that the inhibitor of miR-499a-5p reduced the level of miR-499-5p and increased pol β mRNA level. We then determined the profiles of oxidative DNA base lesions at a single-base resolution in the promoter region of miR-499-5p using DNA damage landscape assay. The results showed that dGs and dCs were the major nucleotides damaged by KBrO₃. We further demonstrated that inhibition of OGG1 activity significantly decreased the level of miR-499a-5p and increased pol β expression. Our results revealed a novel mechanism for how oxidative DNA damage can modulate DNA repair by regulating cellular miRNA expression.

3.3. MATERIALS AND METHODS

3.3.1. Materials

HEK293H cells were purchased from Life Technologies (Carlsbad, CA, USA). Fetal bovine serum (FBS) and Dulbecco's Modified Eagle's Medium (DMEM)

high glucose cell culture medium was purchased from Thermo Fisher Scientific (Waltham, MA, USA). All other standard chemical reagents were from Thermo Fisher Scientific (Waltham, MA, USA) and Sigma-Aldrich (St. Louis, MO, USA).

The genomic DNA isolation kit was purchased from Promega (Madison, WI, USA). The iScript reverse transcription reagent and SYBR Green super mix reagent were purchased from Bio-Rad Laboratories (Hercules, CA, USA). The Lightning Bisulfite Conversion kit was purchased from ZYMO Research (Irvine, CA, USA). The Trizol reagents and the Dream Taq polymerase master mix, and the Original TA Cloning kit were from Invitrogen (Carlsbad, CA, USA). The Rapid DNA Ligation kit was from Thermo Scientific (Waltham, MA, USA).

Oligonucleotide primers for measuring miRNAs and mRNAs levels were synthesized by Integrated DNA Technologies (IDT, Coralville, IA, USA). Oligonucleotide primers for bisulfite-converted PCR and DNA damage landscape assay were purchased from Eurofins (Louisville, KY, USA)

Polyclonal anti-pol β primary antibody (ab26343), monoclonal anti-pol β primary antibody (ab175197), monoclonal anti-beta actin primary antibody (ab8226), polyclonal anti-mouse secondary antibody (ab6728), and monoclonal anti-goat secondary antibody (ab13537, Abcam, Cambridge, MA, USA) were from Abcam (Cambridge, MA, USA). Pierce protease inhibitor tablets and ECL reagent were purchased from Thermo Fisher Scientific (Waltham, MA, USA). OGG1 inhibitor was purchased from Tocris (Minneapolis, MN USA). miR-499a-5p inhibitor were purchased from Integrated DNA Technology (IDT).

3.3.2. Determination of miRNA and mRNA levels

HEK293H cells were grown in DMEM with 10% FBS to near confluence in 6 well plates. Cells were treated with 5 mM KBrO₃ for 0, 2, 6, 12, and 24 h. To measure miRNA and mRNA levels at 24 h and 48 h from the recovery of the treatment, cells were treated with 5 mM KBrO₃ for 24 h. Cells were then washed by 1× phosphate-buffered saline (PBS) twice and supplied with fresh culture medium for an additional 24 h and 48 h. To measure the effects of OGG1 inhibition on the level of miR-499-5p, cells were treated with the OGG1 inhibitor, TH5487 (1-10 μM) in the presence or absence of 5 mM KBrO₃. Cells were then harvested, and total RNA was isolated according to the protocol provided by the Invitrogen. The concentration of total RNA was determined using NanoDrop 2000c (Thermo Scientific, Waltham, MA, USA). 1 μg total RNA was used to synthesize cDNA using iScript in 20 μL reaction volume according to the manufacturer's protocol. Quantitative PCR was performed using SYBR Green Super mix (Bio-Rad Laboratories Hercules, CA, USA) in a 25 μL reaction mixture according to the manufacturer's protocols. mRNAs were amplified using a CFX Connect Real-Time PCR Detection System from Bio-Rad Laboratories (Hercules, CA, USA). Ct values that were recorded in CFX Manager Software (Bio-Rad Laboratories, Hercules, CA, USA) during PCR were used for data analysis to evaluate the fold-change between untreated samples and treated samples. The fold-change relative to the internal control (β-actin) was then calculated using $2^{-\Delta\Delta Ct}$

3.3.3. Determination of DNA damage profiles in the promoter region of miR-499a-5p

HEK293H cells were grown in DMEM with 10% FBS to near confluence in 6-well plates. Cells were then exposed to 5 or 10 mM KBrO₃ for 0, 2, 6, 12, and 24 hours. To measure the levels and profiles of oxidative DNA base lesions on the promoter region of miR-499a-5p for 24 h and 48 hours recovery of the treatment, cells treated with KBrO₃ 5 mM KBrO₃ for 24 h were washed by 1×phosphate-buffered saline (PBS) twice and supplied with fresh culture medium and were grown for an additional 24 h and 48 h. Cells were then harvested, and genomic DNA was isolated according to the protocol provided by the Promega genomic DNA isolation kit. The concentration of DNA was measured NanoDrop 2000c (Thermo Fisher Scientific, Waltham, MA, USA). 500 ng of DNA was used to determine the amount and profiles of the oxidized DNA base lesions using DNA damage landscape assay(Rubfiaro A S, 2021). The genomic DNA was treated with OGG1 and APE1 for 1 hour at 37°C to generate single-strand DNA (ssDNA) breaks. The fragmented single-stranded DNAs were converted to double-strand DNAs through reverse primer extension using a reverse primer and deep vent DNA polymerase (New England Biolabs, Boston, MA, USA).

3.3.4. Detection of pol β protein level using Immunoblotting

For detection of pol β in HEK293H cells using immunoblotting, 3 x10⁵ cells were seeded in 2 ml culture medium in a 6-well plate overnight. Cells were treated with 5 mM KBrO₃ for 12h and 24 h. Untreated cells were used as a control. The cells were washed with 1X PBS and collected in PBS and pelleted by

centrifugation at 3000 rpm for 5 min. The pellets were resuspended in ice-cold lysis buffer (0.1 % v/v NP-40, 20% v/v glycerol, 1 mM EDTA, 200 mM KCl and 10 mM Tris-HCl, pH 7.8). The cell lysates were subject to centrifugation at 12,000 rpm for 30 minutes. The supernatant of the lysates was collected. The protein concentrations of cell lysates were determined using the Bradford assay. Cell lysates (30 µg protein) were mixed with 2x loading buffer and denatured at 95°C for 5 min. Proteins were separated by SDS-PAGE and transferred onto PVDF membranes. β-actin was used as a loading control. The PVDF membrane was subject to the blocking in TBST (20 mM Tris-HCl, pH 7.6, 140 mM NaCl, 0.1% (v/v) Tween 20,) containing 1% (w/v) BSA and incubated with primary antibodies (1:1000) (Abcam, ab8226, Cambridge, MA) at 4 °C overnight. The membrane was then washed with TBST three times and was incubated with an HRP-labeled goat anti-mouse secondary antibody (1:10,000) (AbCam, ab6768, Cambridge, MA). The membrane was incubated with the ECL reagent (Pierce, Rockford, IL) for 5 min and exposed to an X-ray film (Fuji). The gel image was then developed by the Konica Minolta film developer (Konica Minota, Wayne, NJ).

3.3.5. Determination of DNA methylation pattern induced by oxidative DNA damage in HEK293H cells

HEK293H cells were grown in DMEM medium to near confluency and treated with 5 mM bromate, and harvested. Genomic DNA was isolated according to the protocol provided by the Promega genomic DNA isolation kit. Genomic DNA was then subject to bisulfite conversion with a Bisulfite Lightning Conversion kit purchased from ZYMO Research. The promoter region of the miR-499-5p gene

(-486 to -3) was amplified by PCR. The PCR products were then cloned into TA vector and sequenced at Florida International University DNA Sequencing Core using the BigDye kit purchased from ThermoFisher Scientific (Waltham, MA, USA).

3.3.6. Transfection of OGG1 siRNA and miR-499-5p inhibitor

HEK293H cells (3.75×10^5) were grown in DMEM with 10% FBS in 6-well plates. Cells were then treated with OGG1 siRNA or miR-499a-5p inhibitor using Lipofectamine™ RNAiMAX (Waltham, MA) according to manufacturers' instructions with or without the treatment of 5 mM KBrO₃. Cells treated with NC siRNA and NC miR inhibitor were used as a control. Cells were washed with 1X PBS, collected in PBS, and pelleted by centrifugation at 3000 rpm for 5 min. Total RNA was isolated according to the protocol provided by the Invitrogen. The concentrations of total RNA were measured using NanoDrop 2000c (Thermo Fisher Scientific, Waltham, MA, USA). 1 µg total RNA was used to synthesize cDNA using iScript 20 µL reaction volume according to the manufacturer's protocol. Quantitative PCR was performed using SYBR Green Super mix (Bio-Rad Laboratories Hercules, CA, USA) in a 25 µL reaction mixture according to the manufacturer's protocols. Samples were amplified using a CFX Connect Real-Time PCR Detection System from Bio-Rad Laboratories (Hercules, CA, USA). Ct values that were recorded in CFX Manager Software (Bio-Rad Laboratories, Hercules, CA, USA) during PCR were used for quantifying data to evaluate the fold change between untreated and treated samples. The fold-change relative to the internal control (β -actin) was then calculated using $2^{-\Delta\Delta Ct}$.

3.4. RESULTS

3.4.1. Oxidative DNA damage altered miR-499a-5p and pol β mRNA levels

To determine the effects of the oxidative DNA damage on the level of miR-499a-5p and mRNA level of pol β , HEK293H cells were treated with 5 mM KBrO₃ at different time intervals. The results showed that the level of miR-499a-5p was significantly increased at 12 h of treatment and continue to increase through 24 h of treatment and started to decrease at 24 h and 48 h of recovery (*Figure 3.1*, blue line). On the other hand, the pol β mRNA level started to decrease at 6 h and 12 h and continue to increase through 24 h of treatment and 24 h of recovery (*Figure 3.1*, red line). The continuous increment of miR-499-5p level throughout the treatment decreased pol β expression at 12 h, suggesting that cells responded to the decreased protein level of pol β by increasing its mRNA level to combat the reduced protein level resulting from oxidative DNA damage-induced miR-499a-5p. Since the upregulation of the miR-499-5p and decreased level of pol β mRNA level may impair DNA repair leading to the accumulation of DNA damage that can cause mutation and cancer development, our results further indicate that oxidative DNA damage can potentially induce genome and epigenome instability by upregulating miR-499-5p.

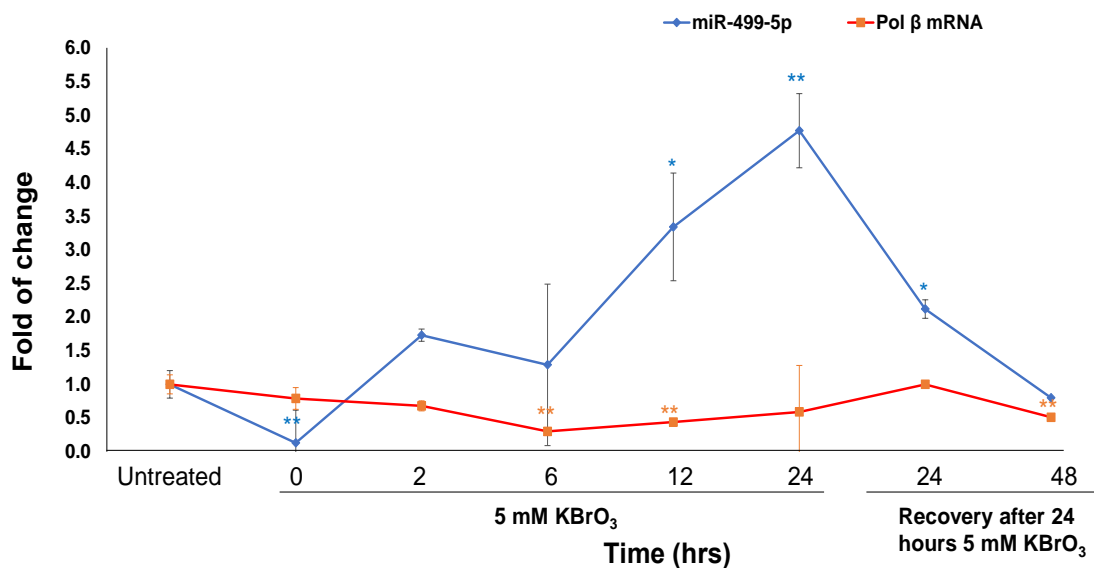


Figure 3.1. Oxidative DNA damage induces alteration of miR-499-5p to deregulate Pol β mRNA level. To test whether oxidative DNA damage alters miR-499-5p level, and this leads to deregulation of Pol β mRNA level, HEK293 cells were treated with 5 mM bromate at a different time frame. The levels of miR-499-5p and pol β mRNA in treated and untreated HEK293 cells was determined using reverse-transcribed qRT-PCR. Our result demonstrated that the levels of miR-499a-5p significantly decreased at 0 h, increased at 12 h and 24 h (blue line) (** P < 0.01) and decreased following recovery at 24 h and 48 h, while pol β mRNA level significantly decreased at 6h, 12 h and starts to increase at 24 h treatment (red line) (** P < 0.01). All experiments were repeated at least in triplicate.

3.4.2. Upregulation of miR-499a-5p leads to a decreased pol β protein level

We then examined if upregulation of miR-499a-5p induced by oxidative DNA damage could decrease the level of pol β protein using immunoblotting. HEK293H cells were treated with 5 mM KBrO₃ for 12 h and 24 h and then allowed to recover for 24 h and 48 h following 24 hours treatment as the miRNA-499-5p and pol β mRNA levels were altered at the times points of the treatments. We found that pol β protein level was significantly decreased at 12 h, 24 h of treatment without or with recovery (*Figure 3.2*).

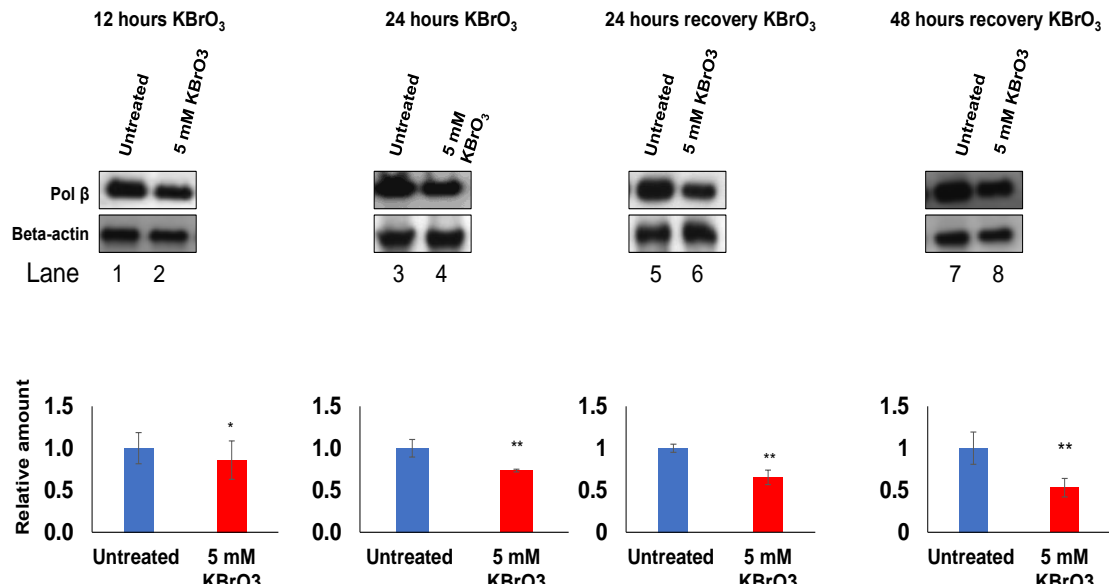


Figure 3.2. Oxidative DNA damage decreases pol β protein level. The protein level of pol β was detected by immunoblotting. The lysates of HEK293H cells without or with the treatment of 5 mM KBrO_3 were subjected to SDS-PAGE. β -actin was used as a control. Lane 2, 4, 6, and 8 represent pol β protein levels in cells treated by KBrO_3 for 12 h, 24 h, and 24- and 48-hours of recovery following 24 h KBrO_3 treatment respectively (the panel on the top). Lane 1, 3, 5, and 7 represent pol β protein levels in untreated cells (the panel on the top). β -actin protein level was used as a loading control. The quantification of the relative protein levels is shown below the gels. The blue bar represents the level of untreated HEK293H cells, whereas the red bar represents the level of pol β in treated HEK293 cells. “*”: $P < 0.05$. All experiments were performed in triplicate.

The pol β protein level remained to be low at 24 h and 48 h of recovery, although the miR-4991-5p level was decreased at 24 h of treatment, and pol β mRNA level was increased at 24 h recovery time (compare the results in Figure 3.1 with those in Figure 3.2). The results suggest that restoring pol β to the normal level in cells took extended recovery time from the treatment. The results further indicate that reduced pol β level could significantly compromise the cellular capacity of base lesion repair leading to the accumulation of DNA strand breaks and genome instability.

3.4.3. OGG1 regulates the expression of miR-499a-5p

We then explored the molecular mechanism by which oxidative DNA damage upregulated miR-499a-5p. We initially tested if the upregulation of miR-499a-5p can result from DNA hypomethylation at the promoter region of the miRNA caused by oxidative DNA damage as DNA methylation in the gene promoter

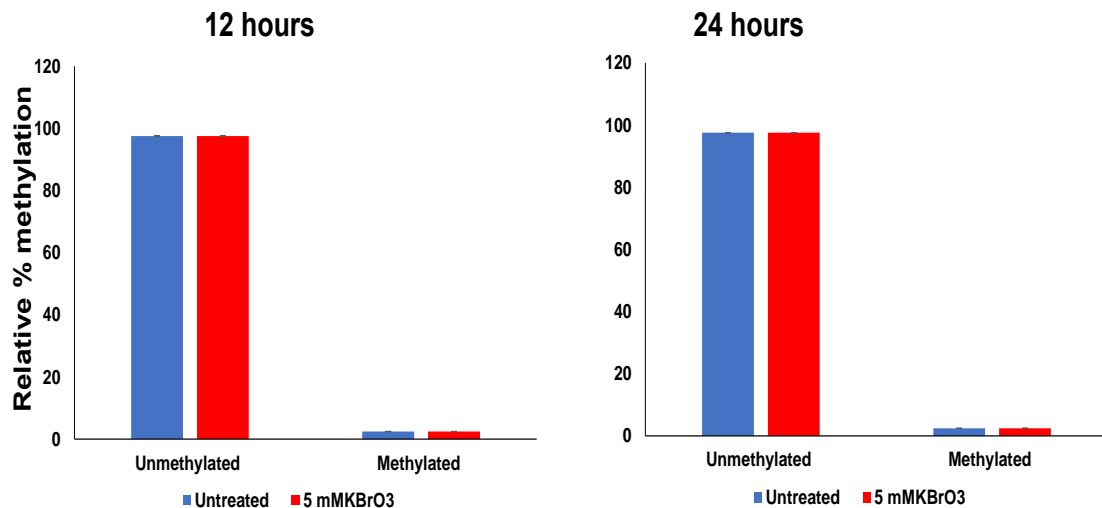


Figure 3.3 Oxidative DNA damage does not alter the DNA methylation pattern in the promoter region of miR-499-5p. HEK293H cells were treated with 5 mM KBrO₃ for 12 h and 24 h. Subsequently, genomic DNA was isolated from cells and subject to bisulfite sequencing. The bar graph represents the percentage of methylation in the promoter region of miR-499-5p (-3 to -483) in HEK293H cells without and with 5 mM bromate treatment. Blue charts represent the results from untreated cells. Red charts represent the results from cells treated by KBrO₃. At least 20 colonies were sequenced to calculate the percentage of methylated CpGs.

regions can be readily modulated by DNA damage and repair (Cortellino et al., 2011; Gong and Zhu, 2011; Niehrs, 2009; Okashita et al., 2014; Yang et al., 2011), and DNA methylation and demethylation play a critical role in regulating gene expression (Cortellino et al., 2011; Gong and Zhu, 2011). However, we found that there was no significant difference in the methylation pattern at the promoter region of miR-499-5p in H EK293H cells without and with KBrO₃

treatment (Figure 3.3). The results indicated that overexpression of miR-499a-5p resulting from KBrO₃-induced oxidative DNA damage was not associated with

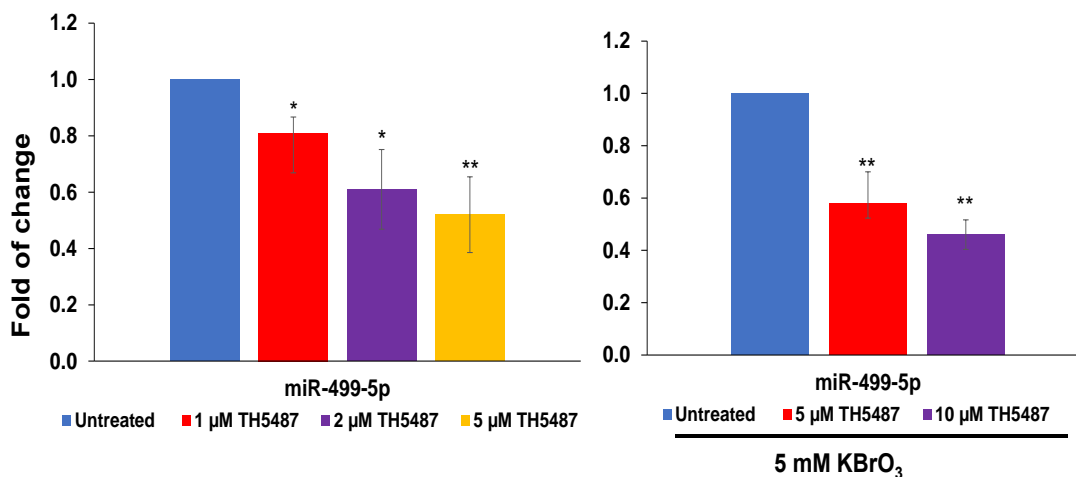


Figure 3.4. inhibition of OGG1 downregulated miR-499a-5p level. miR-499a-5p level in HEK293H cells treated with OGG1 inhibitor, TH5487 with or without KBrO₃ treatment was determined using RT-qPCR. The blue bar represents the relative miR-499a-5p level in untreated cells, and the other bars represent the level of the miRNA relative to that from cells treated with different concentrations of TH5487. The left graph shows miR-499a-5p levels in untreated cells and cells treated with 1, 2, and 5 μM TH5487. The panel on the right shows the level of the miRNA in cells treated with KBrO₃ along with 5 and 10 μM TH5487. “*”: P <0.05, “***”: P <0.01. All experiments were performed in triplicate.

DNA methylation at the promoter region of the miRNA. Since OGG1 can also exhibit the role of a transcription factor by binding to 8-oxoGs, and KBrO₃ primarily generates 8-oxoG (Kawanishi and Murata, 2006), it is possible that 8-oxoG may serve as an epigenetic mark for OGG1 to execute its transcription and epigenetic role. OGG1 is known to modulate the expression of several genes (Ba and Boldogh, 2018; Pan et al., 2017; Wang et al., 2018b). Thus, OGG1 may act as a transcription factor before it removes an 8-oxoG. We then hypothesized that OGG1 binds to the oxidized bases induced by oxidative DNA

damage to upregulate the miR-499a-5p level. To test this, we examined the effects of inhibition of OGG1 substrate binding and reduction of OGG1 protein on the level of miR-499a-5p in HEK293H cells using OGG1 substrate-binding inhibitor, TH5487 (Bristol, UK), and OGG1 gene knockdown using OGG1 siRNA (IDT, Coralville, IA, USA). We found that inhibition of OGG1 substrate binding by TH5487 significantly reduced the level of miR-499a-5p (*Figure 3.4*). However, knockdown of OGG1 at different concentrations of siRNA significantly increased the level of miR-499a-5p and decreased pol β mRNA level (*Figure 3.5*). The results suggest that the recognition and binding of OGG1 to 8-oxoGs play a critical role in upregulating miR-499a-5p in HEK293H cells, and the cells use alternative mechanisms to upregulate miR-499a-5p in the absence of OGG1 protein in responding to oxidative DNA damage. The results further suggest that the binding of OGG1 to 8-oxoG plays a vital role in mediating its role in gene regulation.

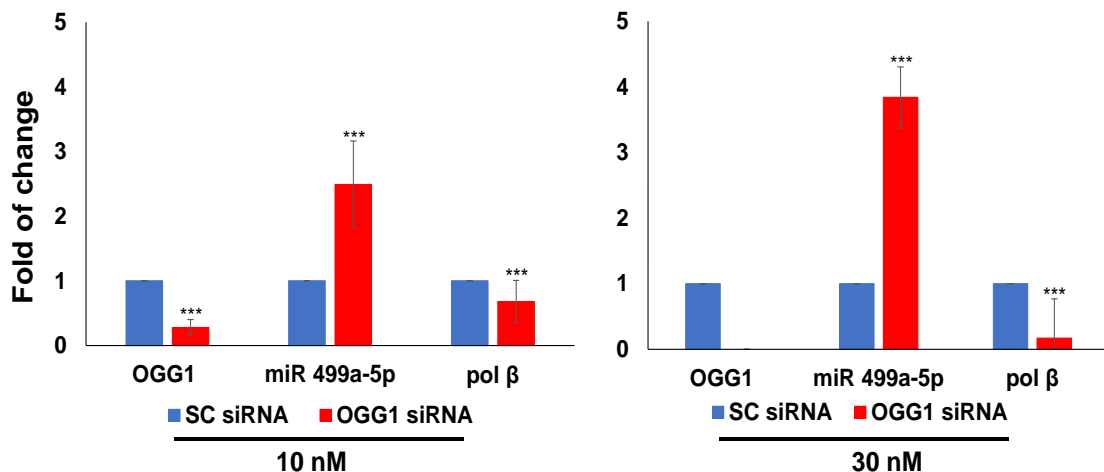


Figure 3.5 miR-499a-5p level is upregulated in OGG1 knockdown HEK293H cells.

HEK293H cells were transfected with 10 nM and 30 nM OGG1 siRNA. The level of miR-499a-5p, pol β , and OGG1 mRNA were determined. Cells transfected with scrambled siRNA (NC siRNA) were used as control. The blue and red bars represent the level of miR-499a-5p, pol β , and OGG1 mRNAs in

cells transfected with NCsiRNA and OGG1 siRNAs, respectively. The left panel shows the level of OGG1, miR-499-5p, and pol β mRNA levels in cells transfected with 10 nM siRNA and NCsiRNA, and the right panel shows the level of OGG1, miR-499-5p, and pol β mRNA levels in cells transfected with 30 nM siRNA transfected cells. “****”: $P < 0.001$. All experiments were performed in triplicate.

3.4.4. The profiles of oxidative DNA damage in the promoter region of miR-499a-5p.

We then mapped the profiles of oxidative DNA damage at the promoter region of miR-499-5p at a single-base resolution using a DNA damage landscape assay developed by the Liu laboratory (Rubfiaro A S, 2021). With this assay, the landscape profiles of the damaged bases in the promoter region of miR-499a-5p, and their level can be mapped based on the length of the DNA fragments generated by converting damaged bases located at different sites into single-strand breaks with BER enzymes. The DNA fragments were then amplified using PCR, and their length was determined by capillary electrophoresis-DNA fragment analysis. Our results demonstrated that guanines followed by cytosines are the majority of damaged bases in the promoter region of miR-499-5p in both untreated and KBrO_3 -treated HEK293H cells (*Figure 3.6*). The results further suggest that 8-oxoG is the most prominent oxidative base lesion generated at the promoter region of the miR-499a-5p. We further correlated the distribution of the base lesions at the promoter region of the miR-499a-5p with the level of the miRNA by dividing the promoter region into three regions, with each region containing 20 nucleotides. We found that the miRNA's percentage of damaged guanine and cytosine at the proximal promoter region (-23 nt to -43 nt) is positively correlated with the increase of the miRNA level

(Figure 3.7, panel on the right). The high percentage of damaged G and C was associated with the high level of miRNA (Figure 3.7, panels on the right). For the damage located at the middle (-43 nt to -63 nt) and distal (-63 nt to -83 nt) regions of the promoter of miR-499a-5p, increased

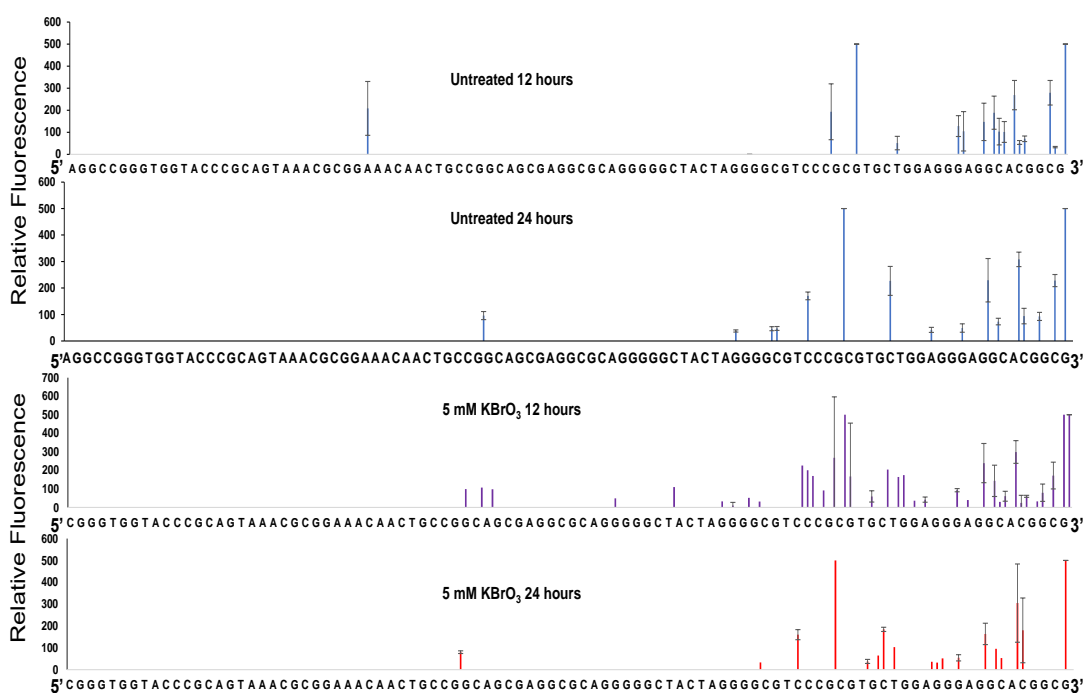


Figure 3.6. DNA damage landscape profiles at the promoter region of miR-499a-5p.

The DNA damage profiles were mapped using DNA damage landscape assay. The panels represent the profiles of DNA base damage in untreated cells and cells treated with 5 mM KBrO₃ 12 h and 24 h (panels from top to bottom). The peaks represent the abundance of DNA breaks generated from base damage at a specific nucleotide at the promoter region of miR-499a-5p. The profiles of base lesions are illustrated in a 5' to 3' direction. The height of the peaks indicates the amount of DNA base damage at specific nucleotide, and nucleotides across the promoter region of miR-499-5p. All experiments were performed in triplicate.

percentage of damaged C correlated with increased level of miR-449a-5p (Figure 3.7, panels on the right). The percentage of damaged G ranging from

2%-4% was correlated with increased miR-499a-5p. However, at a percentage higher than 4%, an increase of the percentage was correlated with decreased miR-449a-5p (*Figure 3.7*, panels in the middle). Increased percentage of damaged G at the distal region (-63 nt to -83 nt) was correlated with decreased miR-449a-5p (*Figure 3.7*, panel on the left). This suggests that the location of the base lesions in the promoter region of the miRNA plays a significant role in regulating the expression of the miRNA.

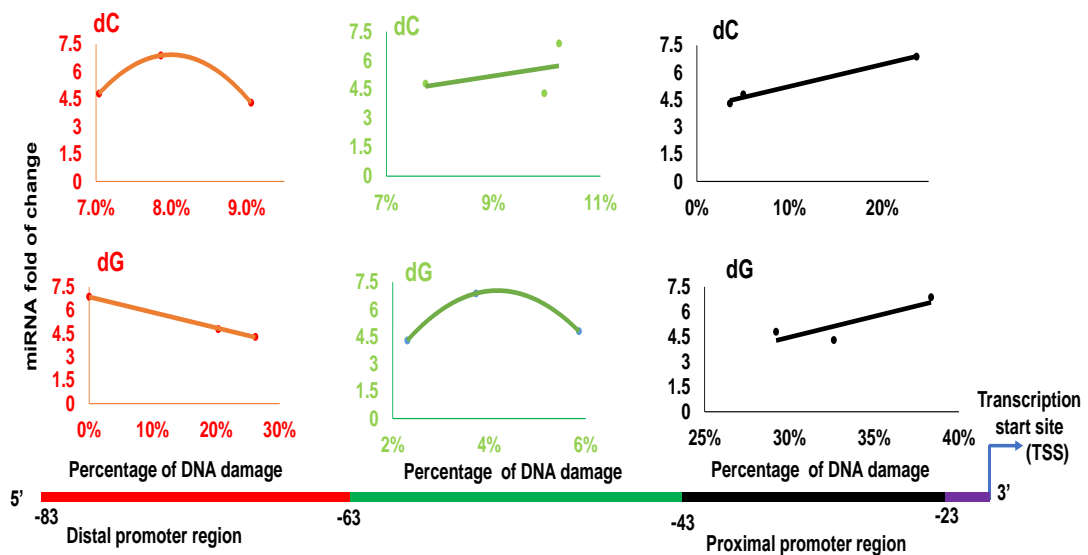


Figure 3.7 DNA base damage is correlated with the expression of miR-499a-5p. The percentage of DNA damage of dG and dC at different regions (proximal, -24 to -43, black, middle, -44 to -63, green, and distal, -64 to -83, red) of the promoter of miRNA-499-5p was correlated with the level of miR-499a-5p. The top panels represent the percentage of damaged C that is correlated with the level of the miRNA. The bottom panels represent the correlation of the percentage of damaged G with the level of the miRNA.

3.5. DISCUSSION

In this study, we explored the effects of oxidative DNA damage on miR-499a-5p expression and the underlying mechanisms. We found that oxidative DNA damage induced by KBrO₃ resulted in the upregulation of miR-499a-5p that in turn downregulated its target pol β expression (*Figure 3.1-Figure 3.2*). We showed that the upregulation of the miRNA was not due to the DNA methylation pattern change at the promoter region (*Figure 3.3*). Instead, the inhibition of OGG1 substrate-binding decreased miR-499a-5p expression independent of KBrO₃ treatment (*Figure 3.4*). Surprisingly, we found that the knockdown of OGG1 significantly increased the level of miR-499a (*Figure 3.5*). The results suggest that cells respond to oxidative DNA damage by overexpressing miR-499a-5p through alternative cellular pathways in the absence of OGG1. Our results provided the first evidence that OGG1 plays a crucial role in mediating cellular response to oxidative stress by regulating miRNA expression.

Our studies also showed that damaged DNA bases predominantly occurred at Gs and Cs at the promoter region of miR-499a-5p (*Figure 3.6*). The percentage of the damaged bases at various sections of the promoter region of the miRNA exhibited a correlation with the expression of miRNA. The results indicate that the locations of the base lesions in the promoter region of the miRNA regulated the expression of the miRNA in responding to oxidative DNA damage. Since 8-oxoG also exhibits an epigenetic function, modulation of OGG1 substrate binding and protein level may also affect the binding of other transcription activators, repressors, and mediators depending on which transcription factor binds at the specific motif that has base lesions.

Previous studies have shown that several genes involved in DNA damage response are regulated by miRNA. For example, miR-34 regulates the expression of p53 (He et al., 2007). miR-106b regulates p21-dependent checkpoint (Ivanovska et al., 2008). miR-15b regulates CDK5, and miR-24 regulates topoisomerase I and H₂AX. miR-26b regulates PTEN (Reasearch, 2008) and others. Here, our results showed the regulation of pol β by miR-499a-5p. Future studies should focus on understanding how this may affect DNA repair capacity.

Since majority of miRNAs are induced in responding to oxidative stress, radiation, and direct DNA damage (Simone et al., 2009), many of the DNA processing pathways may be altered by the deregulation of miRNAs. Although previous studies have shown the deregulation of several miRNAs is involved in responding to different sources of DNA damage, the molecular mechanism by which DNA damage alters the expression of the miRNAs remains elusive. Here, we showed that one possible mechanism of upregulation of miRNA during oxidative DNA damage is mediated by OGG1 substrate binding. As miRNAs response is tissue-specific and DNA damage specific (Wang and Taniguchi, 2013), further studies are needed to understand the association between the modulation of miRNAs and disease development and prevention.

Previous study has shown upregulation of miR-499a-5p enhances cisplatin sensitivity of esophageal carcinoma cells by downregulating the expression of pol β , the core BER enzyme. Our results also showed that upregulation of miR-499a-5p induced by KBrO₃ downregulated the expression of pol β . Subsequently, this may impair BER leading to the accumulation of DNA

damage, DNA breaks, mutations, and genome instability. Considering BER is the major DNA repair mechanism for more than 20, 000 bases lesions generated each day per cell (Barnes and Lindahl, 2004), the outcome of impaired BER would be expected to have a deleterious effect on genome integrity and stability.

REFERENCE

- Abraham, J., and Brooks, P.J. (2011). Divergent effects of oxidatively induced modification to the C8 of. *Environ Mol Mutagen* 52, 287-295.
- Acharya, P.N. (1976). 10th International Congress of Biochemistry. Hamburg, Germany
- Aguilera, A., and Garcia-Muse, T. (2012). R loops: from transcription byproducts to threats to genome stability. *Mol Cell* 46, 115-124.
- Aguilera, A., and Gomez-Gonzalez, B. (2008). Genome instability: a mechanistic view of its causes and consequences. *Nat Rev Genet* 9, 204-217.
- Ahmad, M.K., Amani, S., and Mahmood, R. (2014). Potassium bromate causes cell lysis and induces oxidative stress in human erythrocytes. *Environ Toxicol* 29, 138-145.
- Ahmad, M.K., and Mahmood, R. (2012). Oral administration of potassium bromate, a major water disinfection by-product, induces oxidative stress and impairs the antioxidant power of rat blood. *Chemosphere* 87, 750-756.
- Ahmad, M.K., Naqshbandi, A., Fareed, M., and Mahmood, R. (2012). Oral administration of a nephrotoxic dose of potassium bromate, a food additive, alters renal redox and metabolic status and inhibits brush border membrane enzymes in rats. *Food Chem* 134, 980-985.
- Ajarem, J., Altoom, N.G., Allam, A.A., Maodaa, S.N., Abdel-Maksoud, M.A., and Chow, B.K. (2016). Oral administration of potassium bromate induces neurobehavioral changes, alters cerebral neurotransmitters level and impairs brain tissue of swiss mice. *Behav Brain Funct* 12, 14.
- Ana L. Zamora Perez, G.M.Z.G., Belinda C. Gómez Meda, Blanca P (2016). Periodontal Disease and Nuclear and Oxidative DNA Damage. *IntechOpen* 2, 29-30.
- Anglana, M., Apiou, F., Bensimon, A., and Debatisse, M. (2003). Dynamics of DNA replication in mammalian somatic cells: nucleotide pool modulates origin choice and interorigin spacing. *Cell* 114, 385-394.
- Auerbach, P., Bennett, R.A., Bailey, E.A., Krokan, H.E., and Demple, B. (2005). Mutagenic specificity of endogenously generated abasic sites in *Saccharomyces cerevisiae* chromosomal DNA. *Proc Natl Acad Sci U S A* 102, 17711-17716.
- Autexier, C., and Lue, N.F. (2006). The structure and function of telomerase reverse transcriptase. *Annu Rev Biochem* 75, 493-517.
- Ba, X., and Boldogh, I. (2018). 8-Oxoguanine DNA glycosylase 1: Beyond repair of the oxidatively modified base lesions. *Redox Biol* 14, 669-678.

- Bai, G., Smolka, M.B., and Schimenti, J.C. (2016). Chronic DNA Replication Stress Reduces Replicative Lifespan of Cells by TRP53-Dependent, microRNA-Assisted MCM2-7 Downregulation. *PLoS Genet* 12, e1005787.
- Bailly, V., Derydt, M., and Verly, W.G. (1989). Delta-elimination in the repair of AP (apurinic/aprimidinic) sites in DNA. *Biochem J* 261, 707-713.
- Bailly, V., and Verly, W.G. (1988). Possible roles of beta-elimination and delta-elimination reactions in the repair of DNA containing AP (apurinic/aprimidinic) sites in mammalian cells. *Biochem J* 253, 553-559.
- Baltimore, D. (1985). Retroviruses and retrotransposons: the role of reverse transcription in shaping the eukaryotic genome. *Cell* 40, 481-482.
- Bannister, A.J., and Kouzarides, T. (2011). Regulation of chromatin by histone modifications. *Cell Res* 21, 381-395.
- Barnes, D.E., and Lindahl, T. (2004). Repair and genetic consequences of endogenous DNA base damage in mammalian cells. *Annu Rev Genet* 38, 445-476.
- Bartek, J., Lukas, C., and Lukas, J. (2004). Checking on DNA damage in S phase. *Nat Rev Mol Cell Biol* 5, 792-804.
- Bartel, D.P. (2004a). MicroRNAs: Genomics, biogenesis, mechanism, and function. *Cell* 116, 281-297.
- Bartel, D.P. (2004b). MicroRNAs: genomics, biogenesis, mechanism, and function. *Cell* 116, 281-297.
- Beard, W.A., Osheroff, W.P., Prasad, R., Sawaya, M.R., Jaju, M., Wood, T.G., Kraut, J., Kunkel, T.A., and Wilson, S.H. (1996). Enzyme-DNA interactions required for efficient nucleotide incorporation and discrimination in human DNA polymerase beta. *J Biol Chem* 271, 12141-12144.
- Beard, W.A., and Wilson, S.H. (2006). Structure and mechanism of DNA polymerase Beta. *Chem Rev* 106, 361-382.
- Beard, W.A., and Wilson, S.H. (2014). Structure and mechanism of DNA polymerase beta. *Biochemistry* 53, 2768-2780.
- Beaver, J.M., Lai, Y., Xu, M., Casin, A.H., Laverde, E.E., and Liu, Y. (2015). AP endonuclease 1 prevents trinucleotide repeat expansion via a novel mechanism during base excision repair. *Nucleic Acids Res* 43, 5948-5960.
- Bennett, R.A., Wilson, D.M., 3rd, Wong, D., and Demple, B. (1997). Interaction of human apurinic endonuclease and DNA polymerase beta in the base excision repair pathway. *Proc Natl Acad Sci U S A* 94, 7166-7169.
- Bernstein, B.E., Kamal, M., Lindblad-Toh, K., Bekiranov, S., Bailey, D.K., Huebert, D.J., McMahon, S., Karlsson, E.K., Kulbokas, E.J., Gingeras, T.R., et

al. (2005). Genomic maps and comparative analysis of histone modifications in human and mouse. *Cell* 120, 169-181.

Bernstein, K.A., Gangloff, S., and Rothstein, R. (2010). The RecQ DNA Helicases in DNA Repair. *Annu Rev Genet* 44, 393-417.

Bessman, M.J., Lehman, I.R., Adler, J., Zimmerman, S.B., Simms, E.S., and Kornberg, A. (1958). Enzymatic Synthesis of Deoxyribonucleic Acid. Iii. The Incorporation of Pyrimidine and Purine Analogues into Deoxyribonucleic Acid. *Proc Natl Acad Sci U S A* 44, 633-640.

Bester, A.C., Roniger, M., Oren, Y.S., Im, M.M., Sarni, D., Chaoat, M., Bensimon, A., Zamir, G., Shewach, D.S., and Kerem, B. (2011). Nucleotide deficiency promotes genomic instability in early stages of cancer development. *Cell* 145, 435-446.

Biade, S., Sobol, R.W., Wilson, S.H., and Matsumoto, Y. (1998). Impairment of proliferating cell nuclear antigen-dependent apurinic/aprimidinic site repair on linear DNA. *J Biol Chem* 273, 898-902.

Birincioglu, M., Jaruga, P., Chowdhury, G., Rodriguez, H., Dizdaroglu, M., and Gates, K.S. (2003). DNA base damage by the antitumor agent 3-amino-1,2,4-benzotriazine 1,4-dioxide (tirapazamine). *J Am Chem Soc* 125, 11607-11615.

Blackburn, E.H. (1992). Telomerases. *Annu Rev Biochem* 61, 113-129.

Boguszewska, K., Szewczuk, M., Kazmierczak-Baranska, J., and Karwowski, B.T. (2021). How (5'S) and (5'R) 5',8-Cyclo-2'-Deoxypurines Affect Base Excision Repair of Clustered DNA Damage in Nuclear Extracts of *xrs5* Cells? A Biochemical Study. *Cells* 10(4):725.

Boiteux, S., and Guillet, M. (2004). Abasic sites in DNA: repair and biological consequences in *Saccharomyces cerevisiae*. *DNA Repair (Amst)* 3, 1-12.

Brambati, A., Zardoni, L., Nardini, E., Pellicioli, A., and Liberi, G. (2020). The dark side of RNA:DNA hybrids. *Mutat Res* 784, 108300.

Breitling, L.P., Yang, R., Korn, B., Burwinkel, B., and Brenner, H. (2011). Tobacco-smoking-related differential DNA methylation: 27K discovery and replication. *Am J Hum Genet* 88, 450-457.

Brooks, P.J. (2008). The 8,5'-cyclopurine-2'-deoxynucleosides: candidate neurodegenerative DNA lesions in xeroderma pigmentosum, and unique probes of transcription and nucleotide excision repair. *DNA Repair (Amst)* 7, 1168-1179.

Brooks, P.J., Wise, D.S., Berry, D.A., Kosmoski, J.V., Smerdon, M.J., Somers, R.L., Mackie, H., Spoonde, A.Y., Ackerman, E.J., Coleman, K., *et al.* (2000). The oxidative DNA lesion 8,5'-(S)-cyclo-2'-deoxyadenosine is repaired by the nucleotide excision repair pathway and blocks gene expression in mammalian cells. *J Biol Chem* 275, 22355-22362.

Brooks, S.C., Adhikary, S., Rubinson, E.H., and Eichman, B.F. (2013). Recent advances in the structural mechanisms of DNA glycosylases. *Biochim Biophys Acta* 1834, 247-271.

Bueno, M.J., Gomez de Cedron, M., Laresgoiti, U., Fernandez-Piqueras, J., Zubiaga, A.M., and Malumbres, M. (2010). Multiple E2F-induced microRNAs prevent replicative stress in response to mitogenic signaling. *Mol Cell Biol* 30, 2983-2995.

Cadet, J., Delatour, T., Douki, T., Gasparutto, D., Pouget, J.P., Ravanat, J.L., and Sauvaigo, S. (1999). Hydroxyl radicals and DNA base damage. *Mutat Res* 424, 9-21.

Cadet, J., Douki, T., Gasparutto, D., and Ravanat, J.L. (2003). Oxidative damage to DNA: formation, measurement and biochemical features. *Mutation research* 531, 5-23.

Caglayan, M., Horton, J.K., Dai, D.P., Stefanick, D.F., and Wilson, S.H. (2017). Oxidized nucleotide insertion by pol beta confounds ligation during base excision repair. *Nat Commun* 8, 14045.

Campbell, K.C. (2006). Bromate-induced ototoxicity. *Toxicology* 221, 205-211.

Cappelli, E., Taylor, R., Cevasco, M., Abbondandolo, A., Caldecott, K., and Frosina, G. (1997). Involvement of XRCC1 and DNA ligase III gene products in DNA base excision repair. *J Biol Chem* 272, 23970-23975.

Carthew, R.W., and Sontheimer, E.J. (2009). Origins and Mechanisms of miRNAs and siRNAs. *Cell* 136, 642-655.

Chabosseau, P., Buhagiar-Labarchede, G., Onclercq-Delic, R., Lambert, S., Debatisse, M., Brison, O., and Amor-Gueret, M. (2011). Pyrimidine pool imbalance induced by BLM helicase deficiency contributes to genetic instability in Bloom syndrome. *Nat Commun* 2, 368.

Chagovetz, A.M., Sweasy, J.B., and Preston, B.D. (1997). Increased activity and fidelity of DNA polymerase beta on single-nucleotide gapped DNA. *J Biol Chem* 272, 27501-27504.

Chandramouly, G., Zhao, J., McDevitt, S., Rusanov, T., Hoang, T., Borisonnik, N., Treddinick, T., Lopezcolorado, F.W., Kent, T., Siddique, L.A., *et al.* (2021). Poltheta reverse transcribes RNA and promotes RNA-templated DNA repair. *Sci Adv* 7.

Chatgililoglu, C., Bazzanini, R., Jimenez, L.B., and Miranda, M.A. (2007). (5'S)- and (5'R)-5',8-cyclo-2'-deoxyguanosine: mechanistic insights on the 2'-deoxyguanosin-5'-yl radical cyclization. *Chem Res Toxicol* 20, 1820-1824.

Chatgililoglu, C., D'Angelantonio, M., Kciuk, G., and Bobrowski, K. (2011). New insights into the reaction paths of hydroxyl radicals with 2'-deoxyguanosine. *Chem Res Toxicol* 24, 2200-2206.

Chatgialloglu, C., Ferreri, C., Geacintov, N.E., Krokidis, M.G., Liu, Y., Masi, A., Shafirovich, V., Terzidis, M.A., and Tsegay, P.S. (2019). 5',8-Cyclopurine Lesions in DNA Damage: Chemical, Analytical, Biological, and Diagnostic Significance. *Cells* 8(6):513.

Chaudhuri, A.R., Callen, E., Ding, X., Gogola, E., Duarte, A.A., Lee, J.E., Wong, N., Lafarga, V., Calvo, J.A., Panzarino, N.J., *et al.* (2016). Replication fork stability confers chemoresistance in BRCA-deficient cells. *Nature* 539, 456-456.

Chen, C.W., Tsao, N., Huang, L.Y., Yen, Y., Liu, X., Lehman, C., Wang, Y.H., Tseng, M.C., Chen, Y.J., Ho, Y.C., *et al.* (2016). The Impact of dUTPase on Ribonucleotide Reductase-Induced Genome Instability in Cancer Cells. *Cell Rep* 16, 1287-1299.

Chun, A.C., and Jin, D.Y. (2010). Ubiquitin-dependent regulation of translesion polymerases. *Biochem Soc Trans* 38, 110-115.

Clemente-Ruiz, M., and Prado, F. (2009). Chromatin assembly controls replication fork stability. *Embo Reports* 10, 790-796.

Clifford, R., Louis, T., Robbe, P., Ackroyd, S., Burns, A., Timbs, A.T., Wright Colopy, G., Dreau, H., Sigaux, F., Judde, J.G., *et al.* (2014). SAMHD1 is mutated recurrently in chronic lymphocytic leukemia and is involved in response to DNA damage. *Blood* 123, 1021-1031.

Constantin, N., Dzantiev, L., Kadyrov, F.A., and Modrich, P. (2005). Human mismatch repair: reconstitution of a nick-directed bidirectional reaction. *J Biol Chem* 280, 39752-39761.

Cortellino, S., Xu, J., Sannai, M., Moore, R., Caretti, E., Cigliano, A., Le Coz, M., Devarajan, K., Wessels, A., Soprano, D., *et al.* (2011). Thymine DNA glycosylase is essential for active DNA demethylation by linked deamination-base excision repair. *Cell* 146, 67-79.

Costanzo, V. (2011). Brca2, Rad51 and Mre11: performing balancing acts on replication forks. *DNA Repair (Amst)* 10, 1060-1065.

Courcelle, J., Crowley, D.J., and Hanawalt, P.C. (1999). Recovery of DNA replication in UV-irradiated *Escherichia coli* requires both excision repair and recF protein function. *J Bacteriol* 181, 916-922.

Crespan, E., Pasi, E., Imoto, S., Hubscher, U., Greenberg, M.M., and Maga, G. (2013). Human DNA polymerase beta, but not lambda, can bypass a 2-deoxyribonolactone lesion together with proliferating cell nuclear antigen. *ACS Chem Biol* 8, 336-344.

Crick, F. (1970). Central dogma of molecular biology. *Nature* 227, 561-563.

Crick, F.H. (1958). On protein synthesis. *Symp Soc Exp Biol* 12, 138-163.

- Crow, Y.J., Leitch, A., Hayward, B.E., Garner, A., Parmar, R., Griffith, E., Ali, M., Semple, C., Aicardi, J., Babul-Hirji, R., *et al.* (2006). Mutations in genes encoding ribonuclease H2 subunits cause Aicardi-Goutieres syndrome and mimic congenital viral brain infection. *Nat Genet* 38, 910-916.
- D'Alessandro, G., Whelan, D.R., Howard, S.M., Vitelli, V., Renaudin, X., Adamowicz, M., Iannelli, F., Jones-Weinert, C.W., Lee, M., Matti, V., *et al.* (2018). BRCA2 controls DNA:RNA hybrid level at DSBs by mediating RNase H2 recruitment. *Nat Commun* 9, 5376.
- Das, R.S., Samaraweera, M., Morton, M., Gascon, J.A., and Basu, A.K. (2012). Stability of N-glycosidic bond of (5'S)-8,5'-cyclo-2'-deoxyguanosine. *Chem Res Toxicol* 25, 2451-2461.
- De Bont, R., and van Larebeke, N. (2004). Endogenous DNA damage in humans: a review of quantitative data. *Mutagenesis* 19, 169-185.
- Derr, L.K., and Strathern, J.N. (1993). A role for reverse transcripts in gene conversion. *Nature* 361, 170-173.
- Dianov, G.L., and Hubscher, U. (2013). Mammalian base excision repair: the forgotten archangel. *Nucleic Acids Res* 41, 3483-3490.
- Dianova, I., Sleeth, K.M., Allinson, S.L., Parsons, J.L., Breslin, C., Caldecott, K.W., and Dianov, G.L. (2004). XRCC1-DNA polymerase beta interaction is required for efficient base excision repair. *Nucleic Acids Res* 32, 2550-2555.
- Dizdaroglu, M. (1992). Measurement of radiation-induced damage to DNA at the molecular level. *Int. J. Radiat. Biol.* 61, 175-183.
- Dizdaroglu, M., Jaruga, P., and Rodriguez, H. (2001). Identification and quantification of 8,5'-cyclo-2'-deoxy-adenosine in DNA by liquid chromatography/mass spectrometry. *Free Radic Biol Med* 30, 774-784.
- Doetsch, P.W., and Cunningham, R.P. (1990). The enzymology of apurinic/apyrimidinic endonucleases. *Mutat Res* 236, 173-201.
- Dominguez-Kelly, R., Martin, Y., Koundrioukoff, S., Tanenbaum, M.E., Smits, V.A., Medema, R.H., Debatisse, M., and Freire, R. (2011). Wee1 controls genomic stability during replication by regulating the Mus81-Eme1 endonuclease. *J Cell Biol* 194, 567-579.
- Dongmei, L., Zhiwei, W., Qi, Z., Fuyi, C., Yujuan, S., and Xiaodong, L. (2015). Drinking water toxicity study of the environmental contaminant--Bromate. *Regul Toxicol Pharmacol* 73, 802-810.
- Donkena, K.V., Young, C.Y., and Tindall, D.J. (2010). Oxidative stress and DNA methylation in prostate cancer. *Obstet Gynecol Int* 2010, 302051.
- Dungrawala, H., Rose, K.L., Bhat, K.P., Mohni, K.N., Glick, G.G., Couch, F.B., and Cortez, D. (2015). The Replication Checkpoint Prevents Two Types of Fork Collapse without Regulating Replisome Stability. *Mol Cell* 59, 998-1010.

Dutta, S., Chowdhury, G., and Gates, K.S. (2007). Interstrand cross-links generated by abasic sites in duplex DNA. *J Am Chem Soc* 129, 1852-1853.

Ehrlich, M., Zhang, X.Y., and Inamdar, N.M. (1990). Spontaneous deamination of cytosine and 5-methylcytosine residues in DNA and replacement of 5-methylcytosine residues with cytosine residues. *Mutat Res* 238, 277-286.

Feng, W.Y. (2017). Mec1/ATR, the Program Manager of Nucleic Acids Inc. *Genes-Basel* 8(1):10.

Fortini, P., Pascucci, B., Parlanti, E., Sobol, R.W., Wilson, S.H., and Dogliotti, E. (1998). Different DNA polymerases are involved in the short- and long-patch base excision repair in mammalian cells. *Biochemistry* 37, 3575-3580.

Francia, S., Cabrini, M., Matti, V., Oldani, A., and d'Adda di Fagagna, F. (2016). DICER, DROSHA and DNA damage response RNAs are necessary for the secondary recruitment of DNA damage response factors. *J Cell Sci* 129, 1468-1476.

Francia, S., Michelini, F., Saxena, A., Tang, D., de Hoon, M., Anelli, V., Mione, M., Carninci, P., and d'Adda di Fagagna, F. (2012). Site-specific DICER and DROSHA RNA products control the DNA-damage response. *Nature* 488, 231-235.

Franklin, A., Milburn, P.J., Blanden, R.V., and Steele, E.J. (2004). Human DNA polymerase-eta, an A-T mutator in somatic hypermutation of rearranged immunoglobulin genes, is a reverse transcriptase. *Immunol Cell Biol* 82, 219-225.

Franzolin, E., Pontarin, G., Rampazzo, C., Miazzi, C., Ferraro, P., Palumbo, E., Reichard, P., and Bianchi, V. (2013). The deoxynucleotide triphosphohydrolase SAMHD1 is a major regulator of DNA precursor pools in mammalian cells. *Proc Natl Acad Sci U S A* 110, 14272-14277.

Friedberg, E.C. (2003). DNA damage and repair. *Nature* 421, 436-440.

Friedberg, E.C. (2005). Suffering in silence: The tolerance of DNA damage. *Nat. Rev. Mol. Cell Biol* 6, 943-953.

Fromme, J.C., Banerjee, A., and Verdine, G.L. (2004). DNA glycosylase recognition and catalysis. *Curr Opin Struct Biol* 14, 43-49.

Frosina, G., Fortini, P., Rossi, O., Carrozzino, F., Raspaglio, G., Cox, L.S., Lane, D.P., Abbondandolo, A., and Dogliotti, E. (1996). Two pathways for base excision repair in mammalian cells. *J Biol Chem* 271, 9573-9578.

Fuss, J.O., and Cooper, P.K. (2006). DNA repair: dynamic defenders against cancer and aging. *PLoS Biol* 4, e203.

Gallo, R.C., Yang, S.S., and Ting, R.C. (1970). RNA dependent DNA polymerase of human acute leukaemic cells. *Nature* 228, 927-929.

- Gandhi, V., Mineishi, S., Huang, P., Chapman, A.J., Yang, Y., Chen, F., Nowak, B., Chubb, S., Hertel, L.W., and Plunkett, W. (1995). Cytotoxicity, metabolism, and mechanisms of action of 2',2'-difluorodeoxyguanosine in Chinese hamster ovary cells. *Cancer Res* 55, 1517-1524.
- Garcia-Muse, T., and Aguilera, A. (2016). Transcription-replication conflicts: how they occur and how they are resolved. *Nat. Rev. Mol. Cell Biol* 17, 553-563.
- Garcia-Muse, T., and Aguilera, A. (2019). R Loops: From Physiological to Pathological Roles. *Cell* 179, 604-618.
- Garcia, A.I., Buisson, M., Bertrand, P., Rimokh, R., Rouleau, E., Lopez, B.S., Lidereau, R., Mikaelian, I., and Mazoyer, S. (2011). Down-regulation of BRCA1 expression by miR-146a and miR-146b-5p in triple negative sporadic breast cancers. *EMBO Mol Med* 3, 279-290.
- Gaschler, M.M., and Stockwell, B.R. (2017). Lipid peroxidation in cell death. *Biochem Biophys Res Commun* 482, 419-425.
- Gates, K.S. (2009). An overview of chemical processes that damage cellular DNA: spontaneous hydrolysis, alkylation, and reactions with radicals. *Chem Res Toxicol* 22, 1747-1760.
- Gay, S., Lachages, A.M., Millot, G.A., Courbet, S., Letessier, A., Debatisse, M., and Brison, O. (2010). Nucleotide supply, not local histone acetylation, sets replication origin usage in transcribed regions. *EMBO Rep* 11, 698-704.
- Gong, Z., and Zhu, J.K. (2011). Active DNA demethylation by oxidation and repair. *Cell research* 21, 1649-1651.
- Goodman, M.F., and Woodgate, R. (2013). Translesion DNA polymerases. *Cold Spring Harb Perspect Biol* 5, a010363.
- Gordenin, D.A., and Resnick, M.A. (1998). Yeast ARMs (DNA at-risk motifs) can reveal sources of genome instability. *Mutat Res* 400, 45-58.
- Grabczyk, E., Mancuso, M., and Sammarco, M.C. (2007). A persistent RNA.DNA hybrid formed by transcription of the Friedreich ataxia triplet repeat in live bacteria, and by T7 RNAP in vitro. *Nucleic Acids Res.* 35, 5351-5359.
- Groh, M., and Gromak, N. (2014). Out of balance: R-loops in human disease. *PLoS Genet* 10, e1004630.
- Groh, M., Lufino, M.M., Wade-Martins, R., and Gromak, N. (2014). R-loops associated with triplet repeat expansions promote gene silencing in Friedreich ataxia and fragile X syndrome. *PLoS Genet* 10, e1004318.
- Grollman, A.P., and Moriya, M. (1993a). Mutagenesis by 8-Oxoguanine - an Enemy Within. *Trends Genet* 9, 246-249.

- Grollman, A.P., and Moriya, M. (1993b). Mutagenesis by 8-oxoguanine: an enemy within. *Trends Genet* 9, 246-249.
- Hamperl, S., Bocek, M.J., Saldivar, J.C., Swigut, T., and Cimprich, K.A. (2017). Transcription-Replication Conflict Orientation Modulates R-Loop Levels and Activates Distinct DNA Damage Responses. *Cell* 170, 774-786 e719.
- Haracska, L., Unk, I., Johnson, R.E., Phillips, B.B., Hurwitz, J., Prakash, L., and Prakash, S. (2002). Stimulation of DNA synthesis activity of human DNA polymerase kappa by PCNA. *Mol Cell Biol* 22, 784-791.
- Haracska, L., Yu, S.L., Johnson, R.E., Prakash, L., and Prakash, S. (2000). Efficient and accurate replication in the presence of 7,8-dihydro-8-oxoguanine by DNA polymerase eta. *Nat Genet* 25, 458-461.
- Hashem, V.I., Pytlos, M.J., Klysik, E.A., Tsuji, K., Khajavi, M., Ashizawa, T., and Sinden, R.R. (2004). Chemotherapeutic deletion of CTG repeats in lymphoblast cells from DM1 patients. *Nucleic Acids Res* 32, 6334-6346.
- Hashem, V.I., and Sinden, R.R. (2002). Chemotherapeutically induced deletion of expanded triplet repeats. *Mutat Res* 508, 107-119.
- Hastings, P.J., Ira, G., and Lupski, J.R. (2009). A microhomology-mediated break-induced replication model for the origin of human copy number variation. *PLoS Genet* 5, e1000327.
- He, L., He, X., Lim, L.P., de Stanchina, E., Xuan, Z., Liang, Y., Xue, W., Zender, L., Magnus, J., Ridzon, D., *et al.* (2007). A microRNA component of the p53 tumour suppressor network. *Nature* 447, 1130-1134.
- He, M., Zhou, W., Li, C., and Guo, M. (2016). MicroRNAs, DNA Damage Response, and Cancer Treatment. *Int J Mol Sci* 17(12):2087.
- Helena, J.M., Joubert, A.M., Grobbelaar, S., Nolte, E.M., Nel, M., Pepper, M.S., Coetzee, M., and Mercier, A.E. (2018). Deoxyribonucleic Acid Damage and Repair: Capitalizing on Our Understanding of the Mechanisms of Maintaining Genomic Integrity for Therapeutic Purposes. *Int J Mol Sci* 19(4):1148.
- Heyer, W.D., Ehmsen, K.T., and Liu, J. (2010). Regulation of homologous recombination in eukaryotes. *Annu Rev Genet* 44, 113-139.
- Hill, J.W., Hazra, T.K., Izumi, T., and Mitra, S. (2001). Stimulation of human 8-oxoguanine-DNA glycosylase by AP-endonuclease: potential coordination of the initial steps in base excision repair. *Nucleic Acids Res* 29, 430-438.
- Hoeijmakers, J.H. (2001). Genome maintenance mechanisms for preventing cancer. *Nature* 411, 366-374.
- Hoeijmakers, J.H. (2009). DNA damage, aging, and cancer. *N Engl J Med* 361, 1475-1485.

Hoogstraten, D., Bergink, S., Ng, J.M., Verbiest, V.H., Luijsterburg, M.S., Geverts, B., Raams, A., Dinant, C., Hoeijmakers, J.H., Vermeulen, W., *et al.* (2008). Versatile DNA damage detection by the global genome nucleotide excision repair protein XPC. *J Cell Sci* 121, 2850-2859.

Hu, M., and Palic, D. (2020). Role of MicroRNAs in regulation of DNA damage in monocytes exposed to polystyrene and TiO₂ nanoparticles. *Toxicol Rep* 7, 743-751.

Huang, Y., Chuang, A., Hao, H., Talbot, C., Sen, T., Trink, B., Sidransky, D., and Ratovitski, E. (2011). Phospho-Delta Np63 alpha is a key regulator of the cisplatin-induced microRNAome in cancer cells. *Cell Death Differ* 18, 1220-1230.

Huertas, P., and Aguilera, A. (2003). Cotranscriptionally formed DNA:RNA hybrids mediate transcription elongation impairment and transcription-associated recombination. *Mol Cell* 12, 711-721.

Ivanovska, I., Ball, A.S., Diaz, R.L., Magnus, J.F., Kibukawa, M., Schelter, J.M., Kobayashi, S.V., Lim, L., Burchard, J., Jackson, A.L., *et al.* (2008). MicroRNAs in the miR-106b family regulate p21/CDKN1A and promote cell cycle progression. *Mol Cell Biol* 28, 2167-2174.

Iyama, T., and Wilson, D.M., 3rd (2013). DNA repair mechanisms in dividing and non-dividing cells. *DNA Repair* 12, 620-636.

Iyer, D.R., and Rhind, N. (2017). Replication fork slowing and stalling are distinct, checkpoint-independent consequences of replicating damaged DNA. *PLoS Genet* 13, e1006958.

Jaruga, P., and Dizdaroglu, M. (2008). 8,5'-Cyclopurine-2'-deoxynucleosides in DNA: mechanisms of formation. *DNA Repair* 7, 1413-1425.

Jasencakova, Z., and Groth, A. (2010). Replication stress, a source of epigenetic aberrations in cancer? *Bioessays* 32, 847-855.

Jasencakova, Z., Scharf, A.N.D., Ask, K., Corpet, A., Imhof, A., Almouzni, G., and Groth, A. (2010). Replication Stress Interferes with Histone Recycling and Predeposition Marking of New Histones. *Mol Cell* 37, 736-743.

Jasti, V.P., Das, R.S., Hilton, B.A., Weerasooriya, S., Zou, Y., and Basu, A.K. (2011). (5'S)-8,5'-cyclo-2'-deoxyguanosine is a strong block to replication, a potent pol V-dependent mutagenic lesion, and is inefficiently repaired in *Escherichia coli*. *Biochemistry* 50, 3862-3865.

Jiang, Z., Xu, M., Lai, Y., Laverde, E.E., Terzidis, M.A., Masi, A., Chatgijialoglu, C., and Liu, Y. (2015a). Bypass of a 5',8-cyclopurine-2'-deoxynucleoside by DNA polymerase beta during DNA. *DNA Repair* 33, 24-34.

Jiang, Z., Xu, M., Lai, Y., Laverde, E.E., Terzidis, M.A., Masi, A., Chatgijialoglu, C., and Liu, Y. (2015b). Bypass of a 5',8-cyclopurine-2'-deoxynucleoside by

DNA polymerase beta during DNA replication and base excision repair leads to nucleotide misinsertions and DNA strand breaks. *DNA Repair* 33, 24-34.

Jobert, L., Skjeldam, H.K., Dalhus, B., Galashevskaya, A., Vagbo, C.B., Bjoras, M., and Nilsen, H. (2013). The human base excision repair enzyme SMUG1 directly interacts with DKC1 and contributes to RNA quality control. *Molcell* 49, 339-345.

Johnson, R.E., Washington, M.T., Haracska, L., Prakash, S., and Prakash, L. (2000a). Eukaryotic polymerases iota and zeta act sequentially to bypass DNA lesions. *Nature* 406, 1015-1019.

Johnson, R.E., Washington, M.T., Prakash, S., and Prakash, L. (2000b). Fidelity of human DNA polymerase eta. *J Biol Chem* 275, 7447-7450.

Kamakura, N., Yamamoto, J., Brooks, P.J., Iwai, S., and Kuraoka, I. (2012a). Effects of 5',8-cyclodeoxyadenosine triphosphates on DNA synthesis. *Chem Res Toxicol* 25, 2718-2724.

Kamakura, N., Yamamoto J Fau - Brooks, P.J., Brooks Pj Fau - Iwai, S., Iwai S Fau - Kuraoka, I., and Kuraoka, I. (2012b). Effects of 5',8-cyclodeoxyadenosine triphosphates on DNA synthesis. *Chem Res Toxicol* 25, 2718-2724.

Kamiya, H., and Kasai, H. (1995). Formation of 2-hydroxydeoxyadenosine triphosphate, an oxidatively damaged nucleotide, and its incorporation by DNA polymerases. Steady-state kinetics of the incorporation. *J Biol Chem* 270, 19446-19450.

Kannouche, P.L., Wing, J., and Lehmann, A.R. (2004). Interaction of human DNA polymerase eta with monoubiquitinated PCNA: A possible mechanism for the polymerase switch in response to DNA damage. *Mol Cell* 14, 491-500.

Kasai, H., and Nishimura, S. (1983). Hydroxylation of the C-8 position of deoxyguanosine by reducing agents in the presence of oxygen. *Nucleic Acids Symp Ser*, 165-167.

Kasai, H., and Nishimura, S. (1984). Hydroxylation of deoxyguanosine at the C-8 position by ascorbic acid and other reducing agents. *Nucleic Acids Res* 12, 2137-2145.

Kastan, M.B., and Bartek, J. (2004). Cell-cycle checkpoints and cancer. *Nature* 432, 316-323.

Kawanishi, S., and Murata, M. (2006). Mechanism of DNA damage induced by bromate differs from general types of oxidative stress. *Toxicology* 221, 172-178.

Kedar, P.S., Kim, S.J., Robertson, A., Hou, E., Prasad, R., Horton, J.K., and Wilson, S.H. (2002). Direct interaction between mammalian DNA polymerase beta and proliferating cell nuclear antigen. *J Biol Chem* 277, 31115-31123.

Keskin, H., Meers, C., and Storici, F. (2016). Transcript RNA supports precise repair of its own DNA gene. *RNA Biol* 13, 157-165.

Khan, N., Sharma, S., and Sultana, S. (2004). Attenuation of potassium bromate-induced nephrotoxicity by coumarin (1,2-benzopyrone) in Wistar rats: chemoprevention against free radical-mediated renal oxidative stress and tumor promotion response. *Redox Rep* 9, 19-28.

Kim, H., and D'Andrea, A.D. (2012). Regulation of DNA cross-link repair by the Fanconi anemia/BRCA pathway. *Genes Dev* 26, 1393-1408.

Kirkali, G., de Souza-Pinto, N.C., Jaruga, P., Bohr, V.A., and Dizdaroglu, M. (2009). Accumulation of (5'S)-8,5'-cyclo-2'-deoxyadenosine in organs of Cockayne syndrome complementation group B gene knockout mice. *DNA Repair (Amst)* 8, 274-278.

Klenow, H., and Henningsen, I. (1970). Selective elimination of the exonuclease activity of the deoxyribonucleic acid polymerase from *Escherichia coli* B by limited proteolysis. *Proc Natl Acad Sci U S A* 65, 168-175.

Klungland, A., and Lindahl, T. (1997). Second pathway for completion of human DNA base excision-repair: reconstitution with purified proteins and requirement for DNase IV (FEN1). *EMBO J* 16, 3341-3348.

Kolodner, R.D., and Marsischky, G.T. (1999). Eukaryotic DNA mismatch repair. *Curr Opin Genet Dev* 9, 89-96.

Kornberg, R.D., and Lorch, Y. (1999). Twenty-five years of the nucleosome, fundamental particle of the eukaryote chromosome. *Cell* 98, 285-294.

Koundrioukoff, S., Carignon, S., Techer, H., Letessier, A., Brison, O., and Debatisse, M. (2013). Stepwise activation of the ATR signaling pathway upon increasing replication stress impacts fragile site integrity. *PLoS Genet* 9, e1003643.

Krokan, H.E., and Bjoras, M. (2013). Base excision repair. *Cold Spring Harb Perspect Biol* 5, a012583.

Kropachev, K., Ding, S., Terzidis, M.A., Masi, A., Liu, Z., Cai, Y., Kolbanovskiy, M., Chatgililoglu, C., Broyde, S., Geacintov, N.E., *et al.* (2014). Structural basis for the recognition of diastereomeric 5',8-cyclo-2'-deoxypurine lesions by the human nucleotide excision repair system. *Nucleic acids research* 42, 5020-5032.

Kuraoka, I., Bender, C., Romieu, A., Cadet, J., Wood, R.D., and Lindahl, T. (2000). Removal of oxygen free-radical-induced 5',8-purine cyclodeoxynucleosides from DNA by the nucleotide excision-repair pathway in human cells. *Proc Natl Acad Sci U S A* 97, 3832-3837.

Kuraoka, I., Robins P Fau - Masutani, C., Masutani C Fau - Hanaoka, F., Hanaoka F Fau - Gasparutto, D., Gasparutto D Fau - Cadet, J., Cadet J Fau -

- Wood, R.D., Wood Rd Fau - Lindahl, T., and Lindahl, T. (2001). Oxygen free radical damage to DNA. Translesion synthesis by human DNA polymerase. *J Biol Chem* 276, 49283-49288.
- Kurokawa, Y., Aoki, S., Matsushima, Y., Takamura, N., Imazawa, T., and Hayashi, Y. (1986). Dose-response studies on the carcinogenicity of potassium bromate in F344 rats after long-term oral administration. *J Natl Cancer Inst* 77, 977-982.
- L, S. The PyMOL Molecular Graphics System. Schrödinger, Inc: New York, NY.
- Lai, Y., Budworth, H., Beaver, J.M., Chan, N.L., Zhang, Z., McMurray, C.T., and Liu, Y. (2016). Crosstalk between MSH2-MSH3 and polbeta promotes trinucleotide repeat expansion during base excision repair. *Nat Commun* 7, 12465.
- Lanz, M.C., Dibitetto, D., and Smolka, M.B. (2019). DNA damage kinase signaling: checkpoint and repair at 30 years. *EMBO J* 38, e101801.
- Laverde, E.E., Lai, Y., Leng, F., Balakrishnan, L., Freudenreich, C.H., and Liu, Y. (2020). R-loops promote trinucleotide repeat deletion through DNA base excision repair enzymatic activities. *J Biol Chem* 295, 13902-13913.
- Lehmann, A.R. (2005). Replication of damaged DNA by translesion synthesis in human cells. *FEBS Lett* 579, 873-876.
- Lehmann, A.R., Niimi, A., Ogi, T., Brown, S., Sabbioneda, S., Wing, J.F., Kannouche, P.L., and Green, C.M. (2007). Translesion synthesis: Y-family polymerases and the polymerase switch. *DNA Repair (Amst)* 6, 891-899.
- Leon-Ortiz, A.M., Svendsen, J., and Boulton, S.J. (2014a). Metabolism of DNA secondary structures at the eukaryotic replication fork. *DNA repair* 19, 152-162.
- Leon-Ortiz, A.M., Svendsen, J., and Boulton, S.J. (2014b). Metabolism of DNA secondary structures at the eukaryotic replication fork. *DNA Repair* 19, 152-162.
- Leung, A.K.L., and Sharp, P.A. (2010). MicroRNA Functions in Stress Responses. *Mol cell* 40, 205-215.
- Levin, D.S., McKenna, A.E., Motycka, T.A., Matsumoto, Y., and Tomkinson, A.E. (2000). Interaction between PCNA and DNA ligase I is critical for joining of Okazaki fragments and long-patch base-excision repair. *Curr Biol* 10, 919-922.
- Li, G., and Reinberg, D. (2011). Chromatin higher-order structures and gene regulation. *Curr Opin Genet Dev* 21, 175-186.
- Li, M., and Wilson, D.M., 3rd (2014). Human apurinic/aprimidinic endonuclease 1. *Antioxid Redox Signal* 20, 678-707.

- Li, X., and Manley, J.L. (2005). Inactivation of the SR protein splicing factor ASF/SF2 results in genomic instability. *Cell* 122, 365-378.
- Lim, S.O., Gu, J.M., Kim, M.S., Kim, H.S., Park, Y.N., Park, C.K., Cho, J.W., Park, Y.M., and Jung, G. (2008). Epigenetic changes induced by reactive oxygen species in hepatocellular carcinoma: methylation of the E-cadherin promoter. *Gastroenterology* 135, 2128-2140.
- Lin, Y., Dent, S.Y., Wilson, J.H., Wells, R.D., and Napierala, M. (2010). R loops stimulate genetic instability of CTG.CAG repeats. *Proc Natl Acad Sci U S A* 107, 692-697.
- Lindahl, T. (1979). DNA glycosylases, endonucleases for apurinic/apyrimidinic sites, and base excision-repair. *Prog Nucleic Acid Res Mol Biol* 22, 135-192.
- Lindahl, T. (1993). Instability and decay of the primary structure of DNA. *Nature* 362, 709-715.
- Lindahl, T., and Andersson, A. (1972). Rate of chain breakage at apurinic sites in double-stranded deoxyribonucleic acid. *Biochemistry* 11, 3618-3623.
- Lindahl, T., and Nyberg, B. (1972). Rate of depurination of native deoxyribonucleic acid. *Biochemistry* 11, 3610-3618.
- Lindahl, T., and Nyberg, B. (1974). Heat-induced deamination of cytosine residues in deoxyribonucleic acid. *Biochemistry* 13, 3405-3410.
- Liu, D., Keijzers, G., and Rasmussen, L.J. (2017). DNA mismatch repair and its many roles in eukaryotic cells. *Mutat Res* 773, 174-187.
- Liu, P.F., Carvalho, C.M.B., Hastings, P.J., and Lupski, J.R. (2012). Mechanisms for recurrent and complex human genomic rearrangements. *Curr Opin Genet Dev* 22, 211-220.
- Liu, Y., Beard, W.A., Shock, D.D., Prasad, R., Hou, E.W., and Wilson, S.H. (2005). DNA polymerase beta and flap endonuclease 1 enzymatic specificities sustain DNA synthesis for long patch base excision repair. *J Biol Chem* 280, 3665-3674.
- Liu, Y., Prasad, R., Beard, W.A., Hou, E.W., Horton, J.K., McMurray, C.T., and Wilson, S.H. (2009). Coordination between polymerase beta and FEN1 can modulate CAG repeat expansion. *J Biol Chem* 284, 28352-28366.
- Liu, Y., Prasad, R., Beard, W.A., Kedar, P.S., Hou, E.W., Shock, D.D., and Wilson, S.H. (2007). Coordination of steps in single-nucleotide base excision repair mediated by apurinic/apyrimidinic endonuclease 1 and DNA polymerase beta. *J Biol Chem* 282, 13532-13541.
- Liu, Y., and Wilson, S.H. (2012). DNA base excision repair: a mechanism of trinucleotide repeat expansion. *Trends Biochem Sci* 37, 162-172.

- Lopes, M., Cotta-Ramusino, C., Pellicioli, A., Liberi, G., Plevani, P., Muzi-Falconi, M., Newlon, C.S., and Foiani, M. (2001a). The DNA replication checkpoint response stabilizes stalled replication forks. *Nature* 412, 557-561.
- Lopes, M., Cotta-Ramusino, C., Pellicioli, A., Liberi, G., Plevani, P., Muzi-Falconi, M., Newlon, C.S., and Foiani, M. (2001b). The DNA replication checkpoint response stabilizes stalled replication forks. *Nature* 412, 557-561.
- Lopes, M., Foiani, M., and Sogo, J.M. (2006). Multiple mechanisms control chromosome integrity after replication fork uncoupling and restart at irreparable UV lesions. *Mol Cell* 21, 15-27.
- Lossaint, G., Larroque, M., Ribeyre, C., Bec, N., Larroque, C., Decaillet, C., Gari, K., and Constantinou, A. (2013). FANCD2 Binds MCM Proteins and Controls Replisome Function upon Activation of S Phase Checkpoint Signaling. *Mol Cell* 51, 678-690.
- Loyola, A., Bonaldi, T., Roche, D., Imhof, A., and Almouzni, G. (2006). PTMs on H3 variants before chromatin assembly potentiate their final epigenetic state. *Molecular Cell* 24, 309-316.
- Loyola, A., Tagami, H., Bonaldi, T., Roche, D., Quivy, J.P., Imhof, A., Nakatani, Y., Dent, S.Y.R., and Almouzni, G. (2009). The HP1 alpha-CAF1-SetDB1-containing complex provides H3K9me1 for Suv39-mediated K9me3 in pericentric heterochromatin. *Embo Reports* 10, 769-775.
- Lu, W.T., Hawley, B.R., Skalka, G.L., Baldock, R.A., Smith, E.M., Bader, A.S., Malewicz, M., Watts, F.Z., Wilczynska, A., and Bushell, M. (2018). Drosha drives the formation of DNA:RNA hybrids around DNA break sites to facilitate DNA repair. *Nat Commun* 9, 532.
- Lu, X., Liu, R., Wang, M., Kumar, A.K., Pan, F., He, L., Hu, Z., and Guo, Z. (2020). MicroRNA-140 impedes DNA repair by targeting FEN1 and enhances chemotherapeutic response in breast cancer. *Oncogene* 39, 234-247.
- Luger, K., and Hansen, J.C. (2005). Nucleosome and chromatin fiber dynamics. *Curr Opin Struct Biol* 15, 188-196.
- Macheret, M., and Halazonetis, T.D. (2015). DNA Replication Stress as a Hallmark of Cancer. *Annu. Rev. Pathol. Mech. Dis* 10, 425-448.
- Macpherson, P., Barone, F., Maga, G., Mazzei, F., Karran, P., and Bignami, M. (2005). 8-oxoguanine incorporation into DNA repeats in vitro and mismatch recognition by MutSalpha. *Nucleic Acids Res* 33, 5094-5105.
- Magdalou, I., Lopez, B.S., Pasero, P., and Larnbert, S.A.E. (2014). The causes of replication stress and their consequences on genome stability and cell fate. *Semin. Cell Dev. Biol.* 30, 154-164.
- Marians, K.J. (2018). Lesion Bypass and the Reactivation of Stalled Replication Forks. *Annu Rev Biochem.* 87:217-238

- Marietta, C., Gulam, H., and Brooks, P.J. (2002). A single 8,5'-cyclo-2'-deoxyadenosine lesion in a TATA box prevents binding of the TATA binding protein and strongly reduces transcription in vivo. *DNA Repair (Amst)* 1, 967-975.
- Masuda, Y., Bennett, R.A., and Demple, B. (1998). Dynamics of the interaction of human apurinic endonuclease (Ape1) with its substrate and product. *J Biol Chem* 273, 30352-30359.
- Masutani, C., Araki, M., Yamada, A., Kusumoto, R., Nogimori, T., Maekawa, T., Iwai, S., and Hanaoka, F. (1999a). Xeroderma pigmentosum variant (XP-V) correcting protein from HeLa cells has a thymine dimer bypass DNA polymerase activity. *EMBO J* 18, 3491-3501.
- Masutani, C., Kusumoto, R., Iwai, S., and Hanaoka, F. (2000). Mechanisms of accurate translesion synthesis by human DNA polymerase eta. *EMBO J* 19, 3100-3109.
- Masutani, C., Kusumoto, R., Yamada, A., Dohmae, N., Yokoi, M., Yuasa, M., Araki, M., Iwai, S., Takio, K., and Hanaoka, F. (1999b). The XPV (xeroderma pigmentosum variant) gene encodes human DNA polymerase eta. *Nature* 399, 700-704.
- Mathews, C.K. (2015). Deoxyribonucleotide metabolism, mutagenesis and cancer. *Nat. Rev. Cancer*. 15, 528-539.
- McIvor, E.I., Polak, U., and Napierala, M. (2010). New insights into repeat instability Role of RNA.DNA hybrids. *Rna Biol* 7, 551-558.
- Mendell, J.T., and Olson, E.N. (2012). MicroRNAs in stress signaling and human disease. *Cell* 148, 1172-1187.
- Mendoza, O., Bourdoncle, A., Boule, J.B., Brosh, R.M., Jr., and Mergny, J.L. (2016). G-quadruplexes and helicases. *Nucleic Acids Res* 44, 1989-2006.
- Mezzina, M., Menck, C.F., Courtin, P., and Sarasin, A. (1988). Replication of simian virus 40 DNA after UV irradiation: evidence of growing fork blockage and single-stranded gaps in daughter strands. *J Virol* 62, 4249-4258.
- Michelini, F., Pitchiaya, S., Vitelli, V., Sharma, S., Gioia, U., Pessina, F., Cabrini, M., Wang, Y., Capozzo, I., Iannelli, F., *et al.* (2017). Damage-induced lncRNAs control the DNA damage response through interaction with DDRNAs at individual double-strand breaks. *Nat Cell Biol* 19, 1400-1411.
- Miller, H., Prasad, R., Wilson, S.H., Johnson, F., and Grollman, A.P. (2000). 8-oxodGTP incorporation by DNA polymerase beta is modified by active-site residue Asn279. *Biochemistry* 39, 1029-1033.
- Mirihana Arachchilage, G., Dassanayake, A.C., and Basu, S. (2015). A potassium ion-dependent RNA structural switch regulates human pre-miRNA 92b maturation. *Chem Biol* 22, 262-272.

- Mirkin, E.V., and Mirkin, S.M. (2007). Replication fork stalling at natural impediments. *Microbiol Mol Biol Rev* 71, 13-35.
- Moldovan, G.L., Pfander, B., and Jentsch, S. (2007). PCNA, the maestro of the replication fork. *Cell* 129, 665-679.
- Morrish, T.A., Gilbert, N., Myers, J.S., Vincent, B.J., Stamato, T.D., Taccioli, G.E., Batzer, M.A., and Moran, J.V. (2002). DNA repair mediated by endonuclease-independent LINE-1 retrotransposition. *Nat Genet* 31, 159-165.
- Murakami, E., Feng, J.Y., Lee, H., Hanes, J., Johnson, K.A., and Anderson, K.S. (2003a). Characterization of novel reverse transcriptase and other RNA-associated catalytic activities by human DNA polymerase gamma: importance in mitochondrial DNA replication. *J Biol Chem* 278, 36403-36409.
- Murakami, M., Ikeda, T., Ogawa, K., and Funaba, M. (2003b). Transcriptional activation of mouse mast cell protease-9 by microphthalmia-associated transcription factor. *Biochem Biophys Res Commun* 311, 4-10.
- Murata, M., Bansho, Y., Inoue, S., Ito, K., Ohnishi, S., Midorikawa, K., and Kawanishi, S. (2001). Requirement of glutathione and cysteine in guanine-specific oxidation of DNA by carcinogenic potassium bromate. *Chem Res Toxicol* 14, 678-685.
- Nakabeppu, Y. (2014). Cellular levels of 8-oxoguanine in either DNA or the nucleotide pool play pivotal roles in carcinogenesis and survival of cancer cells. *Int J Mol Sci* 15, 12543-12557.
- Nash, R.A., Caldecott, K.W., Barnes, D.E., and Lindahl, T. (1997). XRCC1 protein interacts with one of two distinct forms of DNA ligase III. *Biochemistry* 36, 5207-5211.
- Neeley, W.L., and Essigmann, J.M. (2006). Mechanisms of formation, genotoxicity, and mutation of guanine oxidation products. *Chem Res Toxicol* 19, 491-505.
- Nevo-Caspi, Y., and Kupiec, M. (1997). cDNA-mediated Ty recombination can take place in the absence of plus-strand cDNA synthesis, but not in the absence of the integrase protein. *Curr Genet* 32, 32-40.
- Niehrs, C. (2009). Active DNA demethylation and DNA repair. *Differentiation; Res Bio Diver* 77, 1-11.
- Nikolov, I., and Taddei, A. (2016). Linking replication stress with heterochromatin formation. *Chromosoma* 125, 523-533.
- Nordlund, P., and Reichard, P. (2006). Ribonucleotide reductases. *Annu Rev Biochem* 75, 681-706.
- Nyaga, S.G., Jaruga, P., Lohani, A., Dizdaroglu, M., and Evans, M.K. (2007). Accumulation of oxidatively induced DNA damage in human breast cancer cell lines following treatment with hydrogen peroxide. *Cell Cycle* 6, 1472-1478.

- O'Hagan, H.M., Wang, W., Sen, S., Destefano Shields, C., Lee, S.S., Zhang, Y.W., Clements, E.G., Cai, Y., Van Neste, L., Easwaran, H., *et al.* (2011). Oxidative damage targets complexes containing DNA methyltransferases, SIRT1, and polycomb members to promoter CpG Islands. *Cancer Cell* 20, 606-619.
- Ohle, C., Tesorero, R., Schermann, G., Dobrev, N., Sinning, I., and Fischer, T. (2016). Transient RNA-DNA Hybrids Are Required for Efficient Double-Strand Break Repair. *Cell* 167, 1001-1013 e1007.
- Okashita, N., Kumaki, Y., Ebi, K., Nishi, M., Okamoto, Y., Nakayama, M., Hashimoto, S., Nakamura, T., Sugasawa, K., Kojima, N., *et al.* (2014). PRDM14 promotes active DNA demethylation through the ten-eleven translocation (TET)-mediated base excision repair pathway in embryonic stem cells. *Development* 141, 269-280.
- Olejniczak, M., Kotowska-Zimmer, A., and Krzyzosiak, W. (2018). Stress-induced changes in miRNA biogenesis and functioning. *Cell Mol Life Sci* 75, 177-191.
- Pan, L., Hao, W., Zheng, X., Zeng, X., Ahmed Abbasi, A., Boldogh, I., and Ba, X. (2017). OGG1-DNA interactions facilitate NF-kappaB binding to DNA targets. *Sci Rep* 7, 43297.
- Patel, D.R., and Weiss, R.S. (2018). A tough row to hoe: when replication forks encounter DNA damage. *Biochem Soc Trans* 46, 1643-1651.
- Pednekar, V., Weerasooriya S Fau - Jasti, V.P., Jasti Vp Fau - Basu, A.K., and Basu, A.K. (2014). Mutagenicity and genotoxicity of (5'S)-8,5'-cyclo-2'-deoxyadenosine in. *Chem Res Toxicol* 27, 200-210.
- Perron, M.P., and Provost, P. (2008). Protein interactions and complexes in human microRNA biogenesis and function. *Front. Biosci* 13, 2537-2547.
- Pfeifer, G.P., Denissenko, M.F., Olivier, M., Tretyakova, N., Hecht, S.S., and Hainaut, P. (2002). Tobacco smoke carcinogens, DNA damage and p53 mutations in smoking-associated cancers. *Oncogene* 21, 7435-7451.
- Pontarin, G., Fijolek, A., Pizzo, P., Ferraro, P., Rampazzo, C., Pozzan, T., Thelander, L., Reichard, P.A., and Bianchi, V. (2008). Ribonucleotide reduction is a cytosolic process in mammalian cells independently of DNA damage. *Proc Natl Acad Sci U S A* 105, 17801-17806.
- Prakasha Gowda, A.S., *et al.* (2010). Incorporation of gemcitabine and cytarabine into DNA by DNA polymerase beta and ligase III/XRCC1. *Biochemistry* 49(23), p. 4833-4840.
- Prasad, R., Dianov, G.L., Bohr, V.A., and Wilson, S.H. (2000). FEN1 stimulation of DNA polymerase beta mediates an excision step in mammalian long patch base excision repair. *J Biol Chem* 275, 4460-4466.

Prasad, R., Lavrik, O.I., Kim, S.J., Kedar, P., Yang, X.P., Vande Berg, B.J., and Wilson, S.H. (2001). DNA polymerase beta -mediated long patch base excision repair. Poly(ADP-ribose)polymerase-1 stimulates strand displacement DNA synthesis. *J Biol Chem* 276, 32411-32414.

Prasad, R., Liu, Y., Deterding, L.J., Poltoratsky, V.P., Kedar, P.S., Horton, J.K., Kanno, S., Asagoshi, K., Hou, E.W., Khodyreva, S.N., *et al.* (2007). HMGB1 is a cofactor in mammalian base excision repair. *Mol Cell* 27, 829-841.

Pursell, Z.F., McDonald, J.T., Mathews, C.K., and Kunkel, T.A. (2008). Trace amounts of 8-oxo-dGTP in mitochondrial dNTP pools reduce DNA polymerase gamma replication fidelity. *Nucleic Acids Res* 36, 2174-2181.

Rai, P. (2010). Oxidation in the nucleotide pool, the DNA damage response and cellular senescence: Defective bricks build a defective house. *Mutat Res* 703, 71-81.

Ranalli, T.A., Tom, S., and Bambara, R.A. (2002). AP endonuclease 1 coordinates flap endonuclease 1 and DNA ligase I activity in long patch base excision repair. *J Biol Chem* 277, 41715-41724.

Randerath, K., Zhou, G.D., Somers, R.L., Robbins, J.H., and Brooks, P.J. (2001). A 32P-postlabeling assay for the oxidative DNA lesion 8,5'-cyclo-2'-deoxyadenosine in mammalian tissues: evidence that four type II I-compounds are dinucleotides containing the lesion in the 3' nucleotide. *J Biol Chem* 276, 36051-36057.

Reasearch, W.I.f.B. (2008). TargetScanHuman. .

Reddy, K., Tam, M., Bowater, R.P., Barber, M., Tomlinson, M., Edamura, K.N., Wang, Y.H., and Pearson, C.E. (2011). Determinants of R-loop formation at convergent bidirectionally transcribed trinucleotide repeats. *Nucleic Acids Res* 39, 1749-1762.

Reed, A.J., Vyas, R., Raper, A.T., and Suo, Z. (2017). Structural Insights into the Post-Chemistry Steps of Nucleotide Incorporation Catalyzed by a DNA Polymerase. *J Am Chem Soc* 139, 465-471.

Reijns, M.A., Rabe, B., Rigby, R.E., Mill, P., Astell, K.R., Lettice, L.A., Boyle, S., Leitch, A., Keighren, M., Kilanowski, F., *et al.* (2012). Enzymatic removal of ribonucleotides from DNA is essential for mammalian genome integrity and development. *Cell* 149, 1008-1022.

Rhind, N., and Russell, P. (2000). Checkpoints: it takes more than time to heal some wounds. *Curr Biol* 10, R908-911.

Rhind, N., and Russell, P. (2012). Signaling pathways that regulate cell division. *Cold Spring Harb Perspect Biol* 4(10): a005942.

- Robert-Guroff, M., and Gallo, R.C. (1977). Serological analysis of cellular and viral DNA polymerases by an antiserum to DNA polymerase gamma of human lymphoblasts. *Biochemistry* 16, 2874-2880.
- Rodriguez, A., and D'Andrea, A. (2017). Fanconi anemia pathway. *Curr Biol* 27, R986-R988.
- Rondinelli, B., Gogola, E., Yucel, H., Duarte, A.A., van de Ven, M., van der Sluijs, R., Konstantinopoulos, P.A., Jonkers, J., Ceccaldi, R., Rottenberg, S., *et al.* (2017). EZH2 promotes degradation of stalled replication forks by recruiting MUS81 through histone H3 trimethylation. *Nat. Cell Biol.* 19, 1371-1378.
- Rubfiaro A S, T.P.S., Lai Y, Cabello E, Shaver M, Hutcheson J, Liu Y, He J (2021). Scanning Ion Conductance Microscopy Study Reveals the Disruption of the Integrity of the Human Cell Membrane Structure by Oxidative DNA Damage. *ACS Appl Bio Mater* 4 (2), 1632–1639.
- Rudolph, C.J., Upton, A.L., and Lloyd, R.G. (2007). Replication fork stalling and cell cycle arrest in UV-irradiated *Escherichia coli*. *Genes Dev* 21, 668-681.
- Saif, M.W., Syrigos, K.N., and Katirtzoglou, N.A. (2009). S-1: a promising new oral fluoropyrimidine derivative. *Expert Opin Investig Drugs* 18, 335-348.
- Saini, H.K., Griffiths-Jones, S., and Enright, A.J. (2007). Genomic analysis of human microRNA transcripts. *Proc Natl Acad Sci U S A* 104, 17719-17724.
- Santos-Pereira, J.M., and Aguilera, A. (2015). R loops: new modulators of genome dynamics and function. *Nat Rev Genet* 16, 583-597.
- Sczepanski, J.T., Jacobs, A.C., Van Houten, B., and Greenberg, M.M. (2009). Double-strand break formation during nucleotide excision repair of a DNA interstrand cross-link. *Biochemistry* 48, 7565-7567.
- Shibutani, S., Takeshita, M., and Grollman, A.P. (1991). Insertion of specific bases during DNA synthesis past the oxidation-damaged base 8-oxodG. *Nature* 349, 431-434.
- Simone, N.L., Soule, B.P., Ly, D., Saleh, A.D., Savage, J.E., Degraff, W., Cook, J., Harris, C.C., Gius, D., and Mitchell, J.B. (2009). Ionizing radiation-induced oxidative stress alters miRNA expression. *PLoS One* 4, e6377.
- Singh, R.K., Kabbaj, M.H.M., Paik, J., and Gunjan, A. (2009). Histone levels are regulated by phosphorylation and ubiquitylation-dependent proteolysis. *Nat. Cell Biol.* 11, 925-U940.
- Sirbu, B.M., McDonald, W.H., Dungalwala, H., Badu-Nkansah, A., Kavanaugh, G.M., Chen, Y., Tabb, D.L., and Cortez, D. (2013). Identification of proteins at active, stalled, and collapsed replication forks using isolation of proteins on nascent DNA (iPOND) coupled with mass spectrometry. *J. Biol. Chem.* 288, 31458-31467.

Storici, F., Bebenek, K., Kunkel, T.A., Gordenin, D.A., and Resnick, M.A. (2007). RNA-templated DNA repair. *Nature* *447*, 338-341.

Su, Y., Meador, J.A., Geard, C.R., and Balajee, A.S. (2010). Analysis of ionizing radiation-induced DNA damage and repair in three-dimensional human skin model system. *Exp Dermatol* *19*, e16-22.

Sutherland, G.R., Baker, E., and Richards, R.I. (1998). Fragile sites still breaking. *Trends Genet* *14*, 501-506.

Swanson, A.L., J, W., and Y, W. (2012a). Accurate and efficient bypass of 8,5'-cyclopurine-2'-deoxynucleosides by human and yeast DNA polymerase η . *Chem Res Toxicol* *25*, 1682-1691.

Swanson, A.L., Wang J Fau - Wang, Y., and Wang, Y. (2012b). Accurate and efficient bypass of 8,5'-cyclopurine-2'-deoxynucleosides by human. *Chem Res Toxicol* *25*, 1682-1691.

Szatrowski, T.P., and Nathan, C.F. (1991). Production of large amounts of hydrogen peroxide by human tumor cells. *Cancer Res* *51*, 794-798.

Techer, H., Koundrioukoff, S., Carignon, S., Wilhelm, T., Millot, G.A., Lopez, B.S., Brison, O., and Debatisse, M. (2016). Signaling from Mus81-Eme2-Dependent DNA Damage Elicited by Chk1 Deficiency Modulates Replication Fork Speed and Origin Usage. *Cell Rep* *14*, 1114-1127.

Techer, H., Koundrioukoff, S., Nicolas, A., and Debatisse, M. (2017). The impact of replication stress on replication dynamics and DNA damage in vertebrate cells. *Nat Rev Genet* *18*, 535-550.

Tom, S., Henricksen, L.A., and Bambara, R.A. (2000). Mechanism whereby proliferating cell nuclear antigen stimulates flap endonuclease 1. *J Biol Chem* *275*, 10498-10505.

Trincao, J., Johnson, R.E., Escalante, C.R., Prakash, S., Prakash, L., and Aggarwal, A.K. (2001). Structure of the catalytic core of *S. cerevisiae* DNA polymerase ϵ : implications for translesion DNA synthesis. *Mol Cell* *8*, 417-426.

Trott, O., and Olson, A.J. (2010). AutoDock Vina: improving the speed and accuracy of docking with a new scoring function, efficient optimization, and multithreading. *J Comput Chem* *31*, 455-461.

Tsegay, P.S., Lai, Y., and Liu, Y. (2019). Replication Stress and Consequential Instability of the Genome and Epigenome. *Molecules* *24*.

Turk, P.W., Laayoun, A., Smith, S.S., and Weitzman, S.A. (1995). DNA adduct 8-hydroxyl-2'-deoxyguanosine (8-hydroxyguanine) affects function of human DNA methyltransferase. *Carcinogenesis* *16*, 1253-1255.

Usdin, K., House, N.C., and Freudenreich, C.H. (2015). Repeat instability during DNA repair: Insights from model systems. *Crit Rev Biochem Mol Biol* 50, 142-167.

Vaisman, A., and Woodgate, R. (2017a). Translesion DNA polymerases in eukaryotes: what makes them tick? *Crit Rev Biochem Mol Biol* 52, 274-303.

Vaisman, A., and Woodgate, R. (2017b). Translesion DNA polymerases in eukaryotes: what makes them tick? *Crit Rev Biochem Mol Biol* 52, 274-303.

Valeri, N., Gasparini, P., Fabbri, M., Braconi, C., Veronese, A., Lovat, F., Adair, B., Vannini, I., Fanini, F., Bottoni, A., *et al.* (2010). Modulation of mismatch repair and genomic stability by miR-155. *Proc Natl Acad Sci U S A* 107, 6982-6987.

Valinluck, V., Tsai, H.H., Rogstad, D.K., Burdzy, A., Bird, A., and Sowers, L.C. (2004). Oxidative damage to methyl-CpG sequences inhibits the binding of the methyl-CpG binding domain (MBD) of methyl-CpG binding protein 2 (MeCP2). *Nucleic Acids Res* 32, 4100-4108.

Voet, D.a.V., J.G. (2011). *Biochemistry* 4th edition p94.

Wallace, S.S. (2002). Biological consequences of free radical-damaged DNA bases. *Free Radic Biol Med* 33, 1-14.

Wallace, S.S. (2014). Base excision repair: a critical player in many games. *DNA Repair* 19, 14-26.

Walmacq, C., Wang, L., Chong, J., Scibelli, K., Lubkowska, L., Gnat, A., Brooks, P.J., Wang, D., and Kashlev, M. (2015). Mechanism of RNA polymerase II bypass of oxidative cyclopurine DNA lesions. *Proc Natl Acad Sci U S A* 112, E410-419.

Wang, G., and Vasquez, K.M. (2014). Impact of alternative DNA structures on DNA damage, DNA repair, and genetic instability. *DNA Repair* 19, 143-151.

Wang, I.X., Grunseich, C., Fox, J., Burdick, J., Zhu, Z., Ravazian, N., Hafner, M., and Cheung, V.G. (2018a). Human proteins that interact with RNA/DNA hybrids. *Genome Res* 28, 1405-1414.

Wang, J., Clauson, C.L., Robbins, P.D., Niedernhofer, L.J., and Wang, Y. (2012). The oxidative DNA lesions 8,5'-cyclopurines accumulate with aging in a tissue-specific manner. *Aging Cell* 11, 714-716.

Wang, J., Yuan, B., Guerrero, C., Bahde, R., Gupta, S., and Wang, Y. (2011). Quantification of oxidative DNA lesions in tissues of Long-Evans Cinnamon rats by capillary high-performance liquid chromatography-tandem mass spectrometry coupled with stable isotope-dilution method. *Anal Chem* 83, 2201-2209.

Wang, R., Hao, W., Pan, L., Boldogh, I., and Ba, X. (2018b). The roles of base excision repair enzyme OGG1 in gene expression. *Cell Mol Life Sci* 75, 3741-3750.

Wang, Y. (2008). Bulky DNA lesions induced by reactive oxygen species. *Chem Res Toxicol* 21, 276-281.

Wang, Y., Feng, J., Zang, W., Du, Y., Chen, X., Sun, Q., Dong, Z., and Zhao, G. (2015). MiR-499 Enhances the Cisplatin Sensitivity of Esophageal Carcinoma Cell Lines by Targeting DNA Polymerase beta. *Cell Physiol Biochem* 36, 1587-1596.

Wang, Y., and Taniguchi, T. (2013). MicroRNAs and DNA damage response: implications for cancer therapy. *Cell Cycle* 12, 32-42.

Wang, Z.B., Zang, C.Z., Rosenfeld, J.A., Schones, D.E., Barski, A., Cuddapah, S., Cui, K.R., Roh, T.Y., Peng, W.Q., Zhang, M.Q., *et al.* (2008). Combinatorial patterns of histone acetylations and methylations in the human genome. *Nat. Genet.* 40, 897-903.

Washington, M.T., Johnson, R.E., Prakash, L., and Prakash, S. (2001). Accuracy of lesion bypass by yeast and human DNA polymerase eta. *Proc Natl Acad Sci U S A* 98, 8355-8360.

Washington, M.T., Johnson, R.E., Prakash, L., and Prakash, S. (2003). The mechanism of nucleotide incorporation by human DNA polymerase eta differs from that of the yeast enzyme. *Mol Cell Biol* 23, 8316-8322.

Waters, L.S., Minesinger, B.K., Wiltrout, M.E., D'Souza, S., Woodruff, R.V., and Walker, G.C. (2009). Eukaryotic translesion polymerases and their roles and regulation in DNA damage tolerance. *Microbiol Mol Biol Rev* 73, 134-154.

Weitzman, S.A., Turk, P.W., Milkowski, D.H., and Kozlowski, K. (1994). Free radical adducts induce alterations in DNA cytosine methylation. *Proc Natl Acad Sci U S A* 91, 1261-1264.

Weng, P.J., Gao, Y., Gregory, M.T., Wang, P., Wang, Y., and Yang, W. (2018a). Bypassing a 8,5'-cyclo-2'-deoxyadenosine lesion by human DNA polymerase eta at atomic resolution. *Proc Natl Acad Sci U S A* 115, 10660-10665.

Weng, P.J., Gao, Y., Gregory, M.T., Wang, P., Wang, Y., and Yang, W.A.-O. (2018b). Bypassing a 8,5'-cyclo-2'-deoxyadenosine lesion by human DNA polymerase eta at. *Proc Natl Acad Sci U S A* 115, 10660-10665.

Whitaker, A.M., Smith, M.R., Schaich, M.A., and Freudenthal, B.D. (2017). Capturing a mammalian DNA polymerase extending from an oxidized nucleotide. *Nucleic Acids Res* 45, 6934-6944.

- Wickramasinghe, C.M., Arzouk, H., Frey, A., Maiter, A., and Sale, J.E. (2015). Contributions of the specialised DNA polymerases to replication of structured DNA. *DNA Repair (Amst)* 29, 83-90.
- Wilhelm, T., Magdalou, I., Barascu, A., Techer, H., Debatisse, M., and Lopez, B.S. (2014). Spontaneous slow replication fork progression elicits mitosis alterations in homologous recombination-deficient mammalian cells. *Proc Natl Acad Sci U S A* 111, 763-768.
- Wilhelm, T., Ragu, S., Magdalou, I., Machon, C., Dardillac, E., Techer, H., Guitton, J., Debatisse, M., and Lopez, B.S. (2016). Slow Replication Fork Velocity of Homologous Recombination-Defective Cells Results from Endogenous Oxidative Stress. *PLoS Genet* 12, e1006007.
- Wilson, D.M., 3rd, Takeshita, M., Grollman, A.P., and Demple, B. (1995). Incision activity of human apurinic endonuclease (Ape) at abasic site analogs in DNA. *J Biol Chem* 270, 16002-16007.
- Wilson, S.H., and Kunkel, T.A. (2000). Passing the baton in base excision repair. *Nat Struct Biol* 7, 176-178.
- Wong, D., and Demple, B. (2004). Modulation of the 5'-deoxyribose-5-phosphate lyase and DNA synthesis activities of mammalian DNA polymerase beta by apurinic/aprimidinic endonuclease 1. *J Biol Chem* 279, 25268-25275.
- Xiang, Y., Laurent, B., Hsu, C.H., Nachtergaele, S., Lu, Z., Sheng, W., Xu, C., Chen, H., Ouyang, J., Wang, S., *et al.* (2017). RNA m(6)A methylation regulates the ultraviolet-induced DNA damage response. *Nature* 543, 573-576.
- Xu, M., Gabison, J., and Liu, Y. (2013). Trinucleotide repeat deletion via a unique hairpin bypass by DNA polymerase beta and alternate flap cleavage by flap endonuclease 1. *Nucleic Acids Res* 41, 1684-1697.
- Xu, M., Lai, Y., Jiang, Z., Terzidis, M.A., Masi, A., Chatgillaloglu, C., and Liu, Y. (2014). A 5', 8-cyclo-2'-deoxypurine lesion induces trinucleotide repeat deletion via a unique lesion bypass by DNA polymerase beta. *Nucleic Acids Res* 42, 13749-13763.
- Yan, S., and Michael, W.M. (2009). TopBP1 and DNA polymerase alpha-mediated recruitment of the 9-1-1 complex to stalled replication forks: implications for a replication restart-based mechanism for ATR checkpoint activation. *Cell Cycle* 8, 2877-2884.
- Yang, L.Q., Liu, Q.C., Gong, C.M., Tao, G.H., Liu, J.J., Hu, G.H., Huang, H.Y., Wang, K.P., and Zhuang, Z.X. (2011). [The effect of DNA methyltransferase 1 low expression on the global genome DNA methylation status of 16HBE cell]. *Zhonghua lao dong wei sheng zhi ye bing za zhi = Zhonghua laodong weisheng zhiyebing zazhi = Chinese journal of industrial hygiene and occupational diseases* 29, 194-197.

- Yang, W., and Gao, Y. (2018). Translesion and Repair DNA Polymerases: Diverse Structure and Mechanism. *Annu Rev Biochem* 87, 239-261.
- You, C., Swanson, A.L., Dai, X., Yuan, B., Wang, J., and Wang, Y. (2013a). Translesion synthesis of 8,5'-cyclopurine-2'-deoxynucleosides by DNA polymerases eta, iota, and zeta. *J Biol Chem* 288, 28548-28556.
- You, C., Swanson A L Fau - Dai, X., Dai X Fau - Yuan, B., Yuan B Fau - Wang, J., Wang J Fau - Wang, Y., and Wang, Y. (2013b). Translesion synthesis of 8,5'-cyclopurine-2'-deoxynucleosides by DNA polymerases. *J Biol Chem* 288, 28548-28556.
- Zeman, M.K., and Cimprich, K.A. (2014b). Causes and consequences of replication stress. *Nat Cell Biol* 16, 2-9.
- Zhang, C., Chen, L., Peng, D., Jiang, A., He, Y., Zeng, Y., Xie, C., Zhou, H., Luo, X., Liu, H., *et al.* (2020). METTL3 and N6-Methyladenosine Promote Homologous Recombination-Mediated Repair of DSBs by Modulating DNA-RNA Hybrid Accumulation. *Mol Cell* 79, 425-442.
- Zhang, X., Wan, G., Berger, F.G., He, X., and Lu, X. (2011). The ATM kinase induces microRNA biogenesis in the DNA damage response. *Mol Cell* 41, 371-383.
- Zhao, Y., Gregory, M.T., Biertumpfel, C., Hua, Y.J., Hanaoka, F., and Yang, W. (2013). Mechanism of somatic hypermutation at the WA motif by human DNA polymerase eta. *Proc Natl Acad Sci U S A* 110, 8146-8151.
- Zhou, V.W., Goren, A., and Bernstein, B.E. (2011). Charting histone modifications and the functional organization of mammalian genomes. *Nat Rev Genet* 12, 7-18.

VITA

PAWLOS S. TSEGAY

Miami, FL

2017-2021 Biochemistry Ph.D. Candidate
Florida International University
Miami, FL

2010-2016 Graduate teaching and research assistant
Asmara College of Health Sciences,
Asmara, Eritrea

2010 B.Sc. Clinical Laboratory Science
Asmara College of Health Sciences,
Asmara, Eritrea
Publications

Qu F, Tsegay PS, Liu Y. (2021) N6-methyladenosine, DNA repair, and genome stability. *Front. Mol. Biosci.* (8):104.

Rubfiaro AS, Tsegay PS, Lai Y, Cabello E, Shaver M, Hutcheson J, Liu Y, and He J. (2021). Scanning Ion Conductance Microscopy Study Reveals the Disruption of the Integrity of the Human Cell Membrane Structure by Oxidative DNA Damage. *ACS Appl. Bio Mater.* 4 (2), 1632-1639.

Jiang Z, Lai Y, Beaver JM, Tsegay PS, Zhao ML, Horton JK, Zamora M, Rein HL, Miralles F, Shaver M, Hutcheson JD, Agoulnik I, Wilson SH, Liu Y. (2020) Oxidative DNA Damage Modulates DNA Methylation Pattern in Human Breast Cancer 1 (BRCA1) Gene via the Crosstalk between DNA Polymerase β and a *de novo* DNA Methyltransferase. *Cells* 9(1): 225.

Tsegay PS, Lai Y, Liu Y. (2019). Replication stress and consequential instability of the genome and epigenome. *Molecules* 24 (21), 3870.

Chatgijialoglu, C, Ferreri, C, Geacintov, E, Krokidis, M, Liu, Y, Masi, A, Shafirovich, V, Terzidis, M and Tsegay, PS. (2019). 5',8-Cyclopurine Lesions in DNA Damage: Chemical, Analytical, Biological, and Diagnostic Significance. *Cells* 2019, 8, 513.

Tsegay P, Christopher Brache, Liu Y.; Environmental toxicants alter miRNAs associated with DNA repair genes. Poster presented at the 51st Annual

Meeting of Environmental Mutagenesis and Genomics Society (EMGS), Sep. 12-16, 2020, virtual meeting.

Tsegay P, Lai Y, Liu Y.; Incorporation of 5'8-cyclodeoxyadenosine lesions to the promoter sequence of miRNA by repair DNA polymerases. Poster presented SoFL-ACS Chemical Science Symposium, Aug 1st, 2020, virtual meeting.

Tsegay P, Lai Y, Liu Y.; Incorporation of 5'8-cyclodeoxyadenosine lesions to the promoter sequence of miRNA by repair DNA polymerase. Poster presented at FIU Biomolecular Sciences Institute symposium, July 30-31, 2020, Miami, FL, virtual meeting.

Tsegay P, Lai Y, Liu Y.; Incorporation of 5'8-cyclodeoxyadenosine lesions to the promoter sequence of miRNA. Poster presented at the 50th Annual Meeting of Environmental Mutagenesis and Genomics Society (EMGS), Sep. 19-23, 2019, Washington, DC.

Tsegay P, Jiang Z, Lai Y, Liu Y.; Oxidative DNA damage alters miRNAs level associated with DNA repair genes. Poster presented at FIU Biomolecular Sciences Institute symposium, April 12th, 2019, Miami, FL.

Tsegay P, Jiang Z, Lai Y, Liu Y.; Oxidative DNA damage alters miRNAs level associated with DNA repair proteins. Poster presented at FIU's Graduate Student Appreciation Week (GSAW), April 1st, 2019, Miami, FL.

Tsegay P, Jiang Z, Lai Y, Liu Y.; Oxidative DNA damage alters miRNAs level associated with DNA repair genes. Poster presented at FIU's students visitation day, March 8th, 2019, Miami, FL.

Tsegay P, Jiang Z, Lai Y, Liu Y.; Oxidative DNA damage alters miRNAs level associated with DNA repair genes. Poster presented at FIU Scholarly Forum, April 1st, 2019, Miami, FL.

Tsegay P, Jiang Z, Lai Y, Liu Y.; Oxidative DNA damage alters miRNA expression. Poster presented at the 49th Annual Meeting of Environmental Mutagenesis and Genomics Society (EMGS), Sep. 22-26, 2018, San Antonio, TX.

Tsegay P, Jiang Z, Lai Y, Liu Y.; Oxidative DNA damage alters miRNA expression. Poster presented at the 94th Florida Annual Meeting and Exposition (FAME), May 3-5, 2018, Tampa, FL.